University of Bath

UNIVERSITY OF BATH

PHD

Tracking and predictive simulations of sprinting: a direct collocation optimal control approach
(Alternative Format Thesis)

Haralabidis, Nicos

Award date:
2021

Awarding institution:
University of Bath

Link to publication

Alternative formats
If you require this document in an alternative format, please contact:
openaccess@bath.ac.uk

University of Bath

PHD

Tracking and predictive simulations of sprinting: a direct collocation optimal control approach
(Alternative Format Thesis)

Haralabidis, Nicos

Award date:
2021

Awarding institution:
University of Bath

Link to publication

Alternative formats

If you require this document in an alternative format, please contact:
openaccess@bath.ac.uk

TRACKING AND PREDICTIVE SIMULATIONS OF SPRINTING: A DIRECT COLLOCATION OPTIMAL CONTROL APPROACH

NICOS HARALABIDIS

A thesis submitted for the degree of Doctor of Philosophy

University of Bath

Department for Health

July 2021

COPYRIGHT

Declarations

Declaration of any previous submission of the work

The material presented here for examination for the award of a higher degree by research has not been incorporated into a submission for another degree.

Candidate's Signature:..

Declaration of authorship

I am the author of this thesis, and the work described therein was carried out by myself personally.

Candidate's Signature:..

Abstract

Sprinting is an integral component of sporting performance, and therefore a large body of experimental biomechanics studies have been carried out to identify the kinematics- and kinetics-based variables linked with improved performance. However, to date, very few studies have been performed to assess the influence of technique modifications on sprinting performance, potentially due to the difficulties in doing so using experimental approaches. Furthermore, sprinting, as with many sporting skills, has coaching frameworks that coaches follow when developing athletes, although the recommendations proposed by such frameworks have received minimal support from a scientific perspective. The purpose of this thesis was therefore to develop a computational modelling and simulation framework for sprinting to explore potential performance-enhancing modifications to technique and to assess how they compare to the recommendations proposed by a prevalent coaching framework (front-side mechanics). The first investigation of this thesis featured the development of a computational modelling and simulation framework for sprinting and evaluating its ability to reproduce experimental data for different sprinting phases. The evaluation step was carried out by performing a series of data-tracking calibration and validation simulations. The data-tracking simulations also enabled dynamically consistent simulated outputs to be obtained and foot-ground contact model parameters to be identified. The simulated outputs from the validation simulation were found to be in good agreement with the experimental data, with average root mean squared differences (RMSDs) less than $1.0°$ and 0.3 cm for the rotational and translational kinematics, respectively. The anterior-posterior ground reaction force component had the largest percentage RMSD (11.4%). The second study of this thesis explored how hypothetical modifications to technique affect accelerative sprinting performance by performing a series of (data-tracking and predictive) simulations using the framework developed in the first study. Technique modifications were explored through enabling either individual or combinations of the net lower-limb flexor-extensor joint moments (ankle, knee, and hip) to freely vary within the predictive simulations, whilst the remaining net joint moments were tracked (established from performing a data-tracking simulation). The 'knee-free' simulations led to the greatest improvements to overall performance (22.0%; 1401.2 vs. 1148.7 W) due to modifying the timing and magnitude of the net knee flexor-extensor moments. The kinematics aspects of the front-side mechanics coaching framework were not found to emerge from the performance-enhancing predictive simulations.

Publications

Journal Articles

Haralabidis, N., Serrancolí, G., Colyer, S., Bezodis, I., Salo, A. & Cazzola, D. (2021). Three-dimensional data-tracking simulations of sprinting using a direct collocation optimal control approach. *PeerJ,* **9**, e10975. DOI: https://doi.org/10.7717/peerj.10975

(This published article contains the work conducted in the third chapter of this thesis.)

Conference Proceedings

Haralabidis, N., Serrancolí, G., Colyer, S., Bezodis, I., Salo, A. & Cazzola, D. (2019). Sprinting data-tracking simulation: a direct collocation approach. *Proceedings of the XXXIV BASES Biomechanics Interest Group Meeting.* University of Huddersfield, UK.

(This conference proceeding formed the basis of the work carried out in the third chapter of this thesis.)

Haralabidis, N., Serrancolí, G., Colyer, S., Bezodis, I., Salo, A. & Cazzola, D. (2019). Estimation of kinematics and ground reaction forces during sprint running. *Proceedings of the XVII International Symposium on Computer Simulation in Biomechanics.* Alberta, Canada.

(This conference proceeding was an extension of the previous conference proceeding (Sprinting data-tracking simulation: a direct collocation approach) that contributed towards the work undertaken in the third chapter of this thesis.)

Haralabidis, N., Serrancolí, G., Colyer, S., Bezodis, I., Salo, A. & Cazzola, D. (2020). Data-tracking and predictive simulations of sprint running. *Proceedings of the 38th Conference of the International Society in Biomechanics of Sports.* Liverpool, UK.

(This conference proceeding formed the basis of the work conducted in the fourth chapter of this thesis.)

Acknowledgements

I would like to take this opportunity to thank my supervisors Dr Dario Cazzola, Dr Steffi Colyer and Dr Aki Salo for their guidance, enthusiasm, support, and hard work over the course of my PhD. I cannot express how grateful I am for all your assistance, advice, and feedback over almost the last five years. I would also like to thank Dr Gil Serrancolí for letting me spend a couple of months in his lab at the Polytechnic University of Catalonia and for been on standby to answer any optimal control related issues.

I would also like to express my thanks to present and past Applied Biomechanics Suite staff and students for their friendship throughout my PhD (Adrian, Olli, James, Holly, Luca, Pavlos, Biagio, Lorenzo, Ezio, Polly, Cassie, Elena, Adam, Laurie, Logan, Susann, Andreas, Josh and Mike). A big thanks must also go to the students (Aaron, Carl, Harry, Jon, Matt, and Megan) outside of my discipline within the Department for Health, after a difficult week of PhD work it was always nice to catch up with people over a few drinks and food. A special mention must go to my old flatmate Ollie. Thank you for your friendship and support throughout the PhD journey, it was a pleasure living with you and we shared some great times!

Hampset Cricket Club, thank you to the members for making me feel immediately welcome and part of the club from the onset. At the time of joining the club I barely knew anyone in Bath. Now, almost four years since joining, the people at the club have become friends for life and I have had some of my fondest memories in Bath with those individuals.

A big thank you must also be given to Andrea and Louise from the Doctoral College. Thank you for replying to my emails efficiently, aiding with administrative procedures and for helping me overcome some tricky circumstances.

The final acknowledgement goes to my parents. Mum and Dad, thank you both for your love, encouragement and support throughout my PhD. Whenever either of you visited I always knew I was going to eat well for a couple of days!

Table of Contents

List of Figures

List of Tables

Chapter 1
Introduction

1.1 Motivation for studying sprinting

The purpose of locomotion is to enable movement from one place to another. The two principal forms of terrestrial human locomotion are walking and running, and they collectively enable an individual to horizontally transport their body's centre of mass (CoM) across a broad range of velocities. The preferred form of locomotion at low velocities is walking, and adults typically transition to running when horizontal velocities begin to approach ~2 m/s as it becomes less metabolically demanding to run instead of walk (Saibene and Minetti, 2003). Running can be further categorised as either sprint running (sprinting) or distance running (Mero *et al.*, 1992; Novacheck, 1998). Sprinting enables the greatest horizontal velocities to be achieved, however it can only be sustained for short periods of time as it is heavily reliant upon anaerobic metabolism due to it being performed at maximal intensity. Conversely, distance running enables moderate horizontal velocities to be sustained for much longer periods of time, as the primary source of energy is from aerobic metabolism due to it being performed at submaximal intensity.

Sprinting is an integral component of sporting performance, none more so than for athletes competing within the short distance track and field events (60-400 m) for whom their performance is based on their sprinting ability alone. At the highest levels of competition (e.g., Olympic Games and World Athletics Championships), the winning margin between athletes is often less than several hundredths of a second. For example, in the men's 100 m final at the 2004 Olympic Games in Athens, the first and second place finishers were separated by 0.01 s (IAAF, 2004). Coaches and athletes are therefore continually striving for improvements in sprinting technique which can culminate together to overcome the narrow winning margins. Sprinting is also of paramount importance within team-based sports (e.g., rugby, field hockey and soccer) (Figure 1.1–1) that require short distances to be covered quickly to enable attacking and defensive actions to be completed more effectively than their opponents, thus gaining a competitive advantage (Austin *et al.*, 2011; Faude *et al.*, 2012; Spencer *et al.*, 2004). In rugby league, for example, 35 sprints per match are completed on average (Gabbett, 2012), with these sprints typically occurring during the critical periods of a match (Gabbett and Gahan, 2016). The benefits from understanding sprinting technique and performance have widespread application due to the significance of sprinting towards attaining sporting success, and this

therefore makes it a worthwhile topic to further study. The focus of this thesis will be linear sprinting (0-100 m) in relation to elite athletes (e.g., sprinters and soccer players), specifically from a biomechanical modelling and simulation perspective.

Figure 1.1–1 Examples of sports in which sprinting features prominently. (A & B: short distance track and field events, C: soccer and D: American football)

1.2 Rationale for studying sprinting using a computational modelling and simulation approach

The current body of sprinting literature which has concentrated on enhancing performance and technique suffers from two shortcomings. Firstly, the recommendations for technique modifications are based on cross-sectional group level analyses, which have shown particular biomechanical characteristics to be associated with higher performance levels. Cross-sectional group level analyses are useful for identifying potential trends in techniques between athletes of differing performance levels, and it is possible that the findings from such studies can be transferred to benefit the performance of elite athletes. However, individualised technique modifications are more likely to be necessary for elite athletes to further improve their performance levels by the sought-after small margins. Furthermore, there is also the possibility that applying the findings from the mean of group level analyses may lead to mean levels of overall performance, which is not desirable for elite athletes. Secondly, to date there has been a scarcity of intervention style studies which have attempted to implement the technique-based recommendations from the existing literature (e.g., minimising the horizontal touchdown distance between the CoM and foot) or technical coaching frameworks, such as front-side mechanics (Mann and Murphy, 2015), within a high-performance environment. Moreover, such studies have not succeeded at explaining how specific technique modifications influence sprinting performance. A predictive computer simulation and modelling approach can be used to overcome the issues listed above, particularly given the advancements made with this type of approach (e.g., ease of model development and tractability of performing simulations) since the pioneering long jump predictive simulation study by Hatze (1981). Furthermore, as also highlighted by Lin *et al.* (2018), the ability to perform predictive simulations is the last grand challenge to solve for biomechanists and engineers working within the field of computational modelling and simulation. In fact, the final goal is to enable simulations to be performed routinely and with relative ease to inform changes in the techniques of athletes and the coaching principles. Nevertheless, the usage of a predictive computer simulation and modelling approach with a view to enhance sprinting performance and technique has not yet featured prominently within the literature, thus presenting a potential avenue for further exploration.

1.3 Direct collocation optimal control

Within biomechanics it is common to perform data-tracking and predictive simulations by formulating them as optimal control problems (OCPs) (Ackermann and van den Bogert, 2010; Anderson and Pandy, 1999; Anderson and Pandy, 2001; Falisse *et al.*, 2019b; Lin and Pandy, 2017; Porsa *et al.*, 2016; Serrancolí *et al.*, 2019; van den Bogert *et al.*, 2012). An OCP is solved to determine the optimum state and control variables of a musculoskeletal model that lead to minimising (or maximising) a performance criterion for a specific circumstance, whilst the dynamics of the musculoskeletal model alongside any additional circumstance-specific requirements are satisfied. The standard method for solving an OCP within biomechanics relies on converting it to a nonlinear programming problem (NLP) by means of a direct method (e.g., direct collocation or direct shooting), and using specialised existing NLP solvers (e.g., IPOPT and SNOPT) to solve the problem. Direct collocation optimal control approaches have gained a significant interest from the biomechanics community as they are more computationally efficient, in terms of the amount of time needed to obtain an optimal solution, compared to direct shooting optimal control approaches (Porsa *et al.*, 2016). In addition, this has resulted in the recent release of an open-source software package that utilises direct collocation optimal control approaches for biomechanics applications (Dembia *et al.*, 2020). The computational efficiency of direct collocation optimal control approaches has also enabled researchers to use more sophisticated and realistic musculoskeletal models, such as three-dimensional musculoskeletal models with actuators comprising fast and slow contractile element properties (Lai *et al.*, 2021). In addition, they also provide the opportunity to perform more demanding simulations that were previously viewed as intractable, for example simulating multiple consecutive gait cycles or performing predictive simulations with models representative of numerous participants to permit further statistical analyses of the outputs (Miller and Hamill, 2015). To date, however, the application of a direct collocation optimal control approach together with a complicated three-dimensional musculoskeletal model for the purposes of exploring technique modifications and performance in sprinting has not yet featured within the literature.

1.4 Thesis purpose & aims

The overarching purpose of this thesis was to develop a computational modelling and simulation framework for linear sprinting (0-100 m) to explore potential performance-enhancing modifications to technique. Two studies were subsequently carried out to meet the purpose of this thesis.

Study 1: Three-dimensional data-tracking simulations of sprinting using a direct collocation optimal control approach

The main aims of the first study were to i) develop a computational modelling and simulation framework for sprinting using a direct collocation optimal control approach, and to ii) evaluate its capability of reproducing experimental data by performing a series of data-tracking simulations.

Two secondary aims were also identified for this study: i) to improve the dynamic consistency of the simulations by enforcing the pelvis residuals to be null and ii) to identify foot-ground contact model parameters for performing predictive simulations of sprinting.

Study 2: Modifications to the net knee moments lead to the greatest improvements in accelerative sprinting performance: a predictive simulation study

The main aims of the second study were to i) explore how hypothetical modifications in technique influence accelerative sprinting performance, and ii) investigate how the modifications mirrored the theories of an existing sprinting coaching framework (front-side mechanics).

1.5 Thesis outline

In the following chapters, a literature review of the relevant material together with two studies and a general discussion are presented.

- Chapter 2 features a review of the relevant biomechanical literature pertaining to sprinting and computational modelling and simulation methods.

- Chapter 3 contains the first study, which features the description and basis for initially performing data-tracking simulations of sprinting using the developed computational modelling and simulation framework. A thorough description of an empirical data collection for a single male international-level sprinter is also provided.

- Chapter 4 contains the second study, in which the developed computational modelling and simulation framework is used to explore how hypothetical modifications in technique, through changes in the lower-limb net joint moments, affect performance during accelerative sprinting.

- Chapter 5 provides a summary of the two studies, an overview of the studies' limitations and avenues for further research, and a final conclusion.

Chapter 2
Literature Review

This chapter provides a comprehensive narrative review of the pertinent literature in relation to the broad purpose and aims of this thesis proposed at the end of the first chapter. The review is organised into the following four major themes: 1) sprinting preliminaries, 2) analyses of sprinting technique, 3) application of computer modelling and simulation approaches to sprinting, and 4) biomechanical modelling and simulation approaches. The first theme of the review introduces and outlines the fundamental aspects of sprinting (e.g., phases and spatiotemporal parameters). In the following two themes the key aspects of sprinting technique based upon the findings of intra- and inter-athlete experimental studies are critiqued alongside the findings from predictive computer simulation modelling studies. In addition, these sections also cover the advantages offered by predictive computer simulation modelling approaches to carrying out sprinting research in comparison to more conventional experimental approaches. The latter theme of the review concentrates on reviewing the major elements of biomechanical modelling and simulation approaches (e.g., model construction and evaluation) and includes the advancements made with such approaches, covering their advantages and disadvantages. In the final section of this chapter a more specific restatement of the thesis aims is provided and contextualised based upon the literature provided.

2.1 Sprinting preliminaries

When an athlete performs a sprint, from either standing, jogging or starting blocks, they transition through a series of phases, and these phases are typically referred to as the acceleration, maximum velocity attainment and velocity maintenance phases (Debaere *et al.*, 2013; Delecluse *et al.*, 1995). The acceleration phase has also been recommended to be further subdivided into phases of early, middle, and late acceleration (Nagahara *et al.*, 2014b). From inspection of an athlete's horizontal velocity profile throughout the course of a sprint it is possible to recognise the three major phases (Figure 2.1–1). Successful sprinting performance within each of the phases relies on an athlete's ability to: a) rapidly accelerate their CoM, b) attain maximum horizontal velocity in the least amount of time possible and c) maintain high horizontal CoM velocity (Mero *et al.*, 1992; van Ingen Schenau *et al.*, 1994). The differing biomechanical requirements for achieving a high level of sprinting performance between the phases highlights that been able to perform at a high level in a single phase does not guarantee a high level of performance in the other phases (Delecluse *et al.*, 1992). It is therefore important

to acknowledge these differing requirements when assessments of sprinting performance and technique are made.
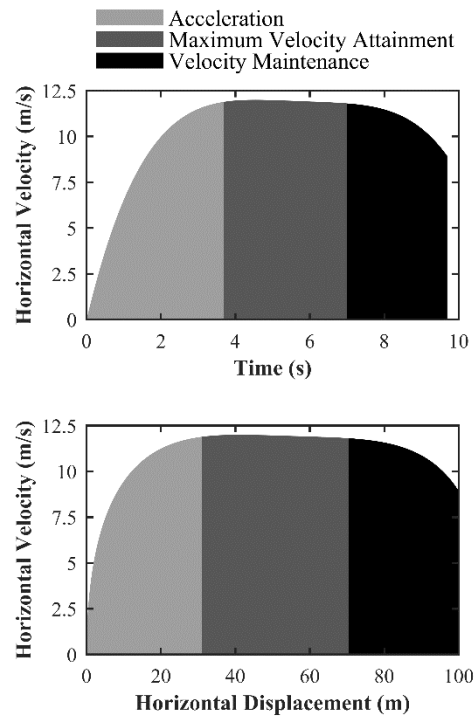
Figure 2.1–1 Exemplar horizontal velocity-time (top) and horizontal velocity-displacement (bottom) profiles of 100 m sprinting to illustrate the three major phases: acceleration (light grey shading), maximum velocity attainment (dark grey shading) and velocity maintenance (black shading). The profiles were created from Usain Bolt's 9.69 s 100 m performance at the 2008 Olympic Games in Beijing, China, using the data presented in Eriksen *et al.* (2009).

The maximum velocity phase is of critical importance to coaches and researchers alike, as the maximum horizontal velocity attained during this phase is strongly associated with the time taken to complete a 100 m sprint (Kersting, 1999; Slawinski *et al.*, 2017), which is the most important measure of sprinting performance. Male sprinters (international-level) and soccer players have been found to achieve horizontal velocities of ~12 and 8.7 m/s, respectively, during the maximum velocity phase (Colyer *et al.*, 2018b; Maćkała and Mero, 2013), and this emphasises the sprinting performance level disparities between specialised sprint athletes and team-based sport athletes. Previous studies have shown that the maximum velocity phase is attained at 30-70 m, with high calibre sprinters attaining the maximum velocity phase at greater distances compared to non-sprinters (Ae *et al.*, 1992; Helene and Yamashita, 2010; Volkov and Lapin, 1979). However, performance during the acceleration phase should not be discounted as it is during this preceding phase where rapid increments in horizontal velocity are aggregated. Furthermore, athletes competing within team-based sports rarely perform sprints that surpass the acceleration phase (Bangsbo *et al.*, 1991; Di Salvo *et al.*, 2010; Gabbett,

2012), and therefore sprinting research based on acceleration phase performance can be readily transferred to improve performance within team-based sports.

Sprinting, as with other forms of terrestrial human locomotion, is achieved by the sequential execution of a series of steps. A step is defined as the instant of touchdown of one foot to the subsequent touchdown of the contralateral foot. Each step whilst sprinting features a stance phase in which contact with the ground is made with one foot, and this is followed by a flight phase which features neither of the feet been in contact with the ground. The stance phase is of a longer duration than the flight phase during the initial acceleration phase, with values reported in the literature ranging between 0.152-0.175 and 0.044-0.079 s, respectively, for the third step of the acceleration phase (von Lieres Und Wilkau *et al.*, 2020; Walker *et al.*, 2019). As horizontal CoM velocity continues to be increased throughout the remainder of the acceleration phase and the maximum velocity phase is reached, more time is spent in the flight phase than the stance phase. Several studies have collectively shown that the stance and flight phase durations during the maximum velocity phase range between 0.076-0.102 and 0.125-0.141 s, respectively, (Kunz and Kaufmann, 1981; von Lieres Und Wilkau *et al.*, 2020). Additionally, the step duration (stance phase duration plus flight phase duration) has been shown to reduce from the early to middle acceleration phases, and then remain relatively constant from the middle to maximum velocity phases (Nagahara *et al.*, 2014a; Nagahara *et al.*, 2014b; von Lieres Und Wilkau *et al.*, 2020).

Given the significance of horizontal velocity towards sprinting performance it therefore seems pertinent to explore its determinants. The horizontal velocity of a given step is the product of the step frequency (the inverse of the time taken to complete one step – stance and flight phase duration) and the step length (the anterior-posterior displacement between the touchdown of one foot and the touchdown of the contralateral foot). It is therefore theoretically possible to increase an individual's horizontal step velocity by either increasing one of the step characteristics (either step frequency or step length) whilst the other step characteristic is kept constant or does not decrease in the same proportion as the other increases, or by increasing both step characteristics simultaneously. The step frequency and step length have been found to range between 4.17-5.36 Hz and 1.08-1.57 m during the early acceleration phase for the finalists competing in the men's 60 m at the 2018 World Indoor Championships (Walker *et al.*, 2019), and between 4.62-4.68 Hz and 2.21-2.29 m during the maximum velocity phase for a male sprinter with a 9.98 s 100 m PB (Bezodis *et al.*, 2008a). Furthermore, step frequency

increases in the early acceleration phase and begins to plateau by approximately the eighth step, whilst step length increases throughout the acceleration phase and is thus responsible for increases in velocity during the late acceleration phase (Nagahara *et al.*, 2014a; Nagahara *et al.*, 2014b).

A large number of studies have been conducted to determine which of the two step characteristics is of most significance to horizontal step velocity (Hunter *et al.*, 2004a; Kuitunen *et al.*, 2002; Kunz and Kaufmann, 1981; Luhtanen and Komi, 1978; Mero and Komi, 1985; Salo *et al.*, 2011), however the conclusions drawn from these studies are inconsistent and conflicted due to the use of intra- and inter-athlete group level analyses. Arguably the most comprehensive study conducted on this topic was carried out by Salo *et al.* (2011), and they concluded that the significance of either step frequency or step length amongst elite-level sprinters (during elite competition) was highly individualised, with a large variety of combinations existing. The step characteristics are readily used by coaches to guide the training and development process of their athletes as they are somewhat easy to measure and can be calculated in almost real-time which enables feedback to be provided in a timely manner. Whilst analyses of the step characteristics provide vital knowledge towards enhancing sprinting technique and performance, much greater insights can be obtained by assessing the processes which are responsible for the step characteristics (Wood, 1987) (Figure 2.1–2).

Horizontal running velocity

Step length

Step rate

Forward progression during flight

Forward progression during contact

Step time

Vertical and horizontal momentum

Flight time

Contact time

Drag force

Ground reaction force

Propulsion time

Landing time

Body segment displacements, velocities and accelerations

Segmental forces and moments of force

Body segment lengths, masses and moments of inertia

Muscle lengths and velocities

Tissue composition

Motor unit activity

Figure 2.1–2 Diagram of the biomechanical processes underlying horizontal sprinting velocity. Adapted from Wood (1987).

The step characteristics achieved together with the CoM motion an athlete undergoes during a step are governed by Newton's Laws of Motion and are the consequence of the behaviour and properties of the neuromusculoskeletal system. The central nervous system is responsible for coordinating the recruitment of the muscles. The muscles in turn generate forces that are applied to the skeleton via tendons, and together with their moment arms they produce moments that cause the segments of the skeleton to accelerate. The acceleration of an athlete's CoM is directly proportional to the external forces applied (Newton's Second Law of Motion),

and the three external forces acting whilst sprinting are the ground reaction force (GRF), gravity and air resistance. During the stance phase of a step, the forces generated by the muscles are transmitted to the ground resulting in an equal and opposite GRF being applied to the foot in contact with the ground (Newton's Third Law of Motion). The forces generated by the muscles during the flight phase can still cause the segments to move, although the CoM acceleration in this case is governed entirely by gravity and air resistance.

The somewhat naïve conclusion from an understanding of the causes of CoM acceleration would be to recommend generating large GRF in short periods of time. However, due to the intrinsic constraints of the neuromusculoskeletal system alongside its nonlinear behaviours (e.g., muscle excitation-force and net joint moments-joint accelerations) achieving a high level of sprinting performance is not so straightforward, and requires a thorough understanding of technique. To obtain further insights into sprinting technique and performance studies to date have been based on analyses of the kinematics (Ae *et al.*, 1992; Kunz and Kaufmann, 1981; Mann and Herman, 1985) and kinetics, external (Hunter *et al.*, 2005; Yu *et al.*, 2016) and internal (Bezodis *et al.*, 2008a; Bezodis *et al.*, 2014; Johnson and Buckley, 2001), obtained from empirical data collections during a discrete step. In the recent past, studies have also developed specialised experimental protocols (Morin *et al.*, 2015b) and research facilities (Nagahara *et al.*, 2014a; Nagahara *et al.*, 2018) to provide a more comprehensive outlook on the kinematics and GRF required by athletes to accelerate their CoM more successfully across successive steps.

Several studies to date have also attempted to elucidate how horizontal velocity increases by analysing the major lower-limb joint kinetics at a range of steady-state horizontal velocities (Belli *et al.*, 2002; Schache *et al.*, 2011; Schache *et al.*, 2015), however the identified techniques may not be representative for when accelerating across successive steps (Dorn *et al.*, 2012; Schache *et al.*, 2014). Alas, minimal literature currently exists which has shown how athletes should coordinate their lower-limb joint kinetics to most successfully accelerate their CoM across successive steps. Lastly, theoretical studies, based on predictive computer simulation and modelling approaches, of sprinting have been performed (Bezodis *et al.*, 2015; Celik and Piazza, 2013; van den Bogert and Ackermann, 2009). However, of the studies cited only one has attempted to explore the relationship between technique and performance, thus there is still great scope and potential to apply a predictive computer simulation and modelling

approach to investigate sprinting technique and performance for the purposes of providing individualised technique modifications and informing coaching practices.

2.2 Analyses of sprinting technique – kinematics and kinetics

The review up to this point has covered the temporal parameters and step characteristics for the different phases of sprinting, and highlighted the need to look beyond those variables to gain further insights into sprinting performance and technique. Thus, for the remainder of this review the findings from studies based on analyses of kinematics and kinetics (external and internal) will be reviewed, with a particular emphasis on studies conducted in relation to the acceleration phase. The decision to narrow the focus of the review to studies conducted during the acceleration phase was due to the significance of acceleration phase performance to overall track and field sprinting performance and the substantial role accelerative sprinting plays in contributing towards success within team-based sports. Lastly, the findings from studies that utilised a predictive computer simulation and modelling approach to study sprinting will be reviewed, irrespective of the phase in which they were conducted due to their scarcity within the existing literature.

2.2.1 Kinematics

Kinematic analyses of the human body are concerned with describing the linear and angular displacements, velocities and accelerations of the body's segments, joints and CoM. Schache and colleagues reported how the major lower-limb joints (hip, knee and ankle) together with the trunk change during discrete steps of high (5.30 m/s^2), medium (2.93 m/s^2) and low (1.32 m/s^2) CoM accelerations throughout the same accelerative sprinting trial (Schache *et al.*, 2019). The time histories of the lower-limb joint and global trunk angles during the stance phase for the different CoM acceleration magnitudes are shown in Figure 2.2-1. At the hip, touchdown was found to commence with a more flexed hip (65°) in the high acceleration condition compared to the low (45°), and the hip was shown to extend by ~60° throughout stance amongst all conditions despite the differences at touchdown. The knee was found to be further flexed at touchdown for the high acceleration condition (65°; 0° represented full extension) and extended until the latter ~5% of the stance phase (50° RoM), in contrast the knee flexion at touchdown for the low condition was ~30° and noticeable flexion-extension during the middle of the stance phase was observed with an overall ~20° RoM. The ankle undergoes flexion-extension during the stance phase irrespective of the acceleration condition.

At touchdown for the high and low acceleration conditions the ankle is dorsiflexed (15°) and plantarflexed (-5°), respectively, and they reach -35° of plantarflexion by the end of the stance phase, which leads to greater RoM in the high acceleration condition (55 vs. 40°).
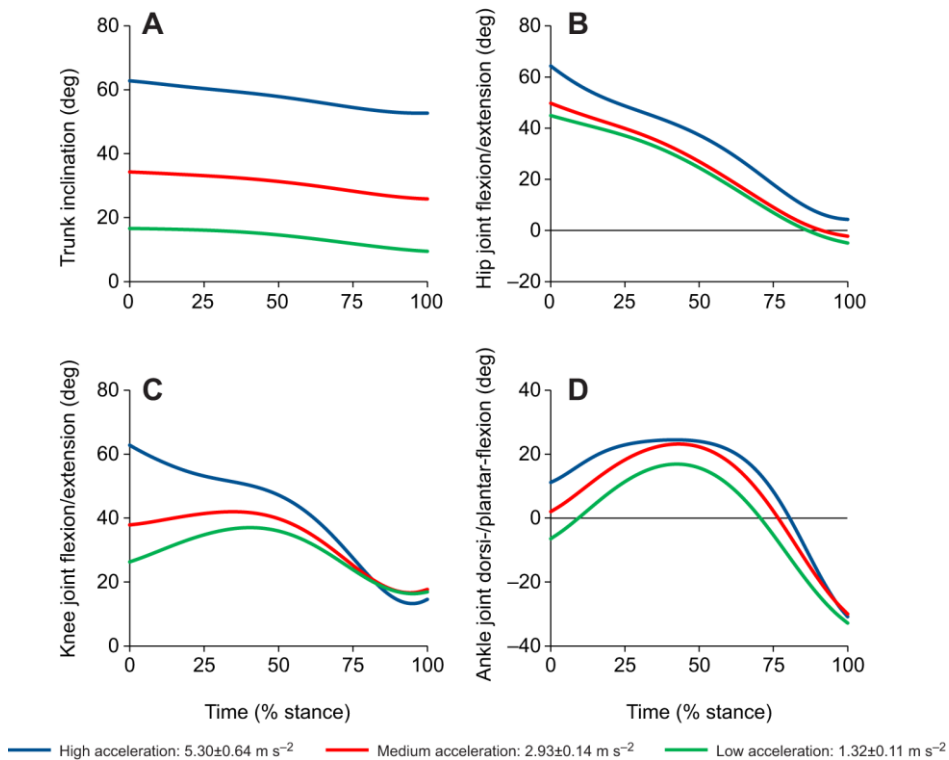
Figure 2.2–1 Group mean global trunk and lower-limb joint angles plotted across the stance phase for the three acceleration conditions (high: blue, medium: red, and low: green). The stance phase was time normalised from 0% (touchdown) to 100% (takeoff). A: trunk (the angle between the trunk segment and the vertical); B: hip (flexion is positive; extension is negative; 0° represents alignment between pelvis and thigh segments); C: knee (flexion is positive; extension is negative; 0° represents alignment between thigh and shank segments); D: ankle (dorsiflexion is positive; plantarflexion is negative; 0° represents plantigrade alignment between shank and foot segments). Figure taken from Schache *et al*. (2019).

Arguably the most noticeable kinematic differences identified by Schache *et al.* (2019) were at the trunk. The trunk angle relative to the vertical started to decrease from ~65° to ~15° between the high and low acceleration conditions at touchdown and became more upright with a ~10-15° RoM during the stance phase of each condition. Nagahara *et al.* (2014a) carried out an extensive study of the kinematics throughout the entire acceleration phase amongst a cohort of 12 sprinters with 100 m PBs ranging between 10.38-11.29 s. Similarly to Schache *et al.* (2019), Nagahara *et al.* (2014a) found that the trunk was more inclined during the early acceleration phase and becomes upright by the 14th step (22.2 m mark). As the trunk becomes more vertical throughout the course of a sprint it is also accompanied with a progressive rise in the CoM height, which rises from ~43% (relative to stature) and begins to plateau at ~53% also by the 14th step (Nagahara *et al.*, 2014a).

The findings from Schache *et al.* (2019) and Nagahara *et al.* (2014a) provide an overview of the acceleration phase kinematics, however they do not enable inferences in terms of the major technique-related kinematic variables differentiating athletes of different performance levels. Nevertheless, very few studies have attempted this in relation to the acceleration phase. One of the rare studies to do so analysed the lower-limb joint kinematics of three male sprinters (100 m PBs: 9.98, 10.22 and 10.51 s) during the first stance phase of the acceleration phase (Bezodis *et al.*, 2008b). They found that the highest performing sprinter, as indicated by their 100 m PB and stance phase average horizontal external power, exhibited greater extension RoM compared with the lowest performing sprinter at both the hip (70 vs. 61°, respectively) and knee (53 vs. 35°, respectively). The findings from this study therefore indicate that greater hip and knee extension are linked with improved early acceleration phase performance.

The sprinting literature during the maximum velocity phase has identified associations between a host of discrete kinematics-based technique variables (e.g., horizontal foot touchdown velocity, horizontal touchdown distance between the CoM and foot, hip and knee angular velocities at touchdown and during the stance phase (mean), hip and knee angles at takeoff, thigh excursion during the stance phase and mean thigh angular velocity during a step) and performance (Ae *et al.*, 1992; Clark *et al.*, 2020; Kunz and Kaufmann, 1981; Mann and Herman, 1985; Sides, 2014). Hunter *et al.* (2005) explored whether a subset of the kinematics-based techniques identified from the maximum velocity phase were also of relevance during the 16 m mark of the acceleration phase. They found that reduced horizontal foot velocity before touchdown, reduced touchdown distance between the CoM and foot, and greater mean hip extension velocity were desirable for improved sprinting performance during the acceleration phase, and these findings coincided with those from studies conducted during the maximum velocity phase (Ae *et al.*, 1992; Kunz and Kaufmann, 1981; Mann and Herman, 1985; Sides, 2014).

Hunter *et al.* (2005) stated that the relevance of greater mean hip extension velocity provided support in favour of the 'hip extensor theory' during the acceleration phase alongside the maximum velocity phase, for which it was originally intended. The 'hip extensor theory' proposes that during the stance phase, the thigh segment is rotated backwards (extended) by the major hip extensor muscles (e.g., gluteus maximus and hamstrings) and that this action is primarily responsible for producing the GRF needed to propel an athlete forward (Hunter *et al.*, 2004b; Mann and Sprague, 1980; Wiemann and Tidow, 1995). However, Hunter *et al.*

(2004b) questioned the 'hip extensor theory' based upon the timing mismatches of the net hip extensor moment in relation to the period of the stance phase which features propulsive GRF generation. In more recent times, the findings by Clark *et al.* (2020) suggest that there is merit in the 'hip extensor theory', although the role of the hip extensor muscles may be to instead produce vertical GRF. The evidence to support this claim is based on the timing of the hip (thigh) kinematics and kinetics in relation to the generation of vertical GRF during the stance phase, as sprinters of a higher performance level have been shown to generate a greater and more asymmetrical vertical GRF (Clark and Weyand, 2014) together with greater thigh excursion during the stance phase (Clark *et al.*, 2020).

The study by Hunter *et al.* (2005) also interestingly found that the hip, knee and ankle angles at takeoff were not relevant to sprinting performance during the acceleration phase. This can be considered a surprising result as it appears to not matter whether the major lower-limb joints are fully extended at takeoff, which Hay (1994) advises to do. Furthermore, this result does not coincide with the front-side mechanics coaching framework (Mann and Murphy, 2015), which is heavily reliant upon kinematics-based criteria, suggesting that the orientation of the major lower-limb joints at takeoff are not as relevant as imagined. The front-side mechanics coaching framework (Figure 2.2–2) was developed by Mann and Murphy (2015), and they suggest that sprinting coaches have been following the principles of the framework for several decades. The front-side mechanics coaching framework advises that athletes should contain the actions of their major lower-limb segments to the front of their body during the stance phase to prevent inefficient GRF production and prolonging the stance phase duration. Nevertheless, the front-side mechanics coaching framework has not been extensively researched and therefore warrants investigation from a scientific standpoint given its suggested prevalence amongst sprinting coaches.

2.2.2 External kinetics

Kinetics refers to both the forces and moments responsible for a body's linear and rotational motion, respectively, and typically in biomechanics a distinction is made between external and internal kinetics (Zatsiorsky, 2002). The external kinetics of most interest to researchers and coaches are the GRF and impulse as they reflect an athlete's ability to generate and transmit muscular forces to the ground in a specific amount of time, and together they are responsible for the linear change in an athlete's CoM velocity during the stance phase. It has been

extensively documented that the stance phase commences with a braking impulse that is followed by a propulsive impulse. The collective findings from studies demonstrate that the proportion of time spent braking during the stance phase increases throughout the course of a sprint. The braking phase has been reported to constitute 6-11%, 24-32% and 40-44% of the stance phase during the early acceleration (Mero and Komi, 1987; Salo *et al.*, 2005; von Lieres Und Wilkau *et al.*, 2020), middle acceleration (von Lieres Und Wilkau *et al.*, 2020; Yu *et al.*, 2016) and maximum velocity (Mero, 1988; von Lieres Und Wilkau *et al.*, 2020; Yu *et al.*, 2016) phases, respectively.

Back-side   **Front-side**
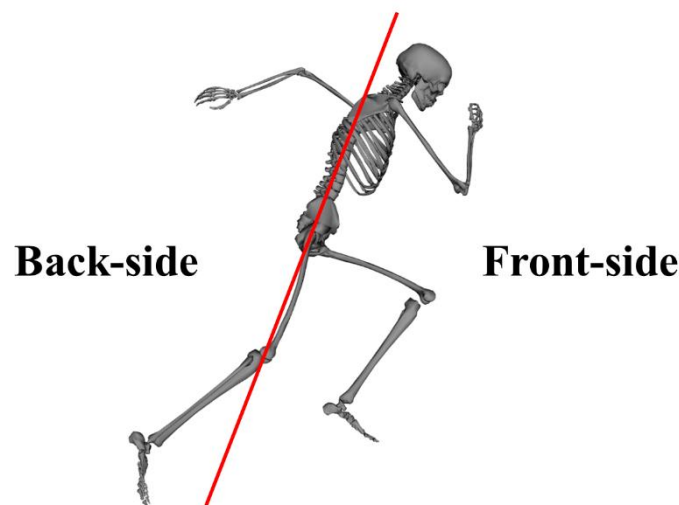
Figure 2.2–2 Schematic diagram highlighting front-side and back-side mechanics during the second step stance phase of a maximal effort sprint. The solid red line drawn parallel to the torso indicates when the lower-limbs are in front of the body and performing front-side mechanics or behind the body and performing back-side mechanics. The definitions of front-side and back-side mechanics are based upon those provided by Mann and Murphy (2015).

An increase in the horizontal CoM velocity during the acceleration phase is due to the production of positive net impulses (sum of braking and propulsive impulses), whilst there is no change in the horizontal CoM velocity during the maximum velocity phase as the net impulse is about zero (although there will be small positive GRF impulses needed to overcome air resistance). Previous studies have reported a net propulsive impulse of 87-92 Ns during the first step (Mero, 1988; Salo *et al.*, 2005), with the net propulsive impulse decreasing to 44 Ns by the fourth step (Salo *et al.*, 2005). The net propulsive impulse has been shown to be 18-19.5 Ns during the 14-16 m mark of the acceleration phase (Hunter *et al.*, 2005; Johnson and Buckley, 2001), whilst during the maximum velocity phase it has been reported to be 3.9-10.8 Ns (Bezodis, 2006; Sides, 2014).

Several studies have shown that sprinting performance is strongly associated with the net propulsive impulse produced (Kawamori *et al.*, 2013; Morin *et al.*, 2015b; Nagahara *et al.*, 2018). It is important to recognise that the CoM velocity across a step can be changed through either reducing the braking impulse and/or increasing the propulsive impulse, and thus several studies have attempted to explore the independent relative importance of braking and propulsive impulses in relation to sprinting (Colyer *et al.*, 2018a; Morin *et al.*, 2015b; Nagahara *et al.*, 2018). The consensus from these studies is that early acceleration phase performance relies on the generation of large propulsive impulses, via greater mean hip extension angular velocity during stance (Hunter *et al.*, 2005), while late acceleration phase performance requires minimising the braking impulses. Strategies for reducing the braking impulse include reducing the horizontal foot touchdown velocity (Hunter *et al.*, 2005; Mann and Sprague, 1983) and horizontal CoM-foot touchdown distance (Mann and Herman, 1985; Mann *et al.*, 1984) by rapid hip extension late in the swing phase. Furthermore, Hunter *et al.* (2005) suggested that intervention studies were warranted to explore these potential mechanisms. It could, however, be argued that a predictive computer simulation and modelling approach is more suited to addressing this type of research, nevertheless application of such an approach has been limited within the sprinting literature.

This section has so far concentrated on the anterior-posterior impulse, however during the stance phase athletes must also generate enough vertical impulse to terminate their downward CoM movement, due to gravity, and propel their CoM upwards for the subsequent flight phase. It has been suggested that athletes should generate the minimum vertical impulse to counter the effect of gravity and enable the lower-limbs to be repositioned for the following flight phase (Hunter *et al.*, 2005), as larger than necessary vertical impulses may be detrimental to performance due to causing longer flight phases and thus reducing step frequency (Nagahara et al., 2018). The study by Nagahara *et al.* (2018) provided evidence to support this, as they found smaller vertical impulses were conducive to greater performance during the acceleration phase. The same study also identified that the ability to generate a large vertical GRF, as opposed to a large vertical impulse, was necessary for improved performance during the maximum velocity phase due to the combination of low stance phase durations together with the requirement of producing the required vertical impulse to maintain performance during this phase. This latter finding has also been supported by studies featuring cohorts of physically active participants (Weyand *et al.*, 2000) and sprinters (von Lieres Und Wilkau *et al.*, 2020),

and they found that applying a larger mean vertical GRF was associated with greater running velocities.

2.2.3 Internal kinetics

Analyses of the internal kinetics are commonly based on the net joint moments, and they are representative of the net sum of all the internal structures (e.g., active contraction of muscle, passive ligament resistance and other soft tissue behaviour) acting across a joint. Through an analysis of the net joint moments it is possible to obtain an understanding of the causes of the joint kinematics, and why the techniques exhibited by athletes of a higher sprinting performance level were able to achieve a superior performance. Furthermore, the net joint moments can be combined with the joint angular velocities to determine the net joint powers and work done by the major lower-limb joints. The net joint powers and work done provide a surrogate measure of whether the major muscle groups, as reflected through the net joint moments, are acting concentrically and generating energy, or eccentrically and absorbing energy (Winter, 2009).

Schache and colleagues performed a comprehensive analysis of the lower-limb net joint kinetics, alongside the lower-limb kinematics, during different magnitudes of CoM acceleration (Schache *et al.*, 2019). The time histories of the ankle, knee, and hip net joint moments and joint powers during the stance phase for the different CoM acceleration magnitudes are shown in Figure 2.2–3 and Figure 2.2–4, respectively. An overview of the main findings for each of the lower-limb joints will be provided separately, commencing with the hip joint.
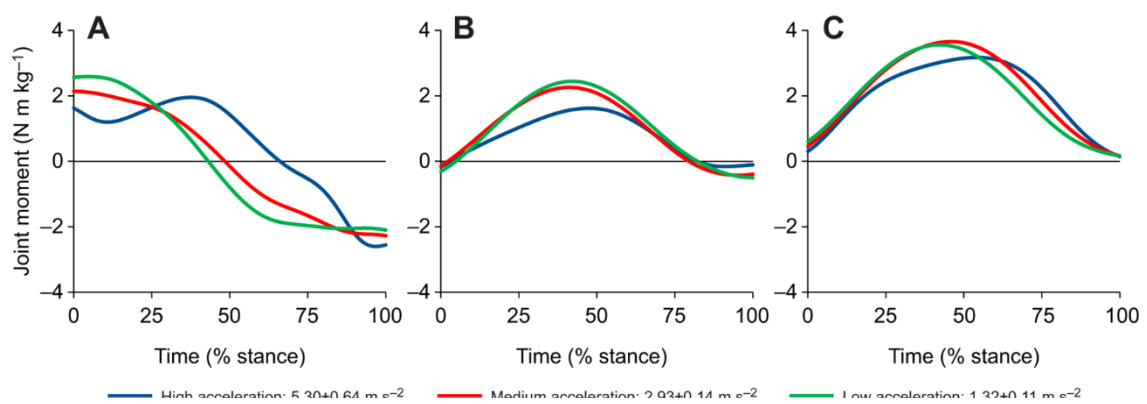
Figure 2.2–3 Group mean lower-limb net flexor-extensor joint moments plotted across the stance phase for the three acceleration conditions (high: blue, medium: red, and low: green). Net joint moments normalised to body mass. The stance phase was time normalised from 0% (touchdown) to 100% (takeoff). A: hip (extensor is positive; flexor is negative); B: knee (extensor is positive; flexor is negative); C: ankle (plantarflexor is positive; dorsiflexor is negative). Figure taken from Schache *et al*. (2019).
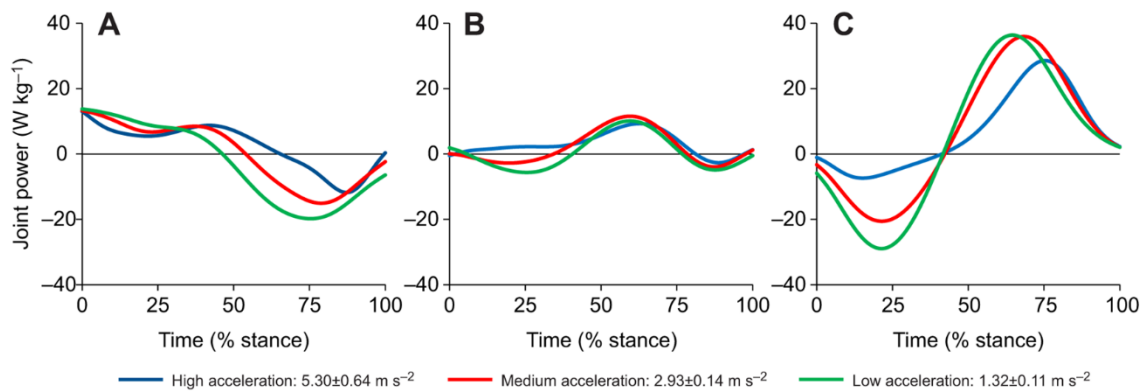
Figure 2.2–4 Group mean lower-limb net joint powers plotted across the stance phase for the three acceleration conditions (high: blue, medium: red, and low: green). Net joint powers were normalised to body mass. Power generation is positive and power absorption is negative. The stance phase was time normalised from 0% (touchdown) to 100% (takeoff). A: hip; B: knee; C: ankle. Figure taken from Schache *et al.* (2019).

At the hip, a greater net extensor moment was identified at touchdown for the low acceleration condition compared to the high (2.5 vs. 1.6 Nm/kg). The net hip moment became flexor at 35% and 65% of the stance phase for the low and high acceleration conditions, respectively, and at takeoff the magnitude was greater for the high acceleration condition compared to the low (-2.3 vs. -2.0 Nm/kg). The net extensor-to-flexor hip moment pattern has been identified as a fundamental aspect of sprinting with front-side mechanics (Mann and Murphy, 2015). The net work done at the hip transitioned from net positive in the high acceleration condition to net negative in the low (0.48 vs. -0.29 J/kg).

A small and similar net knee flexor moment was found at touchdown for the high and low acceleration conditions (-0.15 Nm/kg), and this transitioned to an extensor moment for both conditions at ~5% of the stance phase. The peak net knee extensor moment was greater (2.4 vs. 1.7 Nm/kg) and achieved earlier in the stance phase (40% vs. 48%) for the low acceleration condition compared to the high. At takeoff, the net knee moment became flexor, and the magnitude was greater for the low acceleration condition compared to the high (-0.4 vs. -0.05 Nm/kg). The net work done at the knee decreased across the acceleration conditions but remained net positive across the high and low acceleration conditions (0.56 vs. 0.05 J/kg).

A net ankle plantarflexor moment was identified at touchdown, and the magnitude was greater for the low acceleration condition compared to the high (0.4 vs. 0.2 Nm/kg). The peak net ankle plantarflexor moment was greater (3.8 vs. 3.0 Nm/kg) and achieved earlier in the stance phase

(35% vs. 55%) for the low acceleration condition compared to the high. The net work done at the ankle also decreased across the acceleration conditions but remained net positive across the high and low acceleration conditions (1.19 vs. 0.41 J/kg), and across the acceleration conditions the ankle consistently performed the most net positive work compared to the other joints.

The study by Schache *et al.* (2019) also found positive relationships between the impulse of the extensor moments at the hip and ankle and the acceleration magnitude. The collective findings from this study demonstrate the significance of the ankle and hip joints towards sprinting performance during the acceleration phase. The limited role of the knee joint may be due to the reduced amount of flexion at touchdown as the magnitude of acceleration decreases, thus limiting the RoM over the stance phase for which to generate a net extensor moment. Furthermore, the cross-sectional study design may have omitted important differences at an individual level. Bezodis *et al.* (2015) stated that during the early acceleration phase there is less negative vertical CoM velocity to be reversed, in which case this permits the knee to have a greater role in generating net positive work and consequently contributing towards forward acceleration.

Charalambous *et al.* (2012) analysed the net lower-limb joint kinetics of an international-level male sprint hurdle athlete during the first stance phase of the acceleration phase. They reported that the knee kinematics were dissimilar, lacking flexion, to the middle acceleration (Johnson and Buckley, 2001) and maximum velocity (Bezodis *et al.*, 2008a) phases. They also reported that the knee plays an important role in early acceleration phase sprinting performance, despite the small net extensor moment and power magnitudes compared to the ankle and hip. Charalambous *et al.* (2012) cite that the role of the knee is to stabilise the lower-limb, increase vertical CoM velocity and transfer energy from the hip to the ankle (Jacobs and van Ingen Schenau, 1992). It is also worthwhile noting that the study by Charalambous *et al.* (2012) had the opportunity to explore how changes in the net joint kinetics may have influenced performance during the early acceleration phase on an individualised basis, nevertheless the authors did not choose to do so.

Bezodis *et al.* (2014) also analysed the net lower-limb joint kinetics during the first stance phase of the acceleration phase of three international-level sprinters (100 m PB sprinter A: 10.14, B: 10.28 and C: 12.72 s). In addition, they also attempted to perform a between athlete analysis. Bezodis *et al.* (2014) found that sprinter B achieved the highest performance level

across the stance phase, as indicated by the average horizontal external power, and they found that this sprinter generated greater ankle energy than their counterparts which may have contributed to their superior performance. The authors of this study also noted that sprinter B generated greater knee energy compared to the other athletes, again they also speculated that this may have contributed to their superior performance, noting that this was largely due to an earlier rising and peak net knee extensor moment. Furthermore, Bezodis *et al.* (2014) suggested that the potentially more beneficial net knee extensor moment generated by sprinter B may have been assisted by their improved touchdown kinematics, as they were also found to exhibit a lower horizontal foot touchdown velocity which has been linked with reducing the braking impulse (Mann and Herman, 1985). Lastly, sprinter B was also found to perform greater negative work at the hip, and this strategy has been suggested to be necessary to reduce the backward velocity of the thigh segment. Performing negative work at the hip has been suggested to be important for performance during the maximum velocity phase (Mann and Sprague, 1980; Mann, 1981), and based on these results it also appears to be an important aspect of technique from the very beginning of performing a sprint.

The human skeleton can be modelled as a multibody system comprising rigid segments, and with knowledge of the kinematics and external forces (e.g., GRF) they can be combined to calculate the net joint moments necessary to produce the observed motion by performing inverse dynamics. However, the net joint moments obtained by performing inverse dynamics are known to be sensitive to the processing of the input data (e.g., the choice of filter cut-off frequencies and calculating the derivatives of the kinematics) (Bisseling and Hof, 2006; Hatze, 2005; Kristianslund *et al.*, 2012) and the external force application point (Kim *et al.*, 2007; McCaw and Devita, 1995). Furthermore, imperfections in the model and input data lead to dynamic inconsistencies and violations of Newton's Second of Law of Motion (Delp *et al.*, 2007; Hicks *et al.*, 2015). The dynamic inconsistencies, in the form of residual forces and moments at the unactuated joint of the segment connected to the ground, are commonly disregarded within the sports biomechanics literature, and therefore the validity of the findings from inverse dynamics studies must be questioned. In recent times, data-tracking simulations, formulated as optimal control problems, appear to have gained popularity as they can be performed to obtain dynamically consistent net joint moments (Lin and Pandy, 2017; Meyer *et al.*, 2016; Pallarès-López *et al.*, 2019), however this type of approach has yet to be explored within a highly dynamic task, such as sprinting.

The drivers for motion are the forces generated by muscles, and therefore it seems intuitive that they should be the focus when attempting to improve performance and technique. Nevertheless, measuring muscle forces *in vivo* requires invasive procedures (Pandy and Andriacchi, 2010), and it is therefore not feasible to do so, particularly in tasks such as sprinting. Muscle forces together with their operating conditions (e.g., region on the force-length relationship) can, however, be estimated non-invasively by using a musculoskeletal model in combination with optimisation theory. The application of optimisation theory is necessary to estimate muscle forces as the musculoskeletal system is mechanically redundant, for example, the hip joint is spanned by more than 15 muscles, and consequently a net joint moment can be produced by a multitude of muscle force combinations.

To solve the muscle forces redundancy problem using optimisation theory a performance criterion must either be maximised or minimised subject to a set of constraints. Arguably the two most common optimisation approaches for solving the muscle forces redundancy problem are static and dynamic optimisation (Pandy, 2001; Pandy and Andriacchi, 2010). Static optimisation can be viewed as decomposing the net joint moments into individual muscle forces based on a performance criterion that typically involves minimisation of the sum of squared muscle activations. Dynamic optimisation, which is synonymous with optimal control within the biomechanics community, typically solves the redundancy problem by performing a simulation which aims to track experimental data whilst also simultaneously minimising the sum of squared muscle activations. An advantage of static optimisation is that it can be used to solve the redundancy problem in a timely manner due to solving a separate optimisation problem for each discretised time point of a movement, however using dynamic optimisation can take much longer as it accounts for all the discretised time points of a movement simultaneously. The main benefits of dynamic optimisation are that it permits the use of integrated performance criteria and enables muscle activation and contraction dynamics to be included, as it accounts for all the discretised time points of a movement simultaneously, whilst static optimisation is not suitable for including these features. Lastly, a major benefit of dynamic optimisation is that it can be used in circumstances where no experimental data is available, and thus it enables predictive simulations to be performed.

Hamstring strain injuries are common amongst sports that involve sprinting (Dalton *et al.*, 2015; Duhig *et al.*, 2016). Quantifying the forces generated by those muscles together with their operating conditions is therefore crucial from an injury perspective within sprinting, as

this information could be used to aid in determining the aetiology of hamstring strain injuries and improving the rehabilitation process. Whilst the knowledge of muscle forces is crucial from an injury prevention and conditioning perspective, their application to directly informing sprinting technique and performance must be questioned as providing feedback in relation to muscle forces may be difficult to implement. Conversely, technique-based recommendations related to net joint moments may potentially have a greater application for feedback and intuition.

2.3 Application of predictive computer modelling and simulation approaches to sprinting

To date, very few studies have developed a computer model and used it to perform predictive simulations of sprinting with a view to enhance performance. One of the rare studies to do so was carried out by Bezodis *et al.* (2015). The authors of this study developed a seven-segment two-dimensional model that was kinematically-driven and used it to explore the effects of manipulating horizontal CoM-foot touchdown distance and the range of ankle dorsiflexion during stance on performance in the first step of the acceleration phase. They found a nonlinear relationship between manipulating the horizontal CoM-foot touchdown distance and performance, and confirmed some of the beliefs regarding the benefit of reducing horizontal CoM-foot touchdown distance. External power production was found to decrease as the foot was moved further forward, reach a peak improvement (0.7%) as the foot was moved backwards and then decrease with further backwards movements. Exponential improvements in performance were observed with reductions in ankle dorsiflexion. A major strength of this study was that they performed a comprehensive evaluation of their model by performing a data-tracking simulation and found it was a close match with reality. However, a limitation of this study was that the model was kinematically-driven. Kinematically-driven models have been recommended for movements which are not limited by strength (Yeadon and King, 2007), as the net joint moments can become unwieldy using such an approach, however strength is an important component of sprinting. Future studies attempting to utilise a modelling and predictive simulation approach should consider using a kinetically-driven model with realistic muscle-tendon unit force production capabilities.

Previous studies have performed predictive simulations of walking and running across a single step (Ackermann and van den Bogert, 2010; Falisse *et al.*, 2019b), however they typically impose a terminal constraint that enforces symmetry (e.g., the state and control variables must match at the beginning and end). However, in circumstances such as the acceleration phase,

where CoM velocity continually changes along with the kinematics and kinetics, this type of constraint does not permit multiple steps to be simulated. Celik and Piazza (2013) developed a three-segment two-dimensional model and used it to perform predictive simulations of sprinting across 20 m of the acceleration phase. They found that their model exhibited key features of sprinting during the acceleration phase, for example the trunk segment was initially more inclined and then became more upright with subsequent steps. They also noted that the model began to dive following the last step, which is commonly seen in sprinting to get over the finish line. This study provided evidence for the scope of simulating multiple successive steps without the need to impose a terminal symmetry constraint. However, due to the simplicity of the model it is difficult to translate these findings to an applied environment, and they also did not evaluate their model which would have likely suggested increasing its complexity to ensure it was a closer representation of reality. Lastly, the model's actuators were idealised force and moment generators, and lacked physiological properties, which also makes transferring these findings difficult. Future research should therefore aim to simulate multiple steps of sprinting using a model with actuators governed by muscle physiology properties. Importantly, the model must also initially undergo a thorough evaluation to demonstrate it is suitable for its intended purposes.

2.4 Biomechanical modelling and simulation approaches

Within the field of biomechanics, research questions can be answered using theoretical and experimental approaches. Theoretical approaches rely upon the development of a computer simulation model. A computer model is a set of equations, usually in the form of linear or nonlinear differential equations, that are used to represent a physical system (Alexander, 2003). Most models of the human skeleton are based on a series of interconnected rigid segments and the dynamics equations for these models can be developed by applying Newtonian mechanics. Deriving the dynamics equations of computer models with a limited number of segments and degrees-of-freedom (DOFs) suffices using Newtonian mechanics. However, in circumstances where the human skeleton is modelled with more complexity (e.g., a greater number of segments and DOFs), which is often needed to ensure the model is a closer representation of reality, application of Lagrangian mechanics is more appealing as it leads to a reduced set of dynamics equations and is thus more favourable for subsequent usage (van den Bogert and Nigg, 2007). The Lagrangian formulation is based on describing a model's DOFs with a set of generalised coordinates $q = [q_1 \ q_2 \ ... \ q_n]^T$. Application of the Lagrangian formulation leads

to the following set of coupled second-order nonlinear differential equations to describe the dynamics of the human skeleton:

$$M(q) \cdot a = C(q, v) + G(q) + E + T \qquad (1)$$

where q, v and a are the vectors of generalised coordinates, velocities and accelerations, respectively, $M(q)$ is the mass matrix, $C(q, v)$ is the vector of centrifugal forces, $G(q)$ is the vector of gravitational forces, E is the vector of external forces (e.g., GRF) and T the vector of generalised forces. The generalised forces vector comprises the residual forces and moments, which should be null for unactuated DOFs, and the net joint moments.

The dynamics equations (1) can be restructured as follows:

$$a = M(q)^{-1}[C(q, v) + G(q) + E + T)] \qquad (2)$$

$$M(q) \cdot a - C(q, v) - G(q) - E = T \qquad (3)$$

When the dynamics equations are expressed as per equation (2) they demonstrate the 'natural flow of events' by which humans perform movement (neural-to-muscular-to-skeletal events) (Yamaguchi, 2005). It is possible to integrate these equations forwards in time to determine the motion of the skeleton in response to the inputs, which in this case are the net joint moments. In addition, models of muscle force production and geometry can be used in place of net joint moments. When the dynamics equations are used as per equation (2) it is referred to as forward dynamics, and this is most commonly associated with performing a simulation using a computer model (Vaughan, 1984). Conversely, when the dynamics equations are used as per equation (3) it is known as inverse dynamics, and this permits the net joint moments that must have been necessary to produce an observed motion to be calculated. It is also worthwhile highlighting that studies have developed approaches to perform simulations by using the dynamics equations in an inverse fashion (Falisse *et al.*, 2019a; Meyer *et al.*, 2016; Serrancolí *et al.*, 2019; van den Bogert *et al.*, 2011).

Once a model has been developed it can be used to perform predictive and data-tracking simulations. Predictive simulations have a host of advantages for addressing sports biomechanics research questions which would otherwise not be feasible using experimental approaches, for example they enable 'what if' scenarios to be explored (e.g., hypothetical strength training improvements) and the identification of optimum technique. Data-tracking simulations can be performed to improve the dynamic consistency of modelled outputs, solve the muscle forces redundancy problem and calibrate model parameters (e.g., foot-ground

contact model parameters). Arguably the most beneficial aspect of performing data-tracking simulations is that they enable modelling assumptions to be assessed and they can be used to evaluate whether the model is of sufficient complexity. Yeadon and Challis (1994) stated that computer models used to perform predictive simulations typically undergo very little evaluation and thus their accuracy is unknown. In such cases it is therefore difficult to apply the findings in real world settings due to not knowing the level of accuracy. The evaluation of a computer model is consequently considered a vital step towards the development of a modelling and simulation framework.

2.4.1 Model construction

It is important to highlight that computer models of the human body are simplifications of reality as the human body comprises over 200 bones and 500 muscles (Yeadon and King, 2007). The first step towards developing a computer model is therefore deciding on its complexity, and several authors have stated that the complexity of a model depends on its intended use (Pandy, 2001; Yeadon and King, 2007). For example, if the purpose of a study is to assess muscle coordination, a model which does not include actuators governed by properties of muscle physiology is not likely to be adequate for its intended use.

Within the biomechanics literature, most computer models up until the early 2000s were two-dimensional and grossly simplified, largely due to the limited computational power available at the time. Nevertheless, the benefit of simple computer models is that the results can be more easily interpreted. Whilst the results of simple computer models may be easier to interpret, their overly simplified nature limits the accuracy for which the findings can be applied to the real system. The improvements in computational power together with bespoke biomechanical modelling software (e.g., OpenSim and AnyBody) (Damsgaard *et al.*, 2006; Delp *et al.*, 2007) has seen the rise in three-dimensional computer models with far greater biofidelity. Arguably the greatest strength of these packages is that they come with a library of previously developed models, and this was a major bottleneck in the past as it meant that each model was purpose-built. Now, however, these software packages cater for scaling the generic models to different participants and they permit modifications to be made to the models. Despite the relative ease with which features of a model can be modified within the software packages it is perhaps also one of their major weaknesses, it is therefore imperative to perform checks throughout to ensure

the modifications made produce expected results for simple circumstances and obey the physical laws.

When developing a computer model, an important decision must be made with regards to how the model is driven, as they can be either kinematically- or kinetically-driven. Kinematically-driven models have been previously used for modelling sporting tasks which are not limited by strength, such as the aerial phase of gymnastics manoeuvres (Yeadon *et al.*, 1990). The benefit of kinematically-driven models is that they only require the accelerations of the model's DOFs, however caution should be taken when using this approach as the net joint moments, which can be subsequently calculated, may become greater than feasibly achievable for a human. Kinetically-driven models fall into two categories: muscle and moment. Hereafter these approaches will be referred to as muscle- and moment-driven.

Muscle-driven models involve modelling the geometry and force-producing elements of muscles. The geometry of a muscle is most often modelled as a single line segment between its origin and insertion, and to improve the representation of muscle in different joint configurations via-points and wrapping surfaces are also used. The lengths and moment arms of the modelled muscles using this approach are a function of the skeletal model's generalised coordinates. The force-producing elements of muscle are typically based on the Hill model (Figure 2.4–1), which consists of three elements: an active contractile element, a parallel elastic element and a series elastic element. The contractile and parallel elastic elements are intended to represent the behaviour of the muscle fibres and passive elastic tissue that surrounds the muscle fibres, respectively, whilst the series elastic element is intended to represent the behaviour of the tendon and other tissues responsible for transmitting force from the muscle fibres to the skeleton (van den Bogert *et al.*, 2011) (Figure 2.4–2). A strength of the Hill model is that it is dimensionless and thus force generation can be scaled for different muscles and individuals based on the following parameters: optimum fibre length, tendon slack length, maximum shortening velocity, maximum isometric force and pennation angle at optimum fibre length.

Challenges with muscle-driven models include determining appropriate values for the parameters of the Hill model and accurately capturing the muscle geometry (Hicks *et al.*, 2015). Due to the difficulties outlined, researchers have also utilised moment-driven models for sporting applications (Allen *et al.*, 2013; Felton *et al.*, 2020). Moment-driven models are based

on the moment-angle and moment-angular velocity relationships obtained from dynamometry testing. The greatest strength of this approach is that it permits subject-specific parameters for actuating the model to be determined (Yeadon *et al.*, 2006), and this is particularly important for ensuring that the results from predictive simulations are within the limits of an individual's strength. Nevertheless, this approach is limited to two-dimensional models.
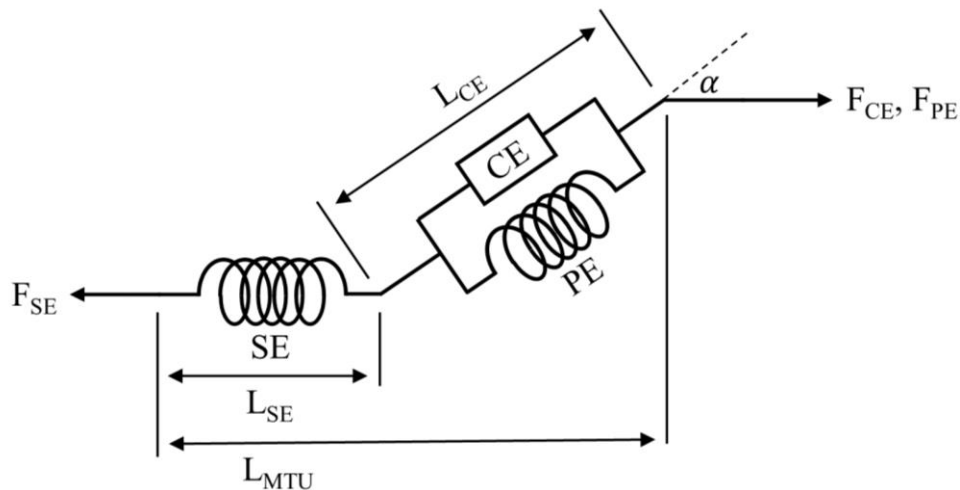
Figure 2.4–1 Schematic of the three-element equilibrium Hill muscle model, consisting of an active contractile element (CE), parallel elastic element (PE) and series elastic element (SE). α is the pennation between the orientation of the CE and SE. L_{MTU}, L_{CE} and L_{SE} are the length of the muscle, CE, and SE, respectively. F_{CE}, F_{PE} and F_{SE} are the force generated by the CE, PE, and SE, respectively.
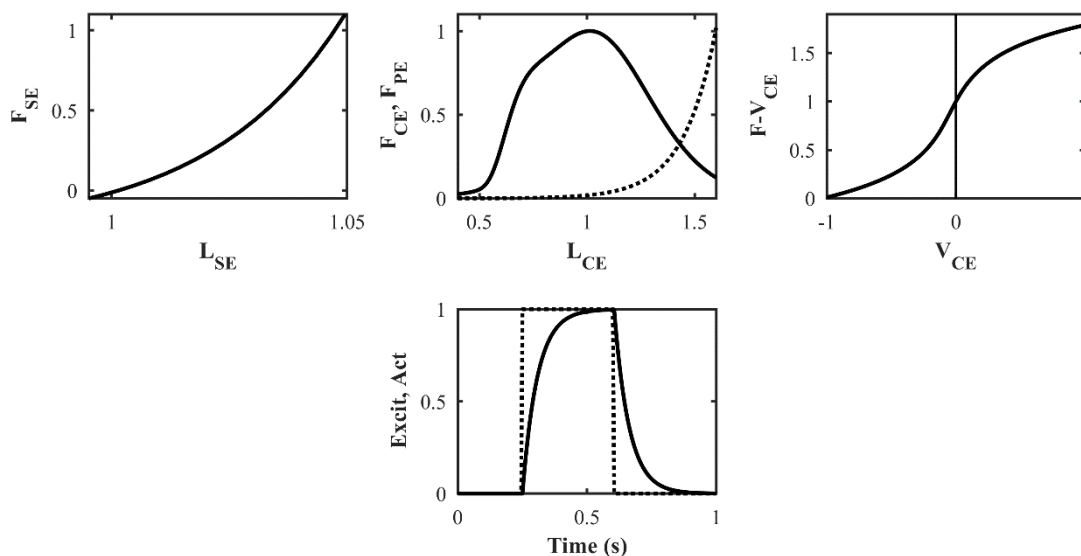
Figure 2.4–2 Characteristic curves describing the behaviour of the Hill model elements. Top left: series elastic element force (F_{SE}) and series elastic element length (L_{SE}) relationship (L_{SE} normalised to tendon slack length). Top middle: contractile element force (F_{CE}), parallel elastic element force (F_{PE}) and contractile element length (L_{CE}) relationships (solid black line represents F_{CE} and dashed black line represents F_{PE}) (L_{CE} normalised to optimum muscle fibre length). Top right: contractile element force velocity multiplier (F-V_{CE}) and contractile element velocity (V_{CE}) relationship (V_{CC} normalised by maximum shortening velocity). Bottom middle: example of the CE activation (Act; solid black) following a maximal burst of excitation (Excit; dashed black).

2.4.2 Simulation

To perform simulations of human movement, forward dynamics, a knowledge of the inputs to the model (e.g., muscle forces or accelerations) together with an integration scheme (e.g., Euler or Runge-Kutta) are needed to advance the model's dynamics equations forwards in time and determine the resulting motion. The major challenge with predictive and data-tracking simulation approaches is the determination of the inputs that lead to a plausible output. A popular approach to determine the inputs relies on the application of optimal control theory. Optimal control theory enables the inputs of a dynamical system that optimise a specified performance criterion to be determined while satisfying any constraints on the behaviour of the system. Optimal control theory can therefore be used to determine the optimal inputs for performing predictive and data-tracking simulations, for example in the predictive scenario maximising jump height or in the data-tracking scenario minimise the error between simulated and measured variables.

The numerical methods for solving optimal control problems (a simulation formulated using optimal control theory) can be divided into two classes: indirect methods and direct methods. Within the biomechanics literature, the direct methods have almost exclusively been used, as the indirect methods rely on applying the calculus of variations to determine the first-order optimality conditions for each optimal control problem, which is not feasible for problems that feature complicated models. Direct methods rely on discretising the original continuous time optimal control problem and converting it to a nonlinear optimisation or nonlinear programming problem (NLP), which can then be solved with an NLP solver (e.g., fmincon, IPOPT). Over the last 10 years within biomechanics, the direct collocation method has gained popularity. Direct collocation relies on discretising the model's control (input) and state variables, whilst direct shooting and multiple shooting only discretise the model's control variables. In the direct collocation method, the model's dynamics equations do not need to be integrated, and instead they are enforced as equality constraints (Figure 2.4–3). In contrast, the direct shooting and multiple shooting methods require the dynamics equation to be integrated, and thus they have the possibility of suffering from integration errors. The direct shooting methods, particularly single shooting, are known to struggle with simulations that feature terminal constraints, and this is a consequence of the control variables at the beginning of the simulation influencing the state variables near the end of the simulation, and thus they are highly sensitive (Betts, 2010). Conversely, the direct collocation method does not suffer from

this issue due to splitting the entire trajectory into different sections and treating each section separately.

$$\frac{x(t_6)-x(t_5)}{t_6-t_5} - f(x(t_5), u(t_5)) = 0$$

$$\frac{x(t_7)-x(t_6)}{t_7-t_6} - f(x(t_6), u(t_6)) = 0$$
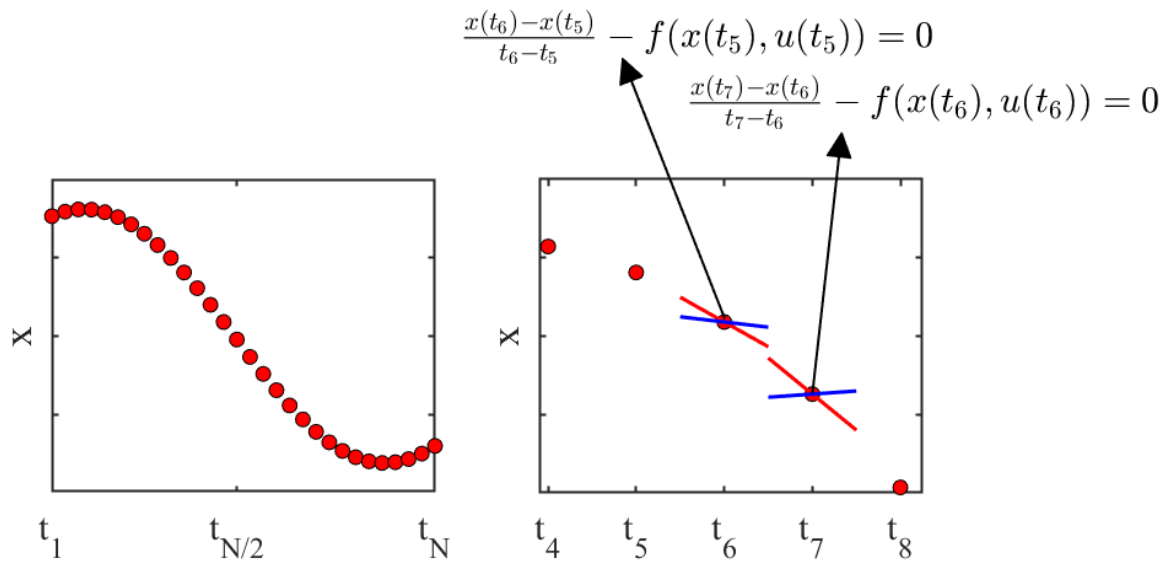
Figure 2.4–3 Schematic of direct collocation process. The left plot features an example of a discretised state variable at N mesh points at a given iteration of the NLP solver. The right plot contains the same data as in the left plot but from t_4 to t_8 and illustrates how a particular model's dynamics are enforced at each of the mesh intervals (in this case for two mesh intervals for visualisation purposes) using a forward Euler scheme.

2.5 Restatement of thesis aims

This section provides a restatement of the aims of this thesis to highlight how they relate to literature reviewed.

Study 1: Three-dimensional data-tracking simulations of sprinting using a direct collocation optimal control approach

From reviewing the sprinting biomechanics literature, it became apparent that very few studies had utilised a predictive computer simulation and modelling approach to study the influence of technique modifications on sprinting performance, despite the advantages offered by such an approach compared to conventional experimental approaches. The rise in the usage of direct collocation optimal control approaches to perform more intricate simulations within biomechanics due to their advantages over (single and multiple) shooting approaches was also highlighted. However, it was also identified that a computational modelling and simulation framework must first undergo a thorough quantitative evaluation, prior to using it to perform predictive simulations, to establish how accurately it can reproduce ground-truth data. This resulted in the following main aims for the first study:

i)   Develop a computational modelling and simulation framework for sprinting using a direct collocation optimal control approach.

ii)   Evaluate the framework's capability of reproducing experimental data by performing a series of data-tracking simulations.

The literature review also identified that the net joint kinetics determined from inverse dynamics can contain dynamic inconsistencies in the form of the residuals, however, seldom are the dynamic inconsistencies acknowledged and dealt with in sports biomechanics applications. Furthermore, the development of a computer model for performing predictive simulations of sprinting necessitates a means of modelling foot-ground interaction and identifying an appropriate set of parameters for the model of foot-ground contact. In the literature review it was discussed that performing data-tracking simulations offers a means of overcoming the dynamic inconsistencies issues and identifying the parameters of a foot-ground contact model. This led to the following secondary aims of the first study:

i)   To improve the dynamic consistency of the simulations by enforcing the pelvis residuals to be null.

ii)   To identify foot-ground contact model parameters for performing predictive simulations of sprinting.

Study 2: Modifications to the net knee moments lead to the greatest improvements in accelerative sprinting performance: a predictive simulation study

From reviewing the literature, accelerative sprinting performance emerged as been of significance to track and field athletes and team-based sports athletes. Furthermore, it was also recognised that the sprinting biomechanics literature contains numerous kinematics- and kinetics-based technique recommendations for improving performance from cross-sectional studies, however very few studies have explored how technique changes influence performance on an individualised basis. It was recognised that a predictive computer simulation and modelling approach was ideal for carrying out such research. Lastly, the primary sprinting coaching framework (front-side mechanics) was discussed, however it was recognised that minimal evidence currently exists to either support or reject it. This subsequently led to the following main aims for the second study:
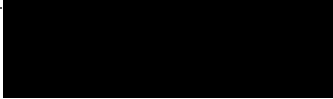
i)   Explore how hypothetical modifications in technique influence accelerative sprinting performance.

ii)   Investigate how the modifications mirrored the theories of an existing sprinting coaching framework (front-side mechanics).

Chapter 3
Three-dimensional data-tracking simulations of sprinting using a direct collocation optimal control approach

3.1 Abstract

Biomechanical simulation and modelling approaches have the possibility to make a meaningful impact within applied sports settings, such as sprinting. However, for this to be realised, such approaches must first undergo a thorough quantitative evaluation against experimental data. We developed a musculoskeletal modelling and simulation framework for sprinting, with the objective to evaluate its ability to reproduce experimental kinematics and kinetics data for different sprinting phases. This was achieved by performing a series of data-tracking calibration (individual and simultaneous) and validation simulations using a direct collocation optimal control approach, that also featured the generation of dynamically consistent simulated outputs and the determination of foot-ground contact model parameters. The simulated values from the calibration simulations were found to be in close agreement with the corresponding experimental data, particularly for the kinematics (average root mean squared differences (RMSDs) less than $1.0°$ and 0.2 cm for the rotational and translational kinematics, respectively) and ground reaction force (GRF) (highest average percentage RMSD of 8.1%). Minimal differences in tracking performance were observed when concurrently determining the foot-ground contact model parameters from each of the individual or simultaneous calibration simulations. The validation simulation yielded results that were comparable (RMSDs less than $1.0°$ and 0.3 cm for the rotational and translational kinematics, respectively) to those obtained from the calibration simulations. This study demonstrated the suitability of the proposed framework for performing future predictive simulations of sprinting, and gives confidence in its use to assess the cause-effect relationships of technique modification in relation to performance. Furthermore, this is the first study to provide dynamically consistent three-dimensional muscle-driven simulations of sprinting across different phases.

This declaration concerns the article entitled:									

Chapter 3 Three-dimensional data-tracking simulations of sprinting using a direct collocation optimal control approach

Publication status (tick one)

Draft manuscript		Submitted		In review		Accepted		Published	✖

Publication details (reference)	Haralabidis, N., Serrancolí, G., Colyer, S., Bezodis, I., Salo, A. & Cazzola, D. (2021). Three-dimensional data-tracking simulations of sprinting using a direct collocation optimal control approach. *PeerJ,* **9**, e10975. DOI: https://doi.org/10.7717/peerj.10975

Copyright status (tick the appropriate statement)

I hold the copyright for this material	✖	Copyright is retained by the publisher, but I have been given permission to replicate the material here	

Candidate's contribution to the paper (provide details, and also indicate as a percentage)	The candidate considerably contributed to and predominantly executed the: **Formulation of ideas: 80%** NH was responsible for carrying out the background research, devising the aims of the study and presenting the idea to supervisors and co-investigators. **Design of methodology: 75%** NH was primarily responsible for selecting the simulation approach used (direct collocation optimal control) and adapting/modifying aspects of the simulation approach originally developed by GS. NH was the main contributor in terms of designing the simulations. **Experimental work: 65%** NH was responsible for liaising with laboratory technicians to ensure the data collection environment had the necessary equipment and software installed. NH played a major role in designing the experimental protocol and processing the acquired experimental data used for this study. **Formal data analysis: 85%** NH setup and carried out the computational simulations and was primarily responsible for the analysis of the simulation results. **Presentation of data in journal format: 80%** NH wrote the first draft of the manuscript, carried out draft revisions, submitted the manuscript to the journal and made the amendments necessary for publication.
Statement from Candidate	This paper reports on original research I conducted during the period of my Higher Degree by Research candidature.
Signed	███████████	Date	25/10/2021

3.2 Introduction

Sprinting is the fastest mode of human bipedal locomotion, and the short distance events (60-400 m) in modern athletics provide a means of assessing the limits of human sprinting performance. The objective for athletes competing within these events is to cover the set distance in the shortest possible time, and often the winning margin is hundredths of a second at the highest levels of competition. Coaches and athletes are therefore continually striving for improvements in technique which can enhance overall performance by such fine margins. Sprinting also plays an important role within team-based sports. For instance, sprinting has been shown to be pivotal in creating goal scoring opportunities within soccer (Faude *et al.*, 2012). Thus, the insights from further understanding sprinting technique and performance can have far reaching applications, as they can also be transferred to benefit performance in other sports.

Most studies to date have advanced the knowledge of how to improve sprinting performance by assessing the ground reaction force (GRF) (Colyer *et al.*, 2018a; Morin *et al.*, 2011), joint kinematics and kinetics (Bezodis *et al.*, 2008a; Schache *et al.*, 2019; Smith *et al.*, 2014), and spatiotemporal parameters (Hunter *et al.*, 2004a; Salo *et al.*, 2011). The studies focusing on joint kinetics (net joint moments, power, and work) potentially bear the most significance, as they can explain the causes of motion. However, the net joint moments calculated from inverse dynamics analyses (IDA) are known to be impacted by several factors (Derrick *et al.*, 2020) (e.g., filtering and soft-tissue artefact), and necessitate fictitious residual forces and moments to be applied at the model's root segment (e.g., pelvis) due to dynamic inconsistencies. These residuals are further exacerbated during explosive tasks, such as sprinting, where experimental errors and modelling assumptions are likely to become more critical. Methods such as the residual reduction algorithm (RRA) within OpenSim (Delp *et al.*, 2007) and optimal control approaches (Lin and Pandy, 2017; Meyer *et al.*, 2016; Pallarès-López *et al.*, 2019) have been introduced to compensate for the residuals, although they have not seen widespread adoption within the sports biomechanics literature. Furthermore, within the sports biomechanics literature these residuals are typically neglected, raising questions on the errors in IDA and the validity of the corresponding findings.

A further limitation within the current body of sprinting literature is that most studies have focused on identifying key aspects of technique from group level analyses. It is possible that the technique-based findings from group level analyses can be transferred to benefit the

performance levels of elite athletes. However, individualised technique modifications are more likely to be necessary for elite athletes to further improve their performance levels by the sought-after small margins. Furthermore, the existing literature provides various technique related factors associated with improved sprinting performance, as opposed to how specific technique modifications influence sprinting performance. Predictive computer simulation and modelling approaches within sports biomechanics can be used to overcome the aforementioned limitations, as they can be used to identify optimum technique on an individualised basis, explore cause-effect relationships, and assess 'what-if' scenarios (Neptune, 2000).

Recently, there has been a noticeable increase in the number of modelling and simulation studies within sports biomechanics adopting an optimal control theory approach (Jansen and McPhee, 2020; Lin and Pandy, 2017; Porsa *et al.*, 2016), also specifically within sprinting (Celik and Piazza, 2013; Schultz and Mombaur, 2010). Celik and Piazza (2013) found that their optimised solution of sprinting demonstrated several salient features that have been observed experimentally (e.g., forward trunk lean during early acceleration), although their model lacked a sufficient representation of the lower-limbs to adequately characterise their actions. Conversely, Schultz and Mombaur (2010) developed a three-dimensional model, and used it in an exploratory sense to determine the feasibility of performing predictive sprinting simulations. However, a limitation common to both of these studies is that they did not explicitly evaluate their outputs against experimental data.

The evaluation of a modelling and simulation framework is needed to ensure that it is fit for its purposes and produces realistic results (Yeadon and Challis, 1994). Furthermore, within applied sports contexts the evaluation step is necessary to ensure that the results from predictive simulations can be transferred with confidence to drive real world changes. To conduct the evaluation step, data-tracking simulations using optimal control theory can be performed (Umberger and Miller, 2017), as they provide the opportunity to quantitatively determine how a modelling and simulation framework performs at reproducing experimental data. In addition, a major benefit of optimal control based data-tracking simulations is that they provide an elegant approach to improve the dynamic consistency of a simulation by either minimising or constraining the residuals, particularly when used with the direct collocation method (Lin and Pandy, 2017; Meyer *et al.*, 2016; Pallarès-López *et al.*, 2019). To date, however, no study has attempted to use this approach within a highly demanding sporting movement, such as sprinting.

Lastly, predictive simulations of sprinting necessitate a means of modelling the foot-ground interaction. One popular approach relies on distributing a finite set of contact elements across the surface of a foot and using a compliant foot-ground contact model to calculate the contact forces at each element (Dorschky *et al.*, 2019; Falisse *et al.*, 2019a; Falisse *et al.*, 2019b; Gilchrist and Winter, 1996; Lin and Pandy, 2017; Serrancolí *et al.*, 2019). The difficulty with using this approach is determining the foot-ground contact model parameters. Previous studies have obtained the foot-ground contact model parameters by fitting their model to mechanical testing data (Dorschky *et al.*, 2019; Miller and Hamill, 2015), thus the values of the parameters can be used by further studies. However, the use of previously published foot-ground contact model parameter values can be problematic due to the differences in the formulations and constitutive laws between compliant foot-ground contact models. It is also possible to determine the values of the foot-ground contact model parameters by manually tuning them (Gilchrist and Winter, 1996), although this approach can be challenging to implement due to the nonlinear interactions of the parameters. An alternative approach is to perform data-tracking simulations, as they enable the foot-ground contact model parameter values to be determined in addition to the evaluation of a modelling and simulation framework (Falisse *et al.*, 2019a; Serrancolí *et al.*, 2019). When using the latter approach, care must be taken to ensure that the parameters obtained are not unrealistic and overfit, particularly if they are determined from tracking a single trial. Consequently, further independent data-tracking simulations using the obtained foot-ground contact model parameters must be performed to ensure that they lead to simulated outputs that closely resemble the experimental data, and to provide confidence for their use within predictive simulations.

The main aims of this study were to develop a musculoskeletal modelling and simulation framework for sprinting, and to evaluate its capability of reproducing experimental data (GRF, kinematics, kinetics, and electromyograms – EMGs) by performing data-tracking simulations. The secondary aims of this study were to improve the dynamic consistency of the simulated outputs by enforcing the residuals to be zero, thus further highlighting the advantages of the approach used, and to identify foot-ground contact model parameters such that they can be used within future predictive simulations of sprinting.

3.3 Methods

3.3.1 Experimental data collection

An international-level male sprinter (age: 24 years; height: 1.79 m; mass: 72.2 kg; 100 m PB: 10.33 s; 200 m PB: 20.27 s) provided written informed consent to participate in the current study. Ethical approval for this study was obtained from the University of Bath's Research Ethics Approval Committee for Health (EP 17/18 238). The data collection took place at the National Indoor Athletics Centre in Cardiff, UK (Figure 3.3–1). The protocol required the athlete to perform a series of maximal sprinting trials whilst GRF, three-dimensional marker trajectories and EMGs were recorded.
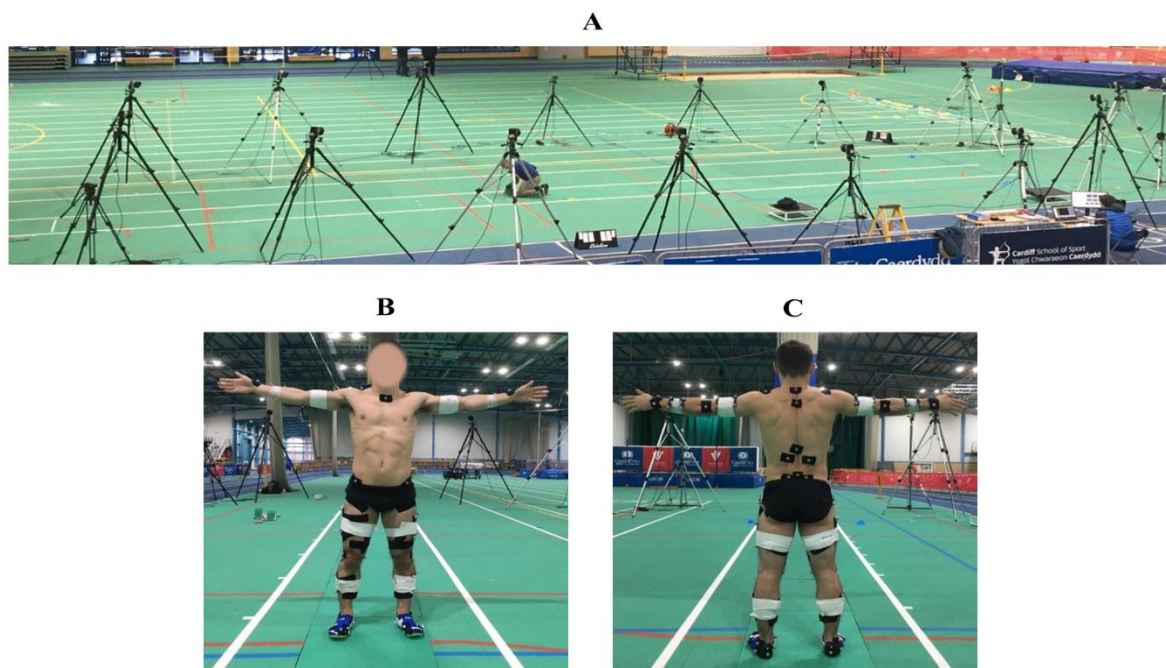
Figure 3.3–1 Experimental data collection setup (A), and placement of retro-reflective markers, acrylic clusters, and EMG electrodes (B and C). The force plates setup provided a 4.5 m segment of the track to capture GRF, and this permitted GRF data from a minimum of two successive steps to be captured for each trial. The calibrated motion capture volume covered 9.5 (length) $\times$ 1.5 (width) $\times$ 2 (height) m^3.

Five force plates ($\times$ 4 type: 9287CA and $\times$ 1 type 9282BA, Kistler, Switzerland) were used to collect GRF at a sampling frequency of 2000 Hz. Three-dimensional marker trajectories were recorded using a 15-camera motion capture system (Qualisys AB, Sweden) sampling at 250 Hz. The motion capture system was positioned on either side of the track segment which enclosed the force plates. Forty-nine retro-reflective markers were attached to the surface of the athlete's skin and shoes using double-sided adhesive and medical tapes (Figure 3.3–1). Eight acrylic marker clusters were also attached to the athlete using double-sided adhesive tape

and medical bandages. Six wireless surface electrodes (Trigno Avanti, Delsys Inc., Boston, MA, USA) sampling at 2000 Hz with a 20-450 Hz bandwidth were used to record EMGs from the following right lower-limb muscles of the athlete: gluteus maximus (GMAX), biceps femoris (BF), medial gastrocnemius (GASTM), tensor fasciae latae (TFL), vastus medialis (VM) and soleus (SOL). The skin preparation and placement of the electrodes was in accordance with previously published guidelines (Hermens *et al.*, 2000).

The data collection commenced with a standing static trial of the athlete being captured. The athlete then performed two successful maximal effort sprints over three distances (0-10, 0-30 and 0-60 m) following the completion of a self-led warm up. The chosen distances covered the three conventional phases (early acceleration, mid-acceleration and maximum velocity) of short distance sprinting events. Different starting positions, relative to the first force plate, were used to enable the sprinter to contact the force plates between 0-5, 10-15 and 45-50 m for each of the distances. A trial was deemed successful if the athlete's entire foot landed within the boundaries of a single force plate whilst not noticeably altering their step. A rest period of up to 10 minutes between each sprint was given to the athlete. Each sprint was initiated by standard '*on your marks*' and '*set*' commands by a member of the research team. The researcher then pressed a trigger button that provided an auditory sound signal through a sounder device (Wee Beastie Ltd, UK), and this also triggered the synchronous acquisition of GRF, three-dimensional marker trajectories and EMGs through Qualisys Track Manager (version 2018.1, Qualisys AB, Sweden).

3.3.2 Model

We started with a generic three-dimensional full-body musculoskeletal OpenSim model (Hamner *et al.*, 2010) (Figure 3.3–2) that had been previously used for applications in sprinting (Dorn *et al.*, 2012; Lai *et al.*, 2016). The original model represented the human skeleton as a multibody system comprising 20 rigid segments and 29 degrees-of-freedom (DOFs). We added DOFs for subtalar inversion-eversion, metatarsophalangeal (MTP) dorsiflexion-plantarflexion, and wrist flexion-extension and adduction-abduction. The configuration of the modified model was uniquely described by a set of generalised coordinates $q \in \mathbb{R}^{37}$, with each DOF being represented by a generalised coordinate. The modified model's 37 DOFs were as follows: 6 DOFs ground-to-pelvis joint, 3 DOFs hip joints, 1 DOF knee joints, 1 DOF ankle joints, 1 DOF

subtalar joints, 1 DOF MTP joints, 3 DOFs back joint, 3 DOFs shoulder joints, 2 DOFs elbow joints and 2 DOFs wrist joints.

The generic modified model was linearly scaled to match the anthropometric and inertial characteristics of the athlete by using a measurement-based approach within OpenSim. Scaling factors for each segment were calculated using the relative distances between markers placed over anatomical landmarks recorded in the static trial and corresponding virtual markers which were placed on the modified generic model. A combination of uniform and non-uniform scaling factors were used to scale the properties of each segment, and the lower- and upper-limbs were scaled to maintain bilateral symmetry.
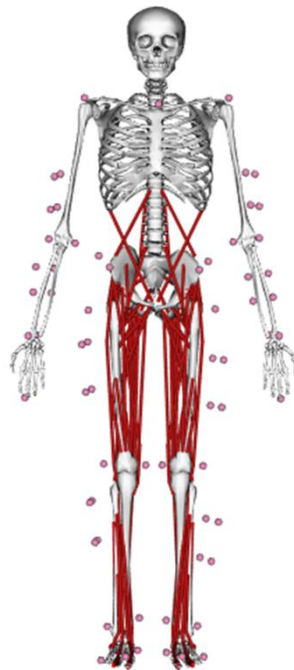
Figure 3.3–2 Three-dimensional musculoskeletal model (Hamner *et al.,* 2010) used in the current study. The same model was used to determine experimental kinematics and kinetics from inverse kinematics and dynamics analyses, respectively, and perform data-tracking simulations. The virtual model markers are denoted by pink spheres.

The upper-limbs were actuated by 14 joint actuators whose limits were set based upon the IDA results. The lower-limbs and trunk were actuated by 92 Hill-type muscle-tendon units (MTUs), and we used the dimensionless characteristic equations presented by De Groote *et al.* (2016) to describe the active and passive (series and parallel) components of force generation for each MTU. Five parameters are used to scale the dimensionless characteristic equations of Hill-type models for a specific MTU: pennation angle at optimum fibre length, optimum fibre length, tendon slack length, maximum shortening velocity and maximum isometric force. In our case

we used the pennation angle at optimum fibre length parameters reported in the generic model, whilst we used the optimum fibre length and tendon slack length parameters obtained following the scaling of our model. The scaling procedure updated those parameters while preserving the ratio between them from the generic model. We set the maximum shortening velocity parameter of all the MTUs to be 12 optimal fibre lengths per second based upon an *in vivo* estimate of the maximum shortening velocity of human muscle (De Ruiter *et al.*, 2000). The maximum isometric force parameters were set to be two times greater than those reported within the generic model, and this enabled the MTUs of the lower-limbs DOFs, except the MTP DOFs, to exert net moments that more closely reflected the training status of our athlete. For example, the four MTUs responsible for extension of the knee DOF had the capacity to exert an isometric net moment that was approximately 18% greater than reported by Erskine *et al.* (2011) for a group of untrained individuals following 9 weeks of resistance training. We also included reserve actuators for each of the lower-limb and trunk DOFs. The upper limits of the reserve actuators for the MTP DOFs and the remaining lower-limb and trunk DOFs were set to 40 and 10 Nm, respectively. The reserve actuators for the MTP DOFs were set with a higher upper limit such that together with the four MTUs spanning each of the MTP DOFs they had the capacity to produce net MTP moments that were in a similar range to those reported from isometric dynamometry testing (Goldmann *et al.*, 2013). To account for the behaviour of the athlete's sprinting spikes and the passive structures surrounding the MTP DOFs we included a simple linear rotational spring. The stiffness of the rotational spring was set to 65 Nm/rad by combining the rotational stiffness of sprinting spikes/sports shoes (Oh and Park, 2017; Toon *et al.*, 2006) with the rotational stiffness used previously for representing the passive structures surrounding the MTP DOFs (Sasaki *et al.*, 2009).

Polynomials were used to describe the lengths, velocities and moment arms of the MTUs as functions of the model's generalised coordinates and velocities (Falisse *et al.*, 2019a). The coefficients of the polynomials were determined by fitting them to the lengths and moment arms of the scaled model's MTUs, which were obtained by performing a Muscle Analysis within OpenSim for a wide range of generalised coordinates values. We opted to describe the lengths, velocities and moment arms of the MTUs with differentiable and continuous polynomial functions as they are ideally suited to the gradient-based optimal control approach we used.

The aerodynamic drag force within sprinting is known to have an influence on overall performance (Quinn, 2003), even when analysing performance across multiple steps with zero wind velocity (Colyer *et al.*, 2018a). To account for the aerodynamic drag force we used the approach presented by Samozino *et al.* (2016), and for this study we assumed that the wind velocity was zero as the experimental data collection took place in an indoor athletics centre. The aerodynamic drag force was applied to the pelvis segment, specifically at the model's CoM position expressed in the local frame of the pelvis segment. We opted to apply the aerodynamic drag force to the pelvis segment as this segment was the closest to the model's CoM position when visualised within the OpenSim graphical user interface for the trials processed.

3.3.3 Data processing & analysis

An open-source MATLAB toolbox (https://simtk.org/projects/matlab_tools) was used to convert the raw data into the file formats compatible with OpenSim (version 3.3, Stanford University, CA,USA) (Delp *et al.*, 2007). For the purposes of this study we used experimental data that spanned an arbitrary right foot stance phase alongside portions of the flight phases prior to touchdown and after take-off from the first early acceleration and mid-acceleration phase trials and from both the maximum velocity phase trials. Touchdown and take-off were determined using a 20 N vertical GRF threshold. The analysed flight phases were identified by searching within the vertical GRF signal 50 frames backwards and forwards from touchdown and take-off, respectively, to then identify the frames which most closely coincided with the sampling intervals of the motion capture system.

Global pelvis and relative joint kinematics for each trial were determined by performing inverse kinematics analyses within OpenSim from the recorded marker trajectories. The kinematics and GRF were filtered using a common 20 Hz fourth-order low-pass Butterworth filter. The cut-off frequency was determined by performing a residual analysis on the kinematics obtained from the inverse kinematics analyses (Winter, 2009). The filtered kinematics were also fitted using B-splines to enable velocities and accelerations to be determined. Net joint moments and pelvis residuals were calculated for each trial by performing IDA using the OpenSim C++ application programming interface. The splined kinematics, net joint moments and filtered GRF served as the experimental data to be tracked within the data-tracking simulations.

The EMGs from each trial were full-wave rectified and filtered at 20 Hz using a fourth-order low-pass Butterworth filter. We selected the cut-off frequency based on previous studies which

assessed EMGs during running and sprinting (Santuz *et al.*, 2020; Yong *et al.*, 2014). Each filtered EMG was normalised to the maximum filtered amplitude of the respective EMG from within all the trials processed. Following the collection of the mid-acceleration and maximum velocity phase trials we noticed that the TFL and SOL electrodes, respectively, became detached from the surface of the athlete's skin, consequently we excluded the TFL and SOL EMG from those trials during data processing and further analysis.

3.3.4 Optimal control problem formulation

The data-tracking simulations (calibration and validation) were formulated as optimal control problems (OCPs). The objective of the data-tracking simulations was to determine the state x and control u variables (plus the foot-ground contact model parameters p for the calibration simulations), that resulted in tracking the experimental data as closely as possible, while satisfying our model's constraints.

The skeletal dynamics of our musculoskeletal model (Figure 3.3–2) were described by a collection of 37 coupled second-order nonlinear differential equations. The contraction and activation dynamics of each MTU were described by two first-order nonlinear differential equations (De Groote *et al.*, 2016; Zajac, 1989). Four state variables ($x = [q\ v\ F_T\ a]$, where q and v are the scaled musculoskeletal model's generalised coordinates and velocities, respectively, and F_T and a are the MTU normalised tendon forces and activations, respectively) were selected to enable the skeletal, contraction and activation dynamics to be represented as a system of first-order differential equations. We also included control variables for the upper-limb joint actuators u_{UL} and the reserve actuators u_{RES} that defined the instantaneous moment those actuators could produce.

We formulated the differential equations governing skeletal and contraction dynamics implicitly (Falisse *et al.*, 2019a) by introducing additional control variables for the time derivatives of the generalised velocities $u_{\dot{v}}$ and normalised tendon forces $u_{\dot{F}_T}$. The implicit formulation led to enforcing the first-order skeletal and contraction dynamics with simple constraints, and additional nonlinear equality path constraints were used to ensure the skeletal and contraction dynamics equations were enforced. Two sets of equality path constraints were used to enforce the skeletal dynamics equations of our model's 37 DOFs. The first set enforced that the pelvis residuals (moments and forces at the 6 pelvis DOFs) obtained from evaluating

the skeletal dynamics equations were zero. The second set enforced that the net joint moments (moments at the 31 relative DOFs) obtained from evaluating the skeletal dynamics equations matched with those obtained from the actuators. The inclusion of the control variables for the upper-limb actuators was not mandatory since we used idealised upper-limb actuators together with an implicit skeletal dynamics formulation. For the contraction dynamics equations we imposed equality path constraints to enforce the Hill-equilibrium condition (the normalised tendon force matched the projected normalised muscle force).

The differential equation describing activation dynamics was also formulated implicitly using the approach presented by De Groote *et al.* (2009), and we introduced additional control variables for the time derivatives of the activations $\boldsymbol{u}_{\dot{a}}$. This again led to enforcing the first-order activation dynamics with simple constraints, and we enforced the activation dynamics equations by imposing two sets of linear inequality path constraints. These constraints can be derived from the original differential equation describing activation dynamics by using the upper and lower bounds of the excitations, which are often used as control variables. By formulating the activation dynamics in this manner we avoided the need to include excitations as control variables, and the resulting path constraints possessed favourable optimisation properties as they were linear.

For the purposes of modelling foot-ground interaction we attached four and two contact spheres to our model's right rearfoot and forefoot segments, respectively. The GRF generated by each of the contact spheres was based on a smooth foot-ground contact model (Serrancolí *et al.*, 2019). The smooth foot-ground contact model was designed to be compatible with gradient-based optimal control approaches and is an approximation of a previously published foot-ground contact model (Sherman *et al.*, 2011). The equations used to calculate the normal and friction forces for the smooth foot-ground contact model can be accessed online at https://simbody.github.io/3.7.0/classSimTK_1_1SmoothSphereHalfSpaceForce.html. The position of each contact sphere relative to the segment it was attached to, and the stiffness and damping coefficients common to all the contact spheres were treated as parameters $\boldsymbol{p}$ to be determined from the data-tracking calibration simulations. A constraint was added to ensure that the contact spheres lie on a horizontal plane when the ankle, subtalar and MTP DOFs were neutral. We used the default parameters for the constants responsible for smoothing the penetration and penetration rate terms, and the constant that enforces the derivative of the penetration term to be non-zero. For each contact sphere, the static, dynamic and viscous

coefficients of friction were set to 0.95, 0.3 and 0.3, respectively, and the transition velocity and radius were set to 0.001 m/s and 0.02 m, respectively. We also introduced GRF control variables $\boldsymbol{u_{GRF}}$ for each of the contact spheres, similarly to Serrancolí *et al.* (2019). GRF control variables were introduced to improve the conditioning of the objective function, as the GRF computed from the contact model is susceptible to large changes with only minor changes in the musculoskeletal model's state variables, which can lead to convergence issues. Equality path constraints were included to ensure the GRF from both the control variables and the contact model matched at the optimal solution.

The objective function J consisted of three terms: a data-tracking term $J_{tracking}$ that minimised the squared errors between the experimental and simulated kinematics, GRF and net joint moments, an effort term J_{effort} that minimised the squared activations, and a control variables term $J_{control}$ that minimised the squared reserve actuators control variables and those control variables introduced due to the use of the implicit differential equations:

$$J = J_{tracking} + J_{effort} + J_{control} \tag{1}$$

$$J_{tracking} = w_1 \sum_{j=1}^{37} \int_{t_0}^{t_f} \left(\frac{q_j^{EXP} - q_j^{SIM}}{range(q_j^{EXP})} \right)^2 dt + w_1 \sum_{n=1}^{3} \int_{t_0}^{t_f} \left(\frac{GRF_n^{EXP} - u_{GRF_n}^{SIM}}{range(GRF_n^{EXP})} \right)^2 dt$$
$$+ w_2 \sum_{k=1}^{29} \int_{t_0}^{t_f} \left(\frac{\tau_k^{EXP} - \tau_k^{SIM}}{range(\tau_k^{EXP})} \right)^2 dt \tag{2}$$

$$J_{effort} = w_3 \sum_{i=1}^{92} \int_{t_0}^{t_f} \left(\frac{F_i^{max} a_i^{SIM^2}}{\sum_{i=1}^{92} F_i^{max}} \right) dt \tag{3}$$

$$J_{control} = w_4 \sum_{m=1}^{17} \int_{t_0}^{t_f} \left(\frac{u_{res_m}^{SIM}}{bound(u_{res_m}^{SIM})} \right)^2 dt + w_5 \sum_{j=1}^{37} \int_{t_0}^{t_f} \left(\frac{u_{\dot{v}_j}^{SIM}}{range(\ddot{q}_j^{EXP})} \right)^2 dt$$
$$+ w_5 \sum_{i=1}^{92} \int_{t_0}^{t_f} \left(\frac{u_{\dot{F}_{T_i}}^{SIM}}{bound\left(u_{\dot{F}_{T_i}}^{SIM}\right)} \right)^2 dt + w_5 \sum_{i=1}^{92} \int_{t_0}^{t_f} \left(\frac{u_{\dot{a}_i}^{SIM}}{bound(u_{\dot{a}_i}^{SIM})} \right)^2 dt \tag{4}$$

where the superscripts *EXP* and *SIM* denote experimental and simulated variables, respectively, t_0 and t_f denote the initial and final times, respectively, of the experimental data

from the trial being tracked, τ_k are the net joint moments, F_i^{max} are the MTU maximal isometric force parameters, and w_i are the weighting factors whose values were set based upon the importance of the term being tracked or minimised ($w = [0.1\ 0.01\ 0.001\ 0.01\ 0.0001]$).

The objective function weighting factors were chosen heuristically, and we placed a greater emphasis on tracking the variables we believed were closer to the ground-truth (kinematics and GRF) whilst ensuring we obtained dynamically consistent solutions. To achieve those objectives it was necessary to place a lower weighting on the tracking of the net joint moments. Furthermore, we opted to not include the tracking of the net MTP moments, as we were not confident in the values obtained from IDA. We included the minimisation of the control variables introduced due to the use of the implicit differential equations with a very small weighting factor to avoid redundancy in the process of obtaining an optimal solution and to improve convergence. The experimental and simulated variable differences within $J_{tracking}$, except for the anterior-posterior pelvis translation difference, and the time derivatives of the generalised velocities control variables were each normalised by 10% of their respective experimental range from the trial being tracked. The anterior-posterior pelvis translation difference was normalised by 0.01 m to ensure it was tracked closely, since the range was much greater in comparison to the other kinematic variables. The remaining variables within $J_{control}$ were normalised by their respective upper bounds.

3.3.5 Optimal control problem solution approach

We converted the data-tracking OCPs described in the previous section to discrete nonlinear programming problems (NLPs) using a direct collocation method. A *flipped* Legendre-Gauss-Radau direct collocation method (Garg *et al.*, 2011) was used to discretise the time horizon of the data-tracking simulations across 80 equally spaced mesh intervals, and each mesh interval was further discretised with 4 points. We set the number of mesh intervals based on a previous study that performed tracking simulations of a running stride using a direct collocation method (Lin and Pandy, 2017), and by considering the trade-off between the time taken for an optimal solution to be reached and the influence of discretising the experimental data to be tracked for different numbers of mesh intervals. The state variables were parameterised with third-order Lagrange polynomials within each mesh interval. The control variables were parameterised at the beginning of each mesh interval and assumed to be piecewise constant throughout a mesh interval. The first-order dynamics constraints were enforced at the collocation points, whilst all

the equality and inequality path constraints were enforced at the beginning of each mesh interval. We also included continuity constraints for the state variables between the ending and beginning of the mesh intervals.

Four data-tracking calibration simulations were performed in total. Three of these calibration simulations featured tracking experimental data from the first trial of each of the sprinting phases (early acceleration, mid-acceleration and maximum velocity) independently whilst also determining the foot-ground contact model parameters (individual calibration simulations). In the fourth calibration simulation we tracked the experimental data from the same three trials simultaneously whilst also determining the foot-ground contact model parameters that were common across the trials (simultaneous calibration simulation). A data-tracking validation simulation was also performed, and we tracked the experimental data from the second maximum velocity phase trial whilst using the foot-ground contact model parameters obtained from the simultaneous calibration simulation. We selected to track the experimental data from the second maximum velocity phase trial for the validation simulation to demonstrate the worst-case scenario from a tracking perspective, as we noticed that the largest tracking errors for the calibration simulations were obtained from the first maximum velocity phase trial.

For each simulation, the initial guess alongside the lower and upper bounds of the state and control variables were set using the experimental data of the trial being tracked where possible. The generalised coordinates and velocities state variables, and the time derivatives of the generalised velocities control variables were initialised using the splined experimental kinematics. The initial guess for the upper-limb joint actuators control variables was set using the results from IDA. The reserve actuators and GRF control variables were initialised as zero for all the simulations. We used the same initial guess as Falisse *et al.* (2019a) for the activations and normalised tendon forces state variables, and the derivatives of the activations and normalised tendon forces control variables for all the simulations. The stiffness and damping parameters for the initial guess were set to 1e6 N/m^2 and 0.5 s/m, respectively, while the contact sphere position parameters were initialised so that they cover a plausible region of foot-ground contact during sprinting.

The lower and upper bounds of the state and control variables pertaining to the skeletal dynamics were set to be 25% less than and more than the minimum and maximum values, respectively, obtained from the experimental data. We set the lower and upper bounds of the

variables pertaining to contraction and activation dynamics in accordance with those used by Falisse *et al.* (2019a). The bounds of the anterior-posterior and medial-lateral positions of the contact sphere parameters were set as to prevent the centres of the spheres from overlapping and to lie within the boundaries of the rearfoot and forefoot segments. The upper bounds of the vertical positions of the contact sphere parameters were set to be the origin of the rearfoot and forefoot segments, whilst the lower bounds of those parameters were set by accounting for length of the spikes attached to athlete's sprinting spikes, the sole height of the sprinting spikes and the behaviour of the compliant foot-ground contact model. The lower and upper bounds of the stiffness and damping parameters were set in line with those reported by previous studies using similar foot-ground contact models (Falisse *et al.*, 2019a; Lin and Pandy, 2017; Porsa *et al.*, 2016; Serrancolí *et al.*, 2019).

The data-tracking simulations were formulated in MATLAB (2016b, MathWorks Inc., Natick, MA, USA) using CasADi (Andersson *et al.*, 2019), and solved using IPOPT (Wächter and Biegler, 2006) with an adaptive barrier parameter strategy and NLP convergence tolerance of 10^{-4}. For each NLP, the variables were scaled to lie on the interval [-1,1] and we also scaled the constraints following the recommendations made by Betts (2010) to improve the convergence rate and numerical conditioning. As an example, the equality path constraints of the pelvis residual forces were scaled by the athlete's bodyweight (BW), thus the largest permissible violation for these constraints was 0.0071 N given our NLP convergence criteria. To further increase the computational efficiency of our simulations we used modified versions of OpenSim and Simbody (Falisse *et al.*, 2019a) for the purposes of evaluating the skeletal dynamic equations. These versions are interfaced with CasADi, which permits the calculation of derivatives using algorithmic differentiation. To evaluate the data-tracking simulations we calculated the root mean squared difference (RMSD) between the tracked experimental and simulated data. For each of the RMSDs reported below we calculated the average RMSD for categories of variables (e.g., global pelvis angles and net lower-limb joint moments), and for the calibration simulations those categorical RMSDs were averaged across the three trials. The GRF RMSD components were expressed relative to the athlete's BW and as a percentage relative to the maximum absolute value of the GRF component obtained experimentally for the trial being tracked. As a further means of evaluating the data-tracking simulations, the filtered EMGs were compared to the corresponding simulated activations.

3.4 Results

The kinematics and GRF obtained from all the data-tracking simulations were a close match with the experimental kinematics (Figures 3.4–1, 3.4–2 and 3.4–3) and GRF (Figures 3.4–4 and 3.4–5). For both sets of calibration simulations, the average RMSDs were less than 1° and 0.2 cm for the global pelvis angles and translations, respectively, and 1° for the relative joint angles (Table 3.4–1). Right ankle plantarflexion-dorsiflexion tended to exhibit the largest RMSD across each of the three trials and for both sets of calibration simulations (4.0° largest RMSD). For the validation simulation, the average RMSDs were less than 1° and 0.3 cm for the global pelvis angles and translations, respectively, and 1° for the relative joint angles. The largest kinematics tracking error for the validation simulation was also obtained for right ankle plantarflexion-dorsiflexion (5.5° RMSD).

For the GRF components, the average percentage RMSDs for both sets of calibration simulations (individual and simultaneous) were 8.2% and 8.0% (anterior-posterior), 4.2% and 4.1% (vertical), and 4.2% and 4.0% (medial-lateral). There was a noticeable trend for the tracking errors of the GRF components to increase from the early acceleration to the mid-acceleration trials and from the mid-acceleration to maximum velocity trials for both sets of calibration simulations (Table 3.4–1). For the validation simulation, the percentage RMSDs of the GRF components were 11.4% (anterior-posterior), 5.9% (vertical) and 7.5% (medial-lateral).
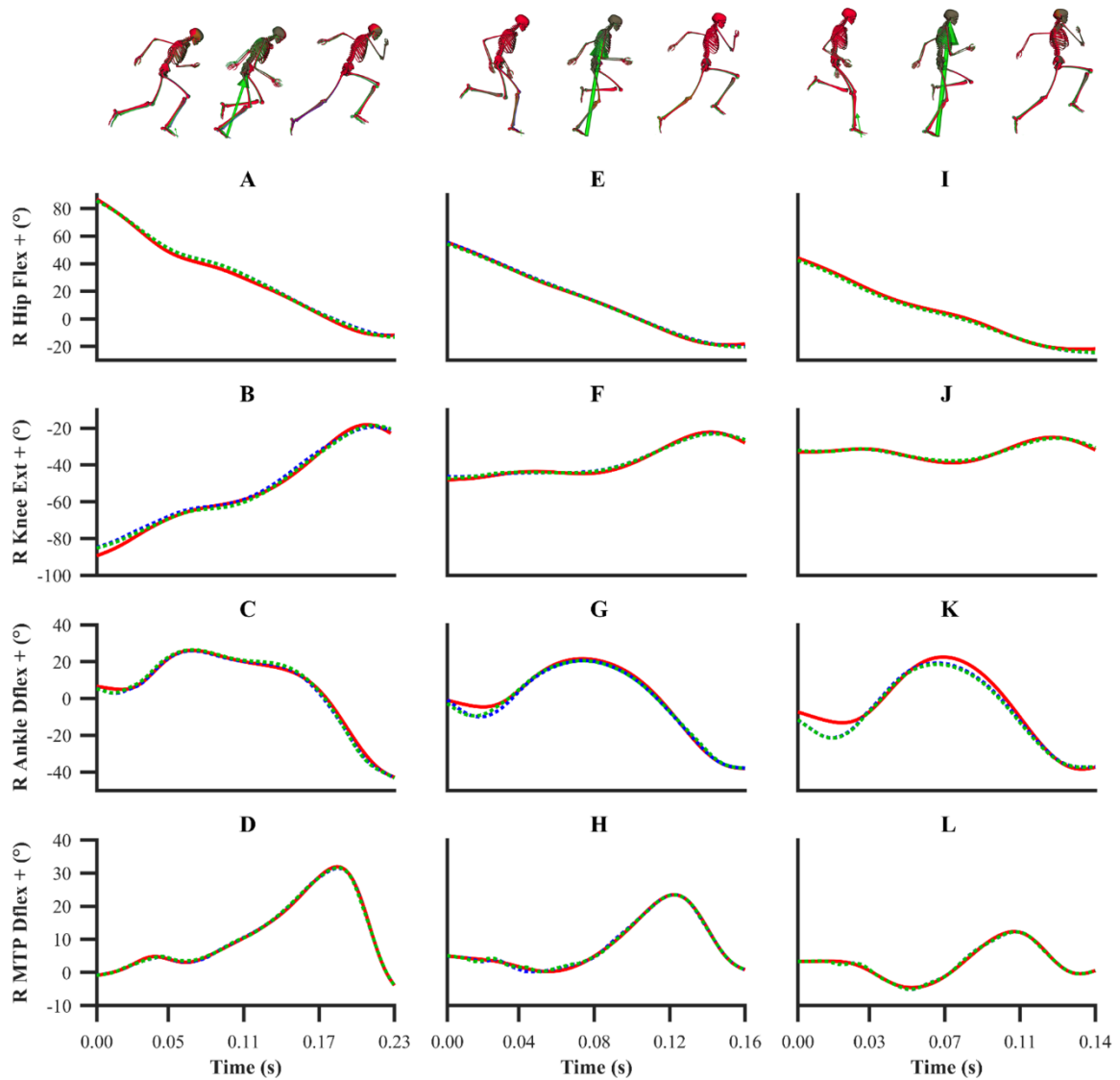
Figure 3.4–1 Subset of right (R) lower-limb joint angles for the first early acceleration (A-D), mid-acceleration (E-H) and maximum velocity (I-L) phase trials. Experimental joint angles are denoted by solid red lines. Simulated joint angles from the individual and simultaneous calibration simulations are denoted by dashed blue and green lines, respectively. Flex: flexion; ext: extension; dflex: dorsiflexion.
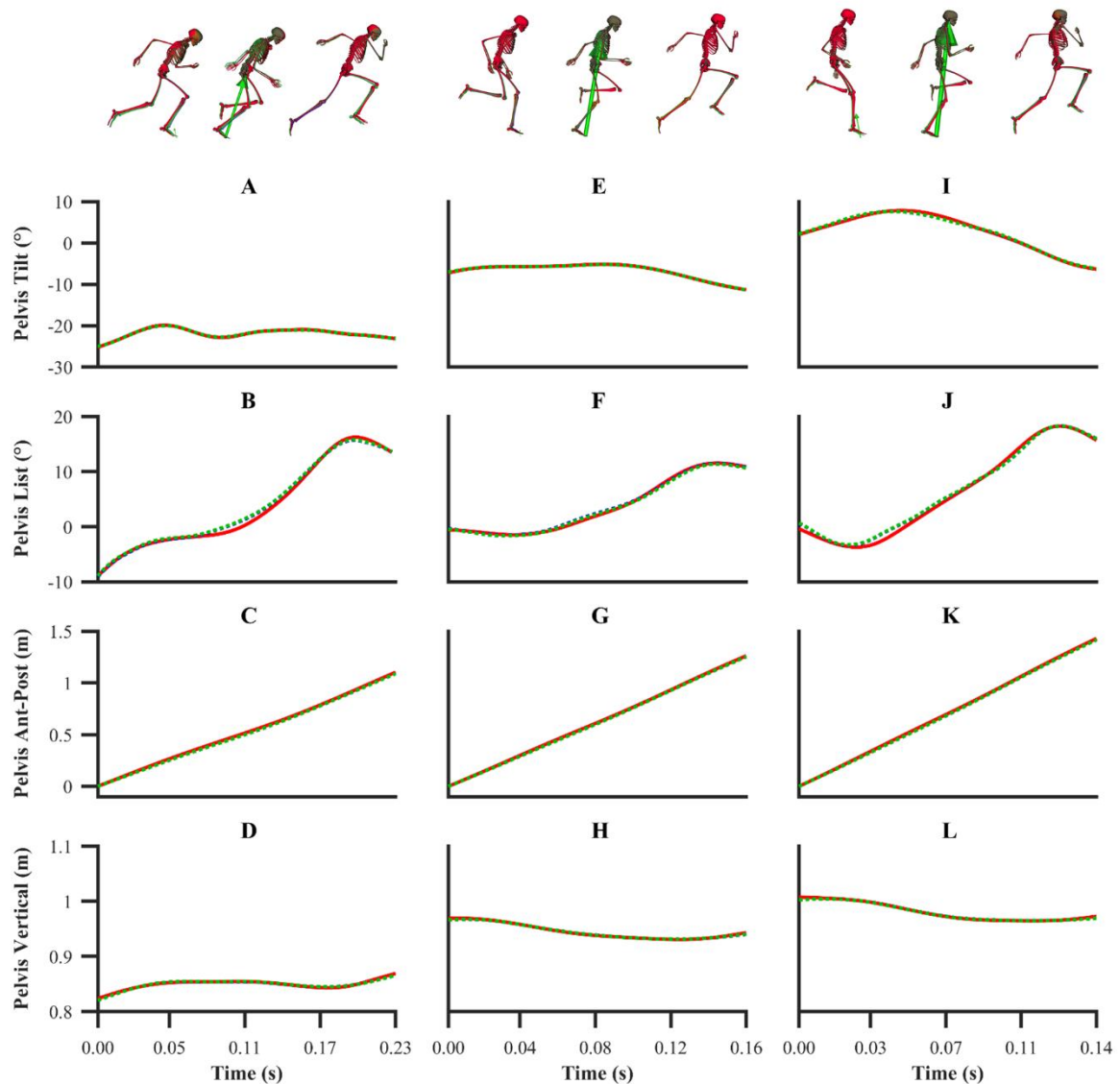
Figure 3.4–2 Subset of global pelvis angles and translations for the first early acceleration (A-D), mid-acceleration (E-H) and maximum velocity (I-L) phase trials. Experimental global pelvis angles and translations are denoted by solid red lines. Simulated global pelvis angles and translations from the individual and simultaneous calibration simulations are denoted by dashed blue and green lines, respectively. Ant-post: anterior-posterior.

The patterns of the net joint moments obtained from the individual and simultaneous data-tracking simulations were found to match the patterns of the experimental net joint moments (Figures 3.5–1 and 3.5–2), with average RMSDs of 16.9 and 17.2 Nm, respectively. The average RMSDs of the net lower-limb joint moments were 19.5 and 19.9 Nm for the individual and simultaneous calibration simulations, respectively (Table 3.5–1). For the validation simulation, the average RMSDs of the net joint moments and the net lower-limb joint moments were 17.7 and 23.6 Nm, respectively. The tracking errors for the validation simulation were lower than the corresponding tracking errors obtained from the individual (24.9 and 28.6 Nm

RMSD) and simultaneous (24.9 and 28.7 Nm RMSD) calibration simulations of the maximum velocity phase trial. For the calibration simulations, the pattern of the untracked net right MTP plantarflexion-dorsiflexion moment was markedly different around touchdown and mid-stance (18.2 Nm largest RMSD), whilst for the validation simulation it was in closer agreement (8.7 Nm RMSD).
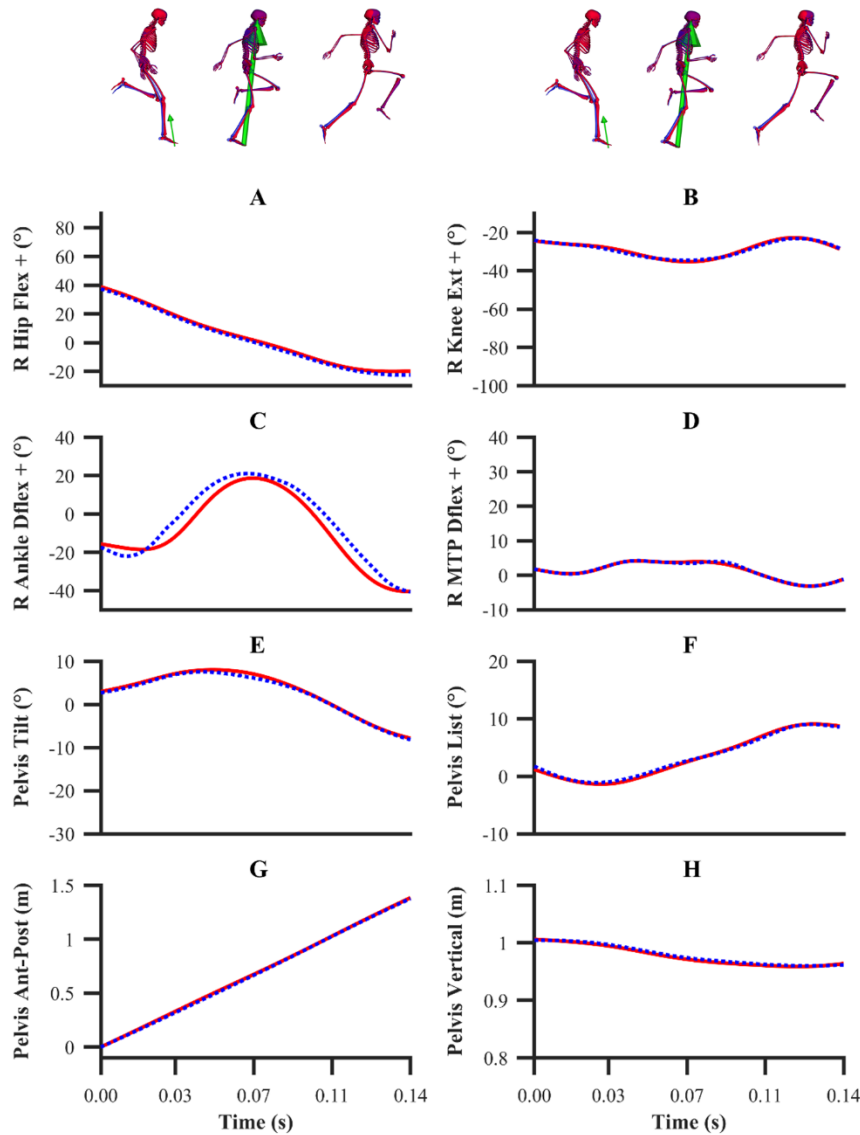
Figure 3.4–3 Subset of right (R) lower-limb joint angles (A-D), and global pelvis angles and translations (E-H) for the second maximum velocity phase trial. Experimental joint angles, and global pelvis angles and translations are denoted by solid red lines. Simulated joint angles, and global pelvis angles and translations from the validation simulation are denoted by dashed blue lines. Flex: flexion; ext: extension; dflex: dorsiflexion; ant-post: anterior-posterior.
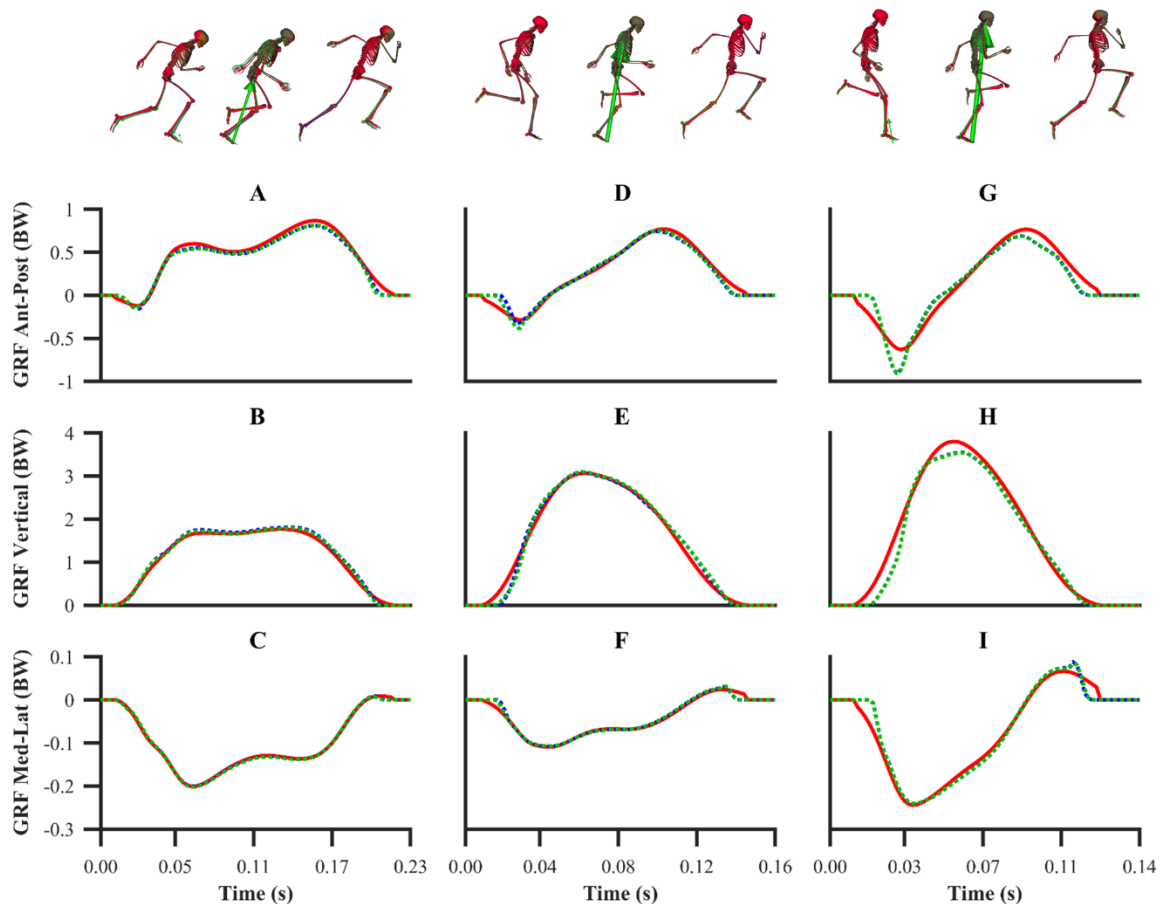
Figure 3.4–4 Normalised GRF components for the first early acceleration (A-C), mid-acceleration (D-F) and maximum velocity (G-I) phase trials. Experimental GRF components are denoted by solid red lines. Simulated GRF components from the individual and simultaneous calibration simulations are denoted by dashed blue and green lines, respectively. Ant-post: anterior-posterior; med-lat: medial-lateral.

The simulated activations of the GASTM, TFL, VM and SOL for both sets of calibration simulations displayed similarities in terms of magnitude and timing with the corresponding EMG data (Figure 3.5–3). The simulated GMAX and BF activations from both sets of calibration simulations were markedly different with respect to the corresponding EMG data. A noticeable difference during the end of the stance phase and the beginning of the following flight phase was observed between the simulated activations and EMG data of the GMAX, BF and GASTM, in which the simulated activations continued to ramp up or remain constant, whilst the EMG data tended to zero. For the validation simulation, the simulated activations of the BF, GASTM and VM displayed strong similarities with the corresponding EMG data (Figure 3.5–4). The simulated BF and GASTM activations for the validation simulation, as per the calibration simulations, continued to ramp up near the end of the stance phase and the beginning of the following flight phase, whilst the corresponding EMG data tended to zero.

The simulated GMAX activation for the validation simulation displayed similarities to the corresponding EMG data, although the magnitude was discernibly different.

The optimised sphere position parameters were for the most part reasonably similar when obtained from the individual and simultaneous calibration simulations (Table 3.5–2 and Figure 3.5–5). The optimised stiffness parameters displayed a trend of increasing from the early acceleration phase trial to the maximum velocity phase trial when determined from the individual calibration simulations. For the simultaneous calibration simulation, the optimised stiffness parameter, was similar to the average value determined from the individual calibration simulations. The optimised damping parameters were found to change minimally between the individual and simultaneous calibration simulations.
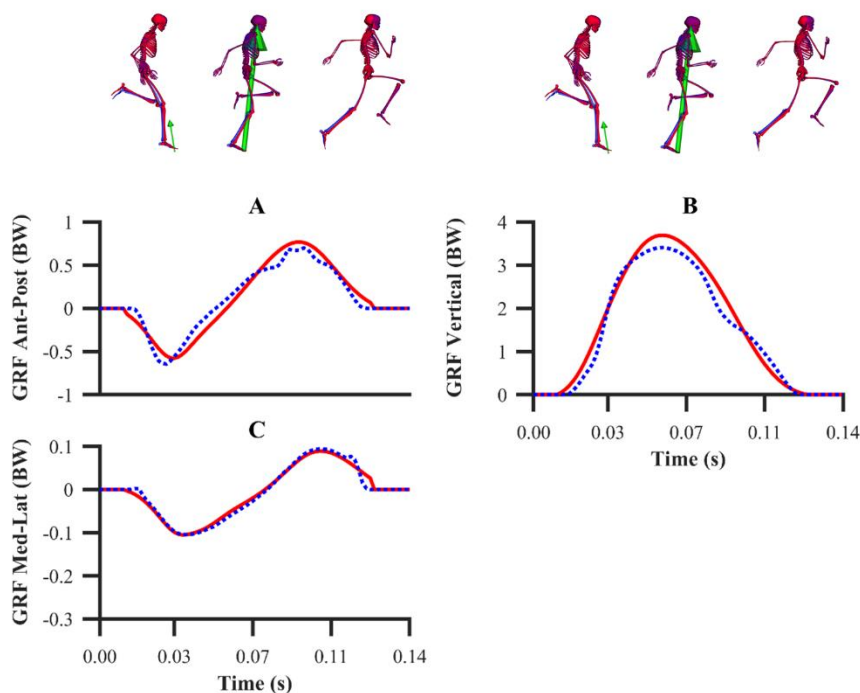
Figure 3.4–5 Normalised GRF components for the second maximum velocity phase trial (A-C). Experimental GRF components are denoted by solid red lines. Simulated GRF components from the validation simulation are denoted by dashed blue lines. Ant-post: anterior-posterior; med-lat: medial-lateral.

Table 3.4–1 The root mean squared difference (RMSD) of the global pelvis translations and angles, subset of lower-limb joint angles and normalised GRF components. Ant-post: anterior-posterior; med-lat: medial-lateral; r: right; l: left; flex: flexion; ext: extension; dflex: dorsiflexion.

RMSD	Early Acc Indiv	Early Acc Simult	Mid-Acc Indiv	Mid-Acc Simult	Max Vel Indiv	Max Vel Simult	Max Vel Valid
Pelvis Translations							
Pelvis Ant-Post (cm)	0.4	0.4	0.3	0.3	0.4	0.4	0.4
Pelvis Vertical (cm)	0.1	0.2	0.1	0.1	0.1	0.1	0.2
Pelvis Med-Lat (cm)	0.1	0.1	0.1	0.1	0.1	0.1	0.1
Pelvis Angles							
Pelvis List (°)	0.1	0.1	0.1	0.1	0.3	0.3	0.4
Pelvis Tilt (°)	0.5	0.6	0.2	0.2	0.3	0.3	0.3
Pelvis Rotation (°)	1.0	1.1	0.7	0.7	0.8	0.8	0.6
Lower-limb Joint Angles							
R Hip Flex (°)	1.8	1.7	0.6	0.7	1.3	1.3	1.4
R Knee Ext (°)	2.0	1.6	0.9	0.8	0.6	0.6	0.5
R Ankle Dflex (°)	1.2	1.5	2.0	1.9	3.7	4.0	5.5
R MTP Dflex (°)	0.3	0.3	0.4	0.4	0.3	0.3	0.2
L Hip Flex (°)	2.7	2.7	1.5	1.3	1.4	1.5	2.7
L Knee Ext (°)	0.3	0.4	0.2	0.2	0.6	0.6	1.4
L Ankle Dflex (°)	0.3	0.3	0.2	0.2	0.2	0.2	0.2
L MTP Dflex (°)	1e-2	1e-2	1e-2	1e-2	1e-2	1e-2	1e-2
GRF							
Ant-Post (BW)	0.042	0.045	0.047	0.041	0.103	0.102	0.088
Vertical (BW)	0.058	0.049	0.112	0.122	0.213	0.213	0.219
Med-Lat (BW)	0.002	0.003	0.005	0.005	0.016	0.016	0.008

Note: The values presented are from the individual (Indiv) and simultaneous (Simult) calibration simulations of the first early acceleration (Early Acc), mid-acceleration (Mid-Acc) and maximum velocity (Max Vel) phase trials, and from the validation (Valid) simulation of the second maximum velocity phase trial.

3.5 Discussion

The primary aims of the current study were to develop a musculoskeletal modelling and simulation framework for sprinting, and to evaluate its capability of reproducing highly dynamic experimental data. The secondary aims of this study were to generate dynamically consistent simulated outputs and to identify foot-ground contact model parameters for subsequent predictive simulations. To achieve our aims, we performed a series of data-tracking calibration and validation simulations, based upon a direct collocation optimal control approach. The data-tracking calibration simulations also enabled the determination of the foot-ground contact model parameters from tracking either an individual trial or multiple trials simultaneously. We found that the outputs from the calibration and validation simulations closely matched the experimental data, and this provides confidence in using the framework to address applied sprinting research questions. Importantly, all the simulated outputs were

dynamically consistent, implying that no fictious residual forces and moments were necessary to satisfy the dynamics equations of our musculoskeletal model. The proposed framework also includes a novel contribution to the biomechanics modelling and simulation literature, as it enables dynamically consistent simulations of an explosive locomotor task to be performed (with the aerodynamic drag force included), whilst also identifying foot-ground contact model parameters. Furthermore, the simultaneous data-tracking calibration simulation enabled the foot-ground contact model parameters to be determined from multiple trials, which is key to avoid overfit bias.
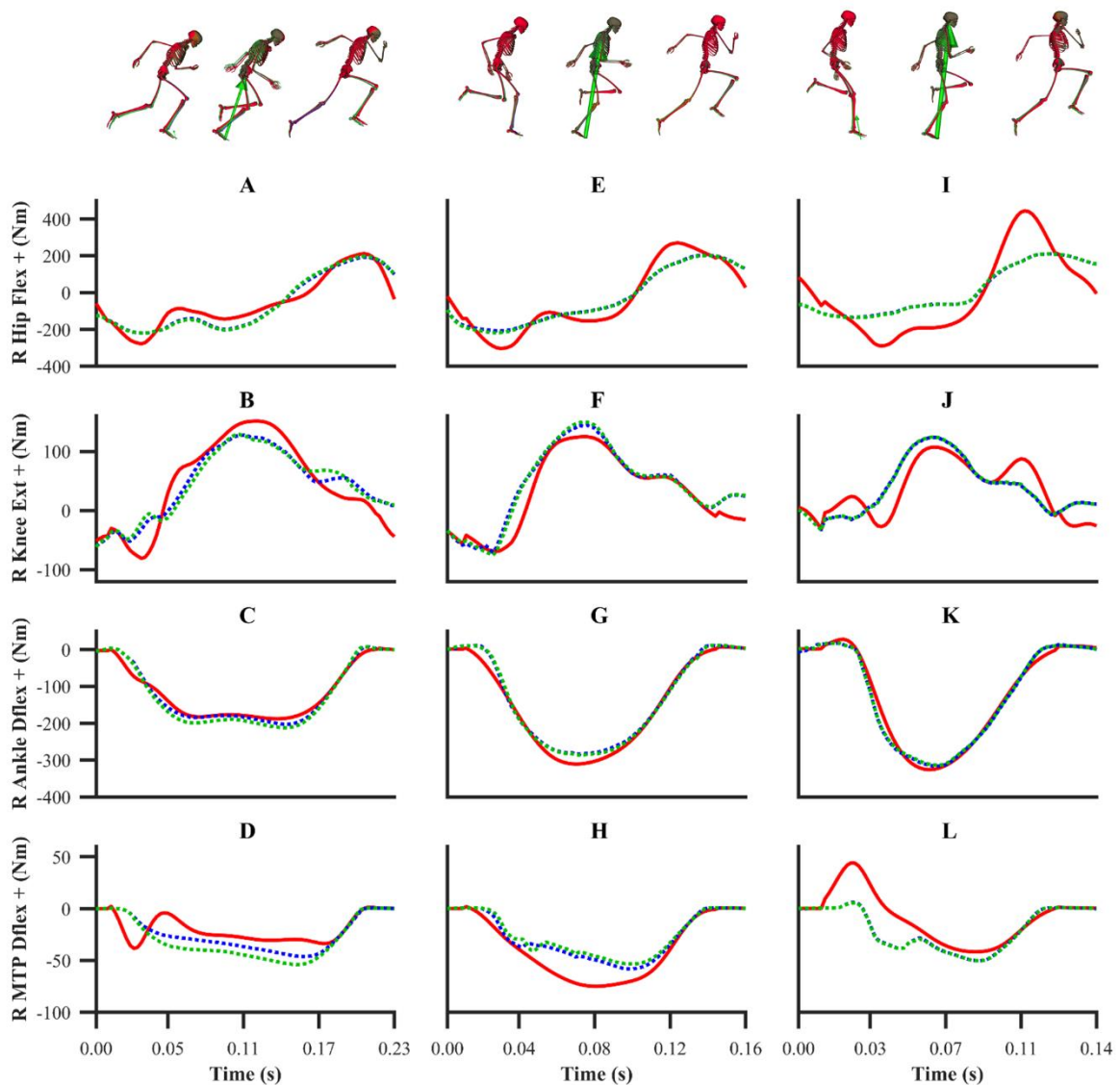
Figure 3.5–1 Subset of right (R) lower-limb net joint moments for the first early acceleration (A-D), mid-acceleration (E-H) and maximum velocity phase trials. Net MTP moments were not tracked. Experimental net joint moments are denoted by solid red lines. Simulated net joint moments from the individual and simultaneous calibration simulations are denoted by dashed blue and green lines, respectively. Flex: flexion; ext: extension; dflex: dorsiflexion.
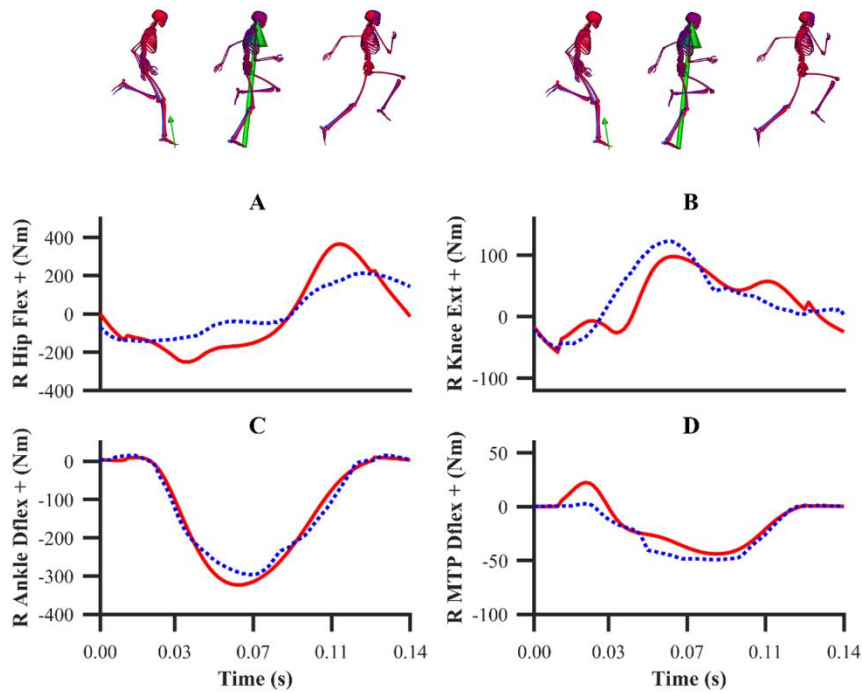
Figure 3.5–2 Subset of right (R) lower-limb net joint moments for the second maximum velocity phase trial (A-D). Net MTP moments were not tracked. Experimental net joint moments are denoted by solid red lines. Simulated net joint moments from the validation simulation are denoted by dashed blue lines. Flex: flexion; ext: extension; dflex: dorsiflexion.

Table 3.5–1 The root mean squared difference (RMSD) of a subset of lower-limb net joint moments. R: right; l: left; flex: flexion; ext: extension; dflex: dorsiflexion.

	Early Acc		Mid-Acc		Max Vel		Max Vel
RMSD	**Indiv**	**Simult**	**Indiv**	**Simult**	**Indiv**	**Simult**	**Valid**
Net Joint Moments (Nm)							
R Hip Flex	46.9	49.8	58.2	57.0	124.2	123.5	99.4
R Knee Ext	26.1	30.3	21.8	21.4	29.1	28.5	30.2
R Ankle Dflex	12.3	18.0	16.9	16.3	14.3	14.1	18.8
R MTP Dflex	11.9	16.9	13.6	15.9	18.0	18.2	8.7
L Hip Flex	33.7	34.1	25.9	26.5	42.4	44.2	40.5
L Knee Ext	6.4	7.1	5.0	4.4	12.7	12.3	16.1
L Ankle Dflex	0.5	0.4	0.3	0.3	0.8	0.9	0.7
L MTP Dflex	2e-2	2e-2	2e-2	2e-2	5e-2	6e-2	5e-2

Note: The values presented are from the individual (Indiv) and simultaneous (Simult) calibration simulations of the first early acceleration (Early Acc), mid-acceleration (Mid-Acc) and maximum velocity (Max Vel) phase trials, and from the validation (Valid) simulation of the second maximum velocity phase trial.

The smooth foot-ground contact model used within our framework has been previously shown to be appropriate for reproducing the GRF within walking (Falisse *et al.*, 2019a) and a sit-to-stand task (Serrancolí *et al.*, 2019). In this study, we showed for the first time that the smooth foot-ground contact model permits accurate reproduction of the GRF from different sprinting phases. Average RMSDs of less than 0.07, 0.15 and 0.01 BW for the anterior-posterior, vertical

and medial-lateral GRF components, respectively, across all the simulations performed are comparable with another study (Lin and Pandy, 2017), in which similar methods were used to perform dynamically consistent data-tracking simulations of running. In our study we also observed that the GRF tracking errors were the highest for the maximum velocity phase trials, which is likely due to the rapid change in GRF dynamics in comparison to the early acceleration phase trial. This result has also been observed by Lin and Pandy (2017), who reported lower GRF tracking error in walking compared to running trials. Additionally, the simulated GRFs we obtained were noticeably smoother than those obtained by Lin and Pandy (2017), which exhibited unrealistic transients. This can potentially be attributed to the generic foot-ground contact model parameters used in that study, whilst in the current study those parameters were determined from the data-tracking calibration simulations. This study therefore adds to the existing literature which has demonstrated that the determination of the foot-ground contact model parameters via data-tracking simulations enables realistic GRF to be obtained (Falisse *et al.*, 2019a; Serrancolí *et al.*, 2019).

The ability to track several different trials simultaneously permits a model's parameters to be obtained with the confidence that they are less likely to suffer from overfitting. We observed that the individual data-tracking calibration simulations resulted in only minor improvements in terms of GRF tracking error when compared to those obtained from the simultaneous data-tracking calibration simulation, thus demonstrating the foot-ground contact model's ability to generalise across different sprinting phases. As a means of further evaluating our framework, we performed a data-tracking validation simulation using the foot-ground contact model parameters obtained from the simultaneous data-tracking calibration simulation. The low GRF tracking errors shown in the simultaneous calibration and validation simulations provide confidence in using the foot-ground contact model parameters obtained from the simultaneous data-tracking calibration simulation to perform future predictive simulations of sprinting. It is also worth highlighting that the formulation of a simultaneous data-tracking calibration simulation is greatly facilitated by the direct collocation method and requires minimal adjustments to the NLP problem formulation of tracking a single trial (increase in the number of variables and constraints). Future studies should therefore consider using a similar approach for circumstances in which the parameters cannot be easily obtained empirically.
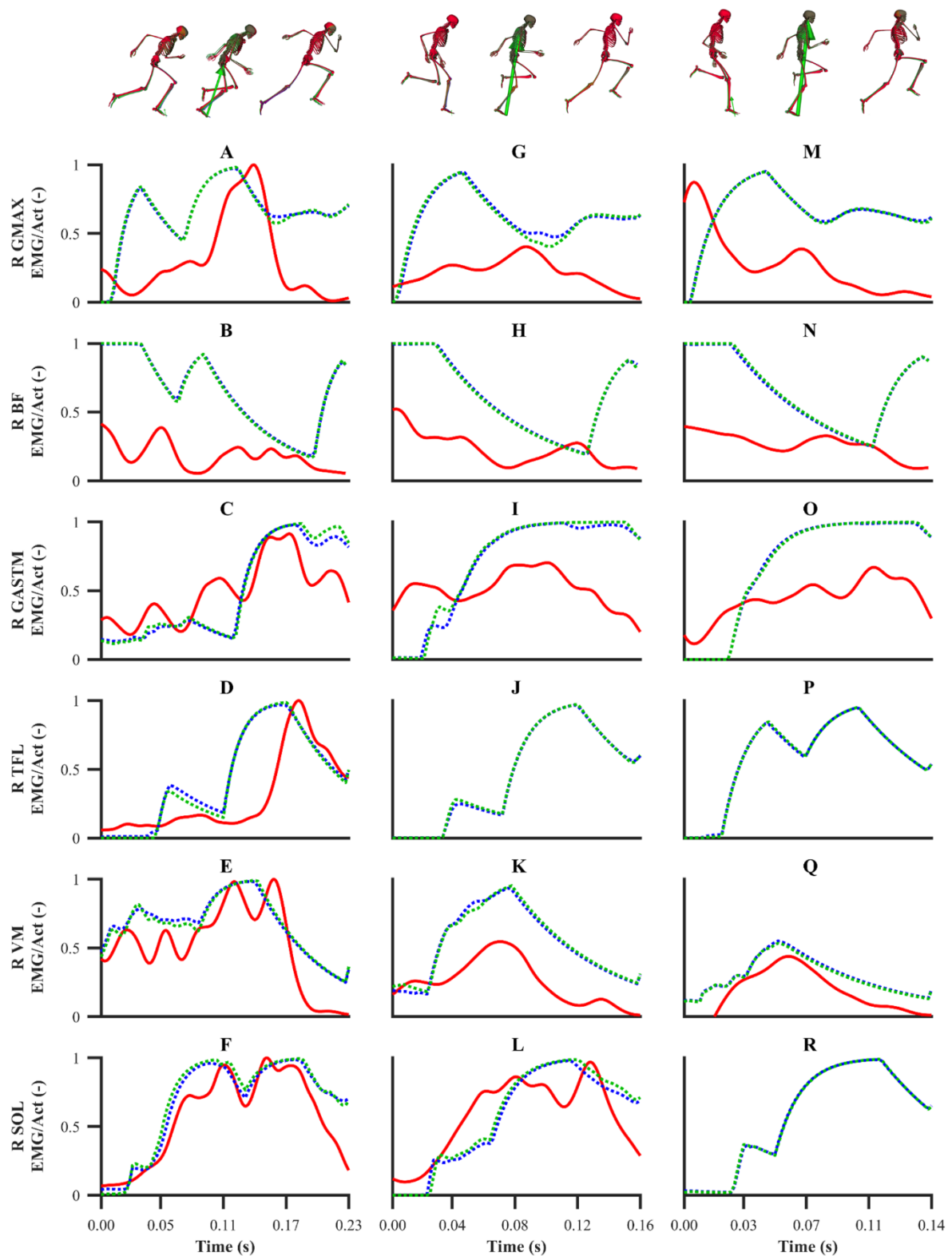
Figure 3.5–3 EMGs and simulated activations from the right (R) lower-limb for the first early acceleration (A-F), mid-acceleration (G-L) and maximum velocity (M-R) phase trials. The TFL EMG during the mid-acceleration and maximum velocity phase trials, and SOL EMG during the maximum velocity phase trial were omitted due to data collection issues. EMGs are denoted by solid red lines. Simulated activations from the individual and simultaneous calibration simulations are denoted by dashed blue and green lines, respectively. GMAX, gluteus maximus; BF, biceps femoris; GASTM; gastrocnemius; TFL, tensor fasciae latae; VM, vastus medialis; SOL, soleus.
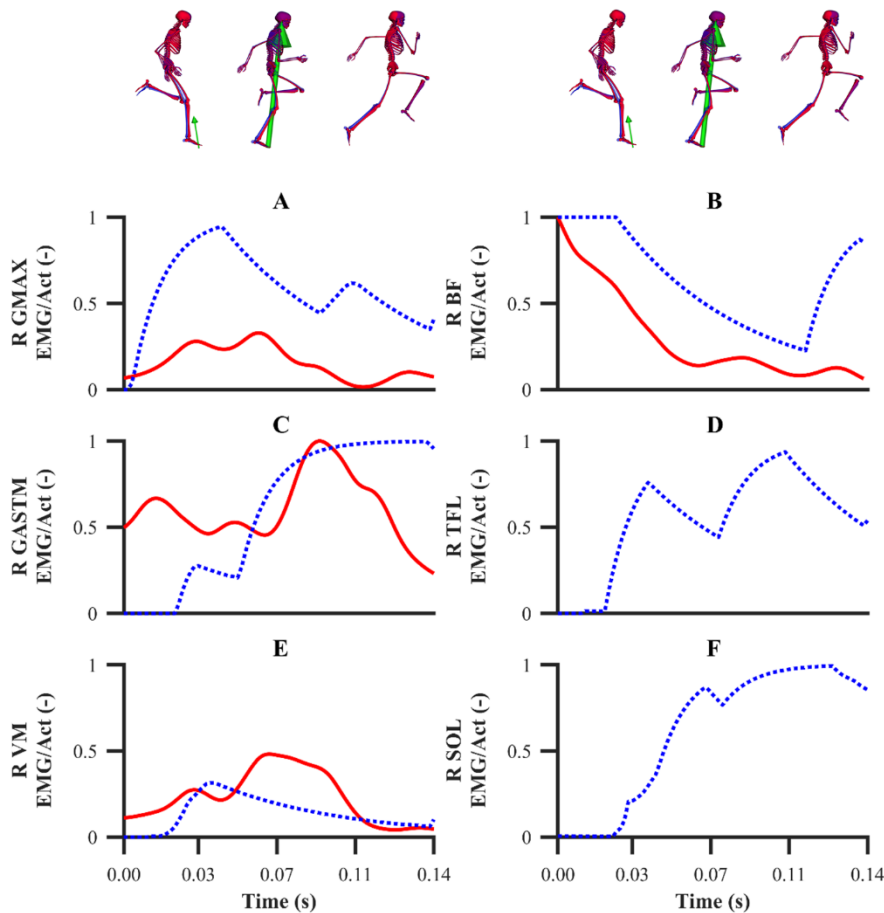
Figure 3.5–4 EMGs and simulated activations from the right (R) lower-limb for the second maximum velocity phase trial (A-F). The TFL and SOL EMGs were omitted due to data collection issues. EMGs are denoted by solid red lines. Simulated activations from the validation simulation are denoted by dashed blue lines. GMAX, gluteus maximus; BF, biceps femoris; GASTM, gastrocnemius; TFL, tensor fasciae latae; VM, vastus medialis; SOL, soleus.

From a kinematics perspective, the magnitude of the tracking errors across all simulations are in line with the study by Lin and Pandy (2017), who reported RMSDs of less than 1.5° and 0.6 cm for rotational and translational tracked kinematics during running, respectively. In general, the patterns of simulated kinematics we obtained are in agreement with previous experimental sprinting kinematics (Lai, 2015; von Lieres Und Wilkau, 2017), and the kinematics errors we observe are in the same order of magnitude of the experimental error related to human motion capture measurement (Alenezi *et al.*, 2016).We therefore believe that the current framework is of a sufficient accuracy to warrant its use within applied sprinting settings. An aspect of our framework which possibly warrants further improvement is the tracking of right ankle plantarflexion-dorsiflexion, for which the maximum RMSD was 5.5° and it was obtained from the data-tracking validation simulation. We were surprised by this result, as we anticipated the kinematics tracking errors from the validation simulation to be more evenly distributed

amongst all the DOFs and higher than those obtained from the equivalent sprinting phase trial of the calibration simulations. In any case, it is worthwhile noting that the smallest detectable difference for peak ankle dorsiflexion during the stance phase of running and bend sprinting is in excess of 10° (Alenezi *et al.*, 2016; Judson *et al.*, 2020), and the largest right ankle dorsiflexion difference we obtained during the stance phase of the validation simulation was 8.9°. Interpreting these findings together suggests that the right ankle kinematics tracking error obtained is likely within the bounds of biological variation and measurement error.

Table 3.5–2 Optimised foot-ground contact model parameters determined from the individual and simultaneous data-tracking calibration simulations.

Parameter	Early Acceleration	Mid-Acceleration	Maximum Velocity	Simultaneous
Sphere s_{1x} (m)	0.070	0.066	0.069	0.070
Sphere s_{1y} (m)	-0.030	-0.030	-0.030	-0.030
Sphere s_{1z} (m)	-0.028	-0.020	-0.030	-0.029
Sphere s_{2x} (m)	0.010	0.035	0.031	0.029
Sphere s_{2y} (m)	-0.030	-0.030	-0.030	-0.030
Sphere s_{2z} (m)	0.045	3.07e-7	3.04e-7	1.52e-8
Sphere s_{3x} (m)	0.150	0.150	0.150	0.150
Sphere s_{3y} (m)	-0.028	-0.028	-0.028	-0.028
Sphere s_{3z} (m)	6.46e-6	5.41e-5	1.12e-6	6.88e-8
Sphere s_{4x} (m)	0.150	0.150	0.150	0.150
Sphere s_{4y} (m)	-0.028	-0.028	-0.028	-0.028
Sphere s_{4z} (m)	-0.025	-4.79e-5	-0.022	-0.023
Sphere s_{5x} (m)	0.120	0.070	0.070	0.070
Sphere s_{5y} (m)	-0.028	-0.028	-0.028	-0.028
Sphere s_{5z} (m)	9.70e-6	0.045	0.045	0.045
Sphere s_{6x} (m)	0.120	0.120	0.120	0.120
Sphere s_{6y} (m)	-0.028	-0.028	-0.028	-0.028
Sphere s_{6z} (m)	-0.025	-2.08e-6	-9.32e-6	-6.09e-8
Stiffness (N/m^2)	1.17e6	1.64e6	1.79e6	1.60e6
Damping (s/m)	0.073	0.110	0.063	0.072

Note: Contact spheres s_1 and s_2 were attached to the forefoot segment, the rest were attached to the rearfoot segment. The x, y and z subscripts for the contact spheres correspond to the anterior-posterior, vertical and medial-lateral axes of the segments to which the spheres were attached.

A wide range of values for the lower-limb net joint moments have been reported within the sprinting literature. For example, the peak net hip flexion-extension moment has been reported to range between ~180 and ~750 Nm during maximum velocity sprinting (Bezodis *et al.*, 2008a; Schache *et al.*, 2019), whilst in the current study the peak value was ~400 Nm. While it is possible that these differences may be attributed to an individual athlete's characteristics (e.g., individual strength differences and anthropometrics) or differences in performance levels, they are also likely to be influenced by the experimental data processing methods and

modelling assumptions applied to determine the net joint moments. We therefore opted to track the net joint moments with a lower weighting compared to the kinematics and GRF, which were considered as the most reliable data to track, due to the various uncertainties known to influence the calculation of net joint moments from an IDA (Derrick *et al.*, 2020). Despite the choice to lower the weight of the net joint moments tracking term, we obtained simulated net joint moments that largely followed the general patterns of the net joint moments we determined from IDA and of those reported within the existing sprinting IDA literature (Bezodis *et al.*, 2008a; Schache *et al.*, 2019). We would also like to emphasise that the simulated net joint moments we obtained were from dynamically consistent simulations, and they were potentially more physiologically plausible due to the use of Hill-type MTUs.
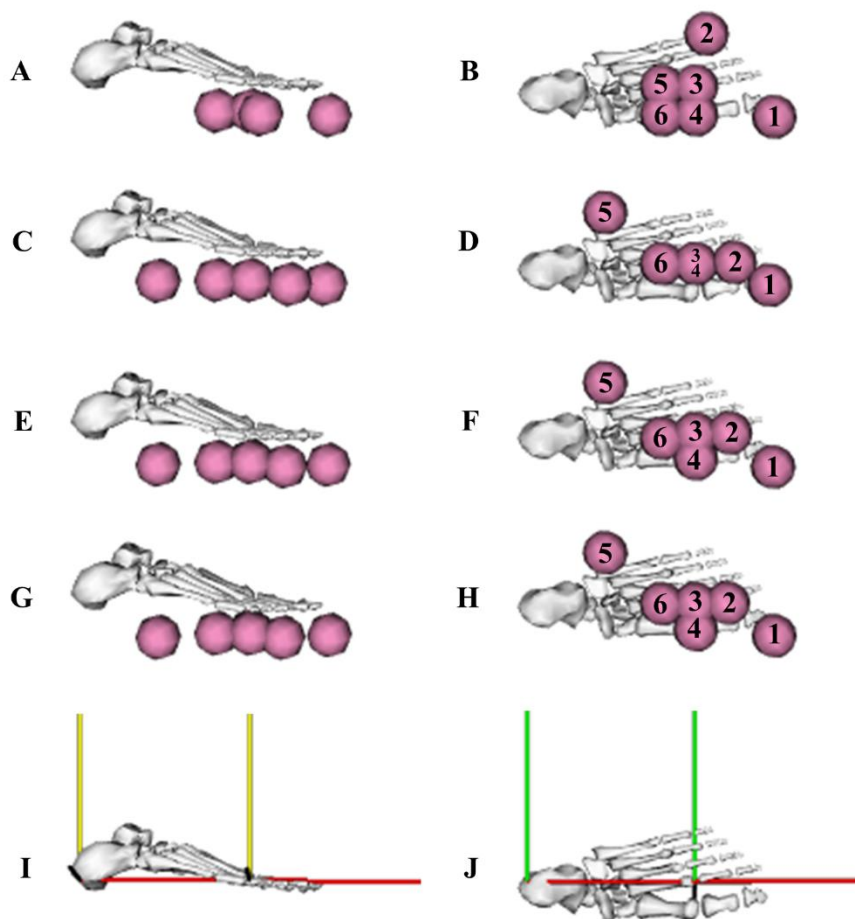
Figure 3.5–5 Optimised contact sphere locations determined from the individual and simultaneous data-tracking calibration simulations. Sagittal and transverse plane views of the optimised contact sphere locations from the first individual early acceleration phase trial (A and B), mid-acceleration phase trial (C and D), maximum velocity phase trial (E and F) calibration simulations, and for the three simultaneous trials calibration simulation (G and H). Contact sphere numbers, and rearfoot and forefoot segment axes (I and J) have been included to aid with the interpretation of the optimised locations presented in Table 3.5–2 (red axis: anterior-posterior (*x*), yellow axis: vertical (*y*) and green axis: medial-lateral (*z*)).

In our data-tracking simulations we avoided tracking the net MTP moments, as we felt that the right net MTP moment was unreliable due to the difficulty to distribute the GRF between the rearfoot and forefoot segments. We believed that the right net MTP moments obtained from all the data-tracking simulations were more physiologically plausible and realistic in comparison to those obtained from IDA, which exhibited fluctuations during the first early acceleration and maximum velocity phase trials. Despite the challenges with calculating the net MTP moment from IDA, the MTP has been previously shown to undergo a substantial range of motion during the contact phase of sprinting (Smith *et al.*, 2014). We therefore included a forefoot segment within our model to permit MTP motion. To date, most modelling and simulation studies have chosen to exclude modelling MTP motion, particularly those in which the model's lower-limbs are actuated by Hill-type MTUs (Dorn *et al.*, 2012; Lai *et al.*, 2016). It is not necessarily surprising that previous studies have neglected modelling MTP motion during sprinting, as existing off the shelf musculoskeletal models, similar to the one we used, do not have the capacity to produce MTP moments that are in a similar magnitude to those obtained from isometric dynamometry testing (Goldmann *et al.*, 2013). In our study, we set the upper limit of the MTP reserve actuators to 40 Nm, such that together with the Hill-type MTUs contained within the original model, they were able to better reflect the moment capacity at the MTP DOFs in relation to the existing literature. Future studies should consider exploring how to better model the MTP moment generating components to minimise the reserve actuator reliance.

An encouraging aspect our study was the similarities between the EMGs and the corresponding simulated activations. We were surprised by the similarities obtained considering the cost function used to resolve the MTU force-sharing problem, minimisation of weighted squared activations, not capturing the time-dependent performance criteria of sprinting. Discrepancies were observed during the end of the stance phase and the beginning of the following flight phase between the simulated activations and EMGs of the BF and GASTM across all the simulations performed. The calibration of the MTU parameters by performing data-tracking simulations and/or the tracking of the EMGs may lead to removing the anomalous simulated activations not observed in the EMGs. The direct collocation optimal control approach we have used in this study also enables the MTU force-sharing problem to be resolved using a cost function that more closely captures the time-dependent performance criteria of sprinting, such as MTU power (Cavagna *et al.*, 1971), and this may also reduce the aforementioned discrepancies.

The major benefit of the modelling and simulation approach used in this study is that it permits dynamically consistent simulations to be obtained. It is not uncommon to obtain large dynamic inconsistencies in the form of pelvis residual forces and moments that surpass 1000 N and 300 Nm, respectively, when performing a standard IDA within sprinting (Aeles *et al.*, 2018). The approach we have used in this study builds on work of other studies (Lin and Pandy, 2017; Pallarès-López *et al.*, 2019) who demonstrated the ability of the direct collocation optimal control approach to reduce residuals within sporting tasks (hopping and running). In this study we demonstrated that it is possible to use this approach to generate dynamically consistent motions in a demanding task that spanned all three planes of motion. Consequently, we recommend that researchers within the sports biomechanics community adopt the approach we have used to increase the fidelity of their results and obtain dynamically consistent motions. A limitation of our study is that we used a generic linearly scaled model. We suspect that the use of a subject-specific model would lead to reduced residuals when performing a standard IDA, due to the model having more representative inertial properties and mass distribution, and we expect that this would improve the tracking of the experimental data due to not needing to overcome the sizeable residuals obtained when using a linearly scaled generic model.

An alternative approach to generating motions that are closer to being dynamically consistent is RRA, which is included within OpenSim (Delp *et al.*, 2007). RRA is based on using a multibody model actuated by a combination of joint and residual actuators, with the objective to track experimental kinematics whilst also minimising the use of the actuators. The reserve actuators are weighted heavily in comparison to the joint actuators such that the new motion obtained is closer to being dynamically consistent. A beneficial feature of RRA is that it provides recommendations for minimally adjusting the mass properties of the model, and this is a useful feature in circumstances when there are discrepancies between the model's and subject's mass distribution. RRA can then be performed again with the model in which the adjustments to the mass properties have been applied to further refine the dynamic consistency. A similar feature could also be incorporated within the data-tracking optimal control approach used in this study, similarly to how the foot-ground contact model parameters were determined. The downsides of RRA are that it must be performed iteratively to obtain a worthwhile dynamically consistent motion and that it necessitates explicit forward integration to satisfy the dynamics, which can be affected by integration errors. In contrast, the direct collocation optimal control approach used in this study needs only to be performed once to obtain a

dynamically consistent solution, and it imposes the dynamics for each time step simultaneously as the state variables are treated as design variables alongside the control variables.

The most challenging elements to simulate were the transitions between touchdown and take-off. For all the data-tracking simulations performed, we observed discrepancies between the simulated and experimental right lower-limb kinematics and GRF around touchdown and take-off, and these discrepancies were most pronounced for the tracked maximum velocity phase trials (Figures 3.4–4 and 3.4–5). Noticeable differences in either knee flexion-extension or ankle plantarflexion-dorsiflexion were accompanied by a mismatch in GRF production timings (largest touchdown and take-off mismatches were 8.0 and 12.6 ms, respectively). More specifically, the right lower-limb appeared to extend earlier and further in the simulations in comparison to the experimental kinematics. This can be explained by the model attempting to position the foot closer to the ground to allow the foot-ground contact model, which is driven by the kinematics, to generate the matching GRF. Future work exploring the geometry of the foot-ground contact model, similar to Ezati *et al.* (2020), is possibly needed to improve the timing of GRF production.

Another explanation for the GRF timing differences may concern the filtering we used to process the experimental GRF. We opted to filter both the experimental kinematics and GRF with the same cut-off frequency as per the current recommendations (Derrick *et al.*, 2020). This was to avoid tracking oscillatory net joint moments, which cannot be produced by muscles as they are unable to activate/deactivate instantaneously. However, in this approach the cut-off frequency to filter the GRF is too low based on a residual analysis, which leads to artificially extending the ground contact phase (Mai and Willwacher, 2019; Robertson and Dowling, 2003). Thus, the GRF onset/offset timing differences, in addition to the right lower-limb extension, can potentially be explained by the tracking of the filtered GRF. In fact, the kinematics during the contact phases are tracked closely, particularly for the calibration simulations, which supports this explanation. A further possibility to improve the GRF timings involves filtering the experimental data using matching time varying cut-off frequencies established from the kinematics data (Davis and Challis, 2020), in an attempt to limit the onset/offset discrepancies between the filtered and raw experimental GRF data. It is important to note that filtering the kinematics and GRF data with matching time-varying frequencies may also lead to oscillatory net joint moments when performing a standard IDA, although this has yet to be explored.

3.6 Conclusion

In conclusion, we have developed a musculoskeletal modelling and simulation framework for sprinting, which is a highly dynamic locomotor task, using an optimal control theory approach. We quantitatively evaluated the framework's ability to reproduce experimental data, which is a first step that is typically ignored within the sports biomechanics modelling and simulation community. The results from the evaluation suggest that the framework can reproduce experimental data from several sprinting phases with low tracking errors, such that we can proceed with performing predictive simulations to assess technique modifications in relation to performance. This is also the first study to provide dynamically consistent three-dimensional muscle-driven simulations of sprinting across different phases. Overlaid videos of the experimental and simulated kinematics, in addition to the corresponding data files, can be accessed online at https://doi.org/10.6084/m9.figshare.12656354.
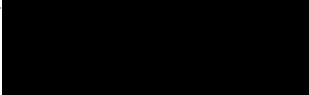
Chapter 4
Modifications to the net knee moments lead to the greatest improvements in accelerative sprinting performance: a predictive simulation study

4.1 Abstract

Accelerative sprinting is an essential skill to improve for athletes participating within short distance track and field events and team-based sports (e.g., soccer and rugby). The current body of sprinting biomechanics literature together with the front-side mechanics coaching framework provide various kinematics- and kinetics-based technique recommendations for improving performance. However, very few studies have attempted to systematically explore technique modifications from a performance enhancement perspective, and the front-side mechanics coaching framework has not been rigorously investigated from a scientific perspective. The aims of this investigation were therefore to i) explore how hypothetical technique modifications affect accelerative sprinting performance, and ii) assess whether the hypothetical modifications support the front-side mechanics coaching framework. A computational modelling and simulation framework, featuring a direct collocation optimal control approach, was used to explore performance improvement via a series of predictive simulations of sprinting during the early acceleration phase. Technique modifications were systematically explored by enabling the framework to change the lower-limb net joint moments with respect to those determined in a data-tracking simulation. Specifically, individual and combinations of the major lower-limb net joint moments (ankle, knee, and hip) were allowed to vary within the predictive simulations. Each predictive simulation was also performed with the aim of improving performance, which was achieved by minimising the time taken to cover a set distance (obtained from the data-tracking simulation). It was found that the 'knee-free' simulations resulted in the greatest improvements to overall performance (22.0%; 1401.2 vs. 1148.7 W) due to modifying the timing and magnitude of the net knee flexor-extensor moments. The 'hip-free' simulations were found to demonstrate an earlier net hip flexor moment during the stance phase, which provides evidence in support of the front-side mechanics coaching framework. However, the kinematics aspects of the front-side mechanics coaching framework (e.g., keeping the lower-limb segments in front of the body at all times) did not emerge from the predictive simulations which improved performance. The results from this study therefore suggest that for athletes to improve their accelerative sprinting performance

they should attempt to modify the actions of the net knee and hip flexor-extensor moments as identified within this investigation.

This declaration concerns the article entitled:

Chapter 4 Modifications to the net knee moments lead to the greatest improvements in accelerative sprinting performance: a predictive simulation study

Publication status (tick one)

Draft manuscript	✘	Submitted		In review		Accepted		Published	

Publication details (reference)	Haralabidis, N., Serrancolí, G., Colyer, S., Salo, A. & Cazzola, D. (2021). Modifications to the net knee moments lead to the greatest improvements in accelerative sprinting performance: a predictive simulation study.

Copyright status (tick the appropriate statement)

I hold the copyright for this material	✘	Copyright is retained by the publisher, but I have been given permission to replicate the material here	

Candidate's contribution to the paper (provide details, and also indicate as a percentage)	The candidate considerably contributed to and predominantly executed the: **Formulation of ideas: 85%** NH acted predominantly independently in conducting the background research and formulating the aims of the study. NH presented the idea to his supervisors, and they provided feedback to aid in refining the study. **Design of methodology: 80%** NH adapted and modified the simulation framework initially developed by GS for the purposes of this study. NH was primarily responsible for setting up the simulations and carrying out any debugging of the simulation code. **Experimental work: 65%** NH liaised with laboratory technicians from a different university to ensure the data collection could take place with the necessary hardware and software. NH significantly contributed to the experimental data collection protocol together with the processing of the data used for this study. **Formal data analysis: 85%** The results of the simulations were primarily analysed by NH with input from his supervisors. **Presentation of data in journal format: 80%** NH wrote the first draft of the manuscript and carried out draft revisions. The figures associated with manuscript were all created by NH.
Statement from Candidate	This paper reports on original research I conducted during the period of my Higher Degree by Research candidature.
Signed	██████████ **Date** 25/10/2021

4.2 Introduction

For athletes competing within the short distance track and field events (60-400 m), their ability to rapidly accelerate their centre of mass (CoM) during the preliminary steps of a race is considered to be of upmost importance (Mero *et al.*, 1992; van Ingen Schenau *et al.*, 1994). In addition, elite athletes are able to achieve well over 50% of their maximum horizontal CoM velocity by the point they complete their second step (Mann and Murphy, 2015). Accelerative sprinting is also believed to play an important role in contributing towards success for team-based sports. For example, within rugby league and soccer 35 and 19 accelerative sprints, respectively, are completed on average during a match (Bangsbo *et al.*, 1991; Gabbett, 2012), with these sprints notably occurring during the key instances of a match (Faude *et al.*, 2012; Gabbett and Gahan, 2016).

Despite the significance of accelerative sprinting towards sporting performance, very few research facilities in the world are equipped with arrays of multiple force plates and optoelectronic motion capture systems to further our understanding of how to improve accelerative sprinting performance from a biomechanical perspective. Consequently, most studies to date have carried out analyses of accelerative sprinting during a discrete step (Bezodis *et al.*, 2014; Hunter *et al.*, 2005; Johnson and Buckley, 2001; Yu *et al.*, 2016). However, from a coaching science perspective it is more beneficial to assess accelerative sprinting performance across multiple steps to capture the changes in technique needed to accelerate most effectively. For this reason, in more recent times, several institutes have developed specialised research facilities (Colyer *et al.*, 2018a; Nagahara *et al.*, 2018) or experimental protocols (Morin *et al.*, 2015b; Schache *et al.*, 2019) to permit such analyses. Of the studies undertaken to date, irrespective of whether they analysed a single step or multiple steps of accelerative sprinting, the main focus of the research has been centred on ground reaction force production. There are three external forces (ground reaction force, gravity and drag) that act on an athlete whilst sprinting, with the most modifiable being the ground reaction force. The change in an athlete's linear horizontal momentum is mainly explained by the net horizontal impulse they are able to generate during the stance phase. Thus, to improve accelerative sprinting performance, an athlete must generate greater horizontal net impulse, either through increasing the propulsive impulse, reducing the braking impulse or by doing both.

One strategy based upon the findings from current literature to reduce the braking impulse relies on an athlete generating high backward lower-limb velocities during the terminal swing phase, through net hip extensor and knee flexor moments (Mann and Sprague, 1983; Mann, 1981). This is believed to reduce the horizontal foot velocity and CoM-foot touchdown distance, and in turn reduce the braking impulse (Hunter *et al.*, 2005; Mann and Sprague, 1980; Mann and Sprague, 1983). Hunter *et al.* (2005) suggested that further research was necessary, in the form of an intervention study, to explore the potential benefits of the aforementioned technique-based recommendations. However, to date, no intervention studies have been carried out to ascertain this, perhaps due to the unwillingness of the athletes and their coaches to participate in such a study given its time-consuming nature and the potential negative effects on their performance. Most importantly, attempting to modify a particular aspect of an athlete's technique in isolation is not feasible, as other aspects of their technique are likely to simultaneously change. Therefore, it is very challenging to assess the effect of modifying a single aspect of an athlete's technique in isolation using a conventional intervention approach (Yeadon and King, 2007). A predictive computer simulation and modelling approach is instead very well-suited to performing such research, as this type of approach requires minimal athlete involvement, allows to systematically modify and assess the effect of single variables in isolation, and enables hypothetical 'what if' scenarios to be explored without the fear of jeopardising an athlete's performance level (Neptune, 2000; Yeadon and King, 2007).

A suggested strategy for maximising the propulsive impulse is to ensure that the thigh segment and hip joint of the stance limb rotate backwards at a high velocity (Mann *et al.*, 1984; Mann and Sprague, 1980), which coincides with the strategy to minimise the braking impulse. Mann and Murphy (2015) suggest that the net hip extensor moment generated during the beginning of the stance phase is crucial for this strategy. The work by Schache *et al.* (2019) provides evidence to support the claim made by Mann and Murphy (2015), as they found that there was a strong association between the impulse of the net hip extensor moment and forward acceleration whilst sprinting. Furthermore, the same study also identified a strong association between the impulse of the net ankle extensor moment and forward acceleration. In a separate study, Bezodis *et al.* (2014) identified that amongst a group of three international calibre sprinters, the most distinguishing feature separating their performance levels during the first stance phase of accelerative sprinting was the magnitude and timing of the net knee extensor moment, which was greater and earlier in the highest performing sprinter. It is interesting to note that the hip generates a net extensor moment for the portion of the stance phase which

mainly involves braking, while the ankle and knee produce net extensor moments that span the braking portion and large parts of the propulsive portion. It is therefore possible that the net extensor moments produced by the knee and ankle may be of greater benefit to propulsive impulse generation.
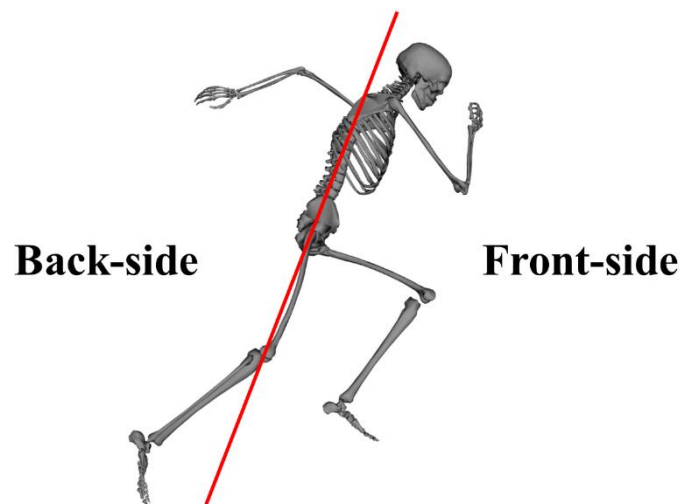
Figure 4.2–1 Front-side and back-side mechanics schematic during the second step stance phase of a maximal effort sprint. The solid red line drawn parallel to the torso indicates when the lower-limbs are in front of the body and performing front-side mechanics or behind the body and performing back-side mechanics.

Mann and Murphy (2015) also recommend that athletes should produce a net hip flexor moment during the latter 75% of the stance phase. The proposed benefit of this technique-based recommendation is that it permits a greater 'high knee' position to be achieved during the swing phase, which subsequently permits the thigh to be accelerated through a greater range of motion in preparation for the next stance phase. The technique-based recommendations proposed by Mann and Murphy (2015) were based on their experiences of working alongside some of the best USA sprinters over the past 20 years, and they have since termed the coaching framework front-side mechanics. The front-side mechanics coaching framework is based on the notion that the lower-limb segments should not extend past an imaginary line drawn parallel to the trunk when viewed from the sagittal plane (Figure 4.2.1), and this is recommended from the onset of sprinting (independent of sprinting phase). In fact, when the lower-limb segments extend past this line, Mann and Murphy (2015) state that athletes sprint with back-side mechanics, which they deem as inefficient as minimal ground reaction force can be produced during back-side mechanics and it leads to a longer stance phase duration.

To date, however, the coaching framework proposed by Mann and Murphy (2015) has received limited attention from a scientific standpoint, with only one study focusing on it (Haugen *et al.*, 2018). Interestingly, the findings in the study by Haugen *et al.* (2018) contradicted the proposed coaching framework, as greater thigh and knee extension at takeoff were associated with greater accelerative sprinting performance. However, the findings from this study were based on sub-elite male sprinters (mean ± standard deviation 100 m PB: 10.86 ± 0.22 s), and Mann and Murphy (2015) suggest that front-side mechanics is only performed by elite level sprinters, which is what sets them apart from the rest of their competitors. It is therefore still plausible that the front-side mechanics coaching framework is correct, however further studies are needed to address this. It is also worthwhile noting that the framework is based on anecdotal evidence, and it is possible that a different technical framework, yet to be uncovered, enables improved performance. Given that the majority of technical coaching within sports is based on anecdotes or information passed down between generations of coaches (Rasmussen *et al.*, 2012), it is possible that a better coaching model exists. For example, consider the variation in the techniques used in the high jump prior to the Fosbury flop technique. Predictive computer simulation and modelling approaches provide the platform for which to optimise the technique of a sporting movement, such as accelerative sprinting, and the usage of such an approach may help to provide further insights into the benefits of the front-side mechanics framework and demonstrate its merits from a scientific standpoint, which are currently lacking within the literature.

Despite the potential opportunities offered by predictive computer simulation and modelling approaches described above, they have scarcely been applied to investigate sprinting, particularly from a technique and performance enhancement perspective. The study by Bezodis *et al.* (2015) is the only study to the authors' knowledge to have done so, and they showed how performance during the first stance phase could be improved by reducing the horizontal CoM-foot touchdown distance and limiting the amount of ankle dorsiflexion. To perform the predictive simulations, Bezodis *et al.* (2015) used a two-dimensional model that was kinematically-driven due to coaches already prescribing technique modifications based on kinematics criteria. However, the kinematics are determined by the kinetics (e.g., net joint moments) and thus it is more appropriate to modify the kinetics to subsequently obtain the desired kinematics. Indeed, a kinematically-driven model can lead to unrealistic net joint moments been produced when used to perform predictive simulations of maximal effort sporting tasks (Yeadon and King, 2007). Musculoskeletal models overcome this limitation as

they rely on actuators governed by principles of muscle physiology which provide limits on their ability to contribute towards the net joint moments of a model.

In this investigation, a modelling and simulation framework was used to perform predictive simulations of the second and third steps of accelerative sprinting, and to assess how modifications in technique affected performance. This framework was previously shown to accurately reproduce sprinting data from multiple phases (early acceleration, mid-acceleration and maximum velocity) (Haralabidis *et al.*, 2021). Technique modifications were explored from a net joint moments paradigm, where individual and combinations of the major flexor-extensor net joint moments (ankle, knee, and hip) were allowed to freely vary within the physiological limits of the model during each of the predictive simulations. The remaining net joint moments were tracked during each of the predictive simulations. The secondary objectives of this investigation were to provide insights into the front-side mechanics coaching framework, and to investigate whether the technique modifications coincided with improvements in performance as explained by the front-side mechanics coaching framework.

4.3 Methods

In this study a three-dimensional musculoskeletal model scaled to an international-male sprinter was used in combination with optimal control theory to perform (data-tracking and predictive) simulations of accelerative sprinting during the preliminary steps. A data-tracking simulation was initially performed to: a) demonstrate that the modelling and simulation framework was able to reproduce experimental sprinting data with sufficient accuracy and b) to provide a reference of performance and technique for comparative purposes with the outputs of the predictive simulations. A series of predictive simulations were then performed to explore how technique modifications, governed through changes in the patterns of selected net joint moments, affected performance.

4.3.1 Musculoskeletal model

The three-dimensional full-body musculoskeletal model described in chapter 3 was used to perform the simulations in this study (Figure 4.3–1). The human skeleton was modelled with 20 rigid segments and 37 degrees-of-freedom (DOFs). The lower-limb and trunk DOFs were actuated by 92 muscle-tendon units (MTUs) together with 17 reserve actuators. Each MTU was modelled as a three-element Hill-type model, with the contraction and activation dynamics

of De Groote *et al.* (2016) and Zajac (1989), respectively. The lengths, velocities, and moment arms of the MTUs were described using differentiable and continuous polynomial functions (Falisse *et al.*, 2019b). The upper-limb DOFs were actuated by 14 joint actuators. The passive properties of sprinting spikes and the structures surrounding the forefoot were modelled by including a linear rotational spring at each of the metatarsophalangeal (MTP) DOFs. Foot-ground interaction was modelled by attaching four and two smooth Hunt-Crossley contact spheres (Serrancolí *et al.*, 2019) to both of the model's lower rearfoot and forefoot segments, respectively. The position of each contact sphere, and the stiffness and damping coefficients common to all the contact spheres were set to the values determined from a previous data-tracking simulation that tracked multiple trials simultaneously (Haralabidis *et al.*, 2021). The aerodynamic drag force was also modelled by using the approach outlined by Samozino *et al.* (2016), and it was applied at the model's CoM expressed in the local reference frame of the pelvis segment.

Figure 4.3–1 The three-dimensional musculoskeletal model used in this study (adapted from Hamner *et al.* (2010)). The human skeleton was modelled with 20 rigid segments: a pelvis, trunk (torso plus head), right and left lower-limbs (thigh, shank, upper rearfoot, lower rearfoot and forefoot) and upper-limbs (upper-arm, lateral forearm, medial forearm and hand). The DOFs of model were as follows: ×6 pelvis-to-ground, ×7 per lower-limb (×3 hip, ×1 knee, ×1 ankle, ×1 subtalar and ×1 MTP), ×3 back, and ×7 per upper-limb (×3 shoulder, ×2 elbow and ×2 wrist). The virtual model markers and smooth Hunt-Crossley contact spheres are denoted by pink and turquoise spheres, respectively. This same model was also used to perform the inverse kinematics and dynamics analyses to determine the kinematics and kinetics experimental tracking data. ***Note:*** inverse dynamics was performed using measured ground reaction forces and without the aerodynamic drag force.

4.3.2 Optimal control problem formulation & discretisation

The simulations were formulated as optimal control problems. The objective of an optimal control problem is to determine the optimal state $\boldsymbol{x}$ and control $\boldsymbol{u}$ variables (plus potentially the duration of the time horizon t_f) of a model that results in a specified performance criterion being minimised whilst also satisfying the model's dynamics and any other additional constraints (e.g., task constraints and state/control variable bounds). Each optimal control problem was converted to a discrete nonlinear programming problem (NLP) by using direct collocation, which involves parameterising both the state and control variables, and in doing so the infinite dimensional optimal control problem becomes finite dimensional. Specifically, the time horizon of the simulations was discretised across 150 equally spaced mesh intervals, with each mesh interval been further discretised with 4 points, by using a *flipped* Legendre-Gauss-Radau (LGR) direct collocation method (Garg *et al.*, 2011). The number of mesh intervals used in this study was greater than we had used in our previous data-tracking simulations of sprinting study (Haralabidis *et al.*, 2021) due to simulating multiple stance phases. The state variables within each mesh interval were parameterised with third-order Lagrange polynomials. The control variables were parameterised at the beginning of a mesh interval and assumed to be piecewise constant throughout a mesh interval. In the following subsections, the model's state and control variables are defined together with a description of how the musculoskeletal model's dynamics were handled within the simulations, and these were common amongst all the simulations. The unique aspects (e.g., performance criterion and additional constraints) to the data-tracking and predictive simulations are also outlined.

4.3.3 Variables & handling of dynamics

The generalised coordinates $\boldsymbol{q}$ and velocities $\boldsymbol{v}$ of the musculoskeletal model, and the normalised tendon forces $\boldsymbol{F_T}$ and activations $\boldsymbol{a}$ of the MTUs were selected as the state variables ($\boldsymbol{x} = [\boldsymbol{q}\ \boldsymbol{v}\ \boldsymbol{F_T}\ \boldsymbol{a}]^T$). The upper-limb joint actuators $\boldsymbol{u_{UL}}$, reserve actuators $\boldsymbol{u_{RES}}$, time derivatives of the generalised velocities $\boldsymbol{u_{\dot{v}}}$, normalised tendon forces $\boldsymbol{u_{\dot{F}_T}}$ and activations $\boldsymbol{u_{\dot{a}}}$, and ground reaction forces $\boldsymbol{u_{GRF}}$ were selected as the control variables ($\boldsymbol{u} = [\boldsymbol{u_{UL}}\ \boldsymbol{u_{RES}}\ \boldsymbol{u_{\dot{v}}}\ \boldsymbol{u_{\dot{F}_T}}\ \boldsymbol{u_{\dot{a}}}\ \boldsymbol{u_{GRF}}]^T$). The chosen state and control variables enabled the differential equations underpinning the dynamics of the musculoskeletal model (skeletal, contraction and activation) to be represented in an implicit, as opposed to explicit, first-order state-space formulation (Falisse *et al.*, 2019a; van den Bogert *et al.*, 2011). The implicit dynamics formulation resulted in enforcing the musculoskeletal model's first-order dynamics with simple

differential constraints, and algebraic path constraints were included to enforce the underlying differential equations of the musculoskeletal model (Table 4.3–1). The first-order dynamics constraints were enforced at the LGR points within a mesh interval, whilst all the algebraic path constraints were enforced at the beginning of each mesh interval. Continuity constraints for the state variables between the ending and beginning of the mesh intervals were also included. Equality path constraints were included to ensure the ground reaction forces from both the control variable and the foot-ground contact model matched at an optimal solution.

Table 4.3–1 Overview of the musculoskeletal model's constraints.

Dynamics Constraints	$\dfrac{d\boldsymbol{q}}{dt} = \boldsymbol{v}$	(1.1)
	$\dfrac{d\boldsymbol{v}}{dt} = \boldsymbol{u}_{\dot{v}}$	(1.2)
	$\dfrac{d\boldsymbol{F_T}}{dt} = \boldsymbol{u}_{\dot{F}_T}$	(1.3)
	$\dfrac{d\boldsymbol{a}}{dt} = \boldsymbol{u}_{\dot{a}}$	(1.4)
Path Constraints	$\boldsymbol{M(q)} \cdot \boldsymbol{u}_{\dot{v}} + \boldsymbol{C(q,v)} + \boldsymbol{G(q)} - \boldsymbol{J_{Ext}}^T \cdot \boldsymbol{Ext(u_{GRF}, AirDrag)} - \begin{bmatrix} \boldsymbol{0} \\ \boldsymbol{\tau} \end{bmatrix} = \boldsymbol{0}$	(2.1)
	$\boldsymbol{F_T} - \cos\bigl(\boldsymbol{\theta(q,F_T)}\bigr) \cdot \bigl(\boldsymbol{F_{CE}(q,v,F_T,a)} + \boldsymbol{F_{PE}(q,F_T)}\bigr) = \boldsymbol{0}$	(2.2)
	$\boldsymbol{0} \le \boldsymbol{u}_{\dot{a}} + \dfrac{\boldsymbol{a}}{\tau_d}; \ \tau_d = 60\ ms$	(2.3)
	$\boldsymbol{u}_{\dot{a}} + \dfrac{\boldsymbol{a}}{\tau_a} \le \dfrac{1}{\tau_a}; \ \tau_a = 15\ ms$	(2.4)
	$\boldsymbol{H}\ \boldsymbol{C_{GRF}(q,v)} - \boldsymbol{u_{GRF}} = \boldsymbol{0}$	(2.5)
Continuity Constraints	$\boldsymbol{x}_i^{END} - \boldsymbol{x}_{i+1}^1 = \boldsymbol{0}$	(3.1)

Note: Skeletal dynamics were enforced as per equation (2.1), where $\boldsymbol{M(q)}$ is the mass matrix, $\boldsymbol{C(q,v)}$ is the vector of centrifugal forces, $\boldsymbol{G(q)}$ is the vector of gravitational forces, $\boldsymbol{J_{Ext}}^T$ is the transpose of the external forces Jacobian matrix, $\boldsymbol{Ext(u_{GRF}, AirDrag)}$ is the vector of external forces and $\boldsymbol{\tau}$ is the vector of net joint moments (consisting of the moments generated by the MTUs, upper-limb and reserve actuators, and springs attached to the MTP DOFs). Contraction dynamics were imposed using the Hill model equilibrium condition (2.2), where the normalised tendon force must equal the projected sum of the normalised contractile $\boldsymbol{F_{CE}(q,v,F_T,a)}$ and passive $\boldsymbol{F_{PE}(q,F_T)}$ muscle forces. Activation dynamics were enforced using the inequality constraint equations (2.2 − 2.3), and they were derived from the original differential equation describing activation dynamics (De Groote *et al.,* 2009). Equation (2.5) was imposed to ensure consistency between the ground reaction forces calculated from the contact model $\boldsymbol{H}\ \boldsymbol{C_{GRF}(q,v)}$ and the controls $\boldsymbol{u_{GRF}}$.

4.3.4 Data-tracking simulation

To perform the data-tracking simulation it was first necessary to perform an empirical data collection. A thorough overview of the data collection procedures can be found in Haralabidis *et al.* (2021), and thus a summary is given here. Three-dimensional marker trajectories (250 Hz, Qualisys AB, Sweden) and ground reaction forces (2000 Hz, Kistler, Switzerland) were

collected from an international-level male sprinter (age: 24 years; height: 1.79 m; mass: 72.2 kg; 100m PB:10.33 s; 200 m PB: 20.27 s) as they performed two successful maximal effort sprints over three distances (0-10, 0-30 and 0-60 m). The participant provided written informed consent to take part in the data collection. The data collection protocol was approved by the University of Bath's Research Ethics Approval Committee for Health (EP 17/18 238). For the purposes of this study, the data collected from between the touchdown of the second step (right foot) to the takeoff of the third step (left foot) during the first 0-10 m trial (early acceleration phase) was extracted for further use. The extracted data together with the model described above were then used to perform inverse kinematics (global pelvis and relative joint angles) and dynamics (net joint moments) analyses within OpenSim (version 3.3, Stanford University, CA, USA) (Delp *et al.*, 2007). The kinematics and ground reaction forces were filtered using a fourth-order low-pass Butterworth filter with a 20 Hz cut-off frequency prior to performing the inverse dynamics analysis. B-splines were also fitted to the filtered kinematics data to enable velocities and accelerations to be determined. The splined kinematics, filtered ground reaction forces and net joint moments served as the experimental data to be tracked within the data-tracking simulation.

For the data-tracking simulation, the objective function $J_{TrackSim}$ consisted of three terms: a tracking term $J_{Tracking}$ that minimised the errors between experimental and simulated kinematics, ground reaction forces and net joint moments (excluding the net MTP moments), an effort term J_{Effort} that minimised the activations, and a control variables term $J_{Control}$ that minimised the reserve actuators control variables and those control variables introduced to permit the use of an implicit dynamics formulation ($\boldsymbol{u}_{\dot{v}}\ \boldsymbol{u}_{\dot{F}_T}\ \boldsymbol{u}_{\dot{a}}$):

$$J_{TrackSim} = J_{Tracking} + J_{Effort} + J_{Control} \tag{4.1}$$

$$J_{Tracking} = w_1 \sum_{j=1}^{37} \int_0^{t_f} \left(\frac{q_j^{EXP} - q_j^{SIM}}{range(q_j^{EXP})} \right)^2 dt + w_2 \sum_{n=1}^{6} \int_0^{t_f} \left(\frac{GRF_n^{EXP} - u_{GRF_n}^{SIM}}{range(GRF_n^{EXP})} \right)^2 dt$$

$$+ w_3 \sum_{k=1}^{29} \int_0^{t_f} \left(\frac{\tau_k^{EXP} - \tau_k^{SIM}}{range(\tau_k^{EXP})} \right)^2 dt \tag{4.2}$$

$$J_{Effort} = w_4 \sum_{i=1}^{92} \int_0^{t_f} \left(\frac{F_i^{max} a_i^{SIM^2}}{\sum_{i=1}^{92} F_i^{max}} \right) dt \tag{4.3}$$

$$J_{Control} = w_5 \sum_{m=1}^{17} \int_0^{t_f} \left(\frac{u_{res_m}^{SIM}}{bound\left(u_{res_m}^{SIM}\right)} \right)^2 dt + w_6 \sum_{j=1}^{37} \int_0^{t_f} \left(\frac{u_{\dot{v}_j}^{SIM}}{range\left(\ddot{q}_j^{EXP}\right)} \right)^2 dt$$

$$+ w_7 \sum_{i=1}^{92} \int_0^{t_f} \left(\frac{u_{\dot{F}_{T_i}}^{SIM}}{bound\left(u_{\dot{F}_{T_i}}^{SIM}\right)} \right)^2 dt + w_7 \sum_{i=1}^{92} \int_0^{t_f} \left(\frac{u_{\dot{a}_i}^{SIM}}{bound\left(u_{\dot{a}_i}^{SIM}\right)} \right)^2 dt \qquad (4.4)$$

where the superscripts EXP and SIM denote the experimental and simulated variables, respectively, t_f (0.436 s) denotes the duration of the extracted data from the trial being tracked, τ_k are the net joint moments, F_i^{max} are the MTU maximal isometric force parameters, and w_i are the weights whose values were set based upon the importance provided to the term being tracked or minimised ($w = [0.1\,0.05\,0.01\,0.01\,0.001\,0.0001\,0.1]$). The net MTP moments from the inverse dynamics analysis were not tracked due to experimental challenges related to the centre of pressure. The calculated differences between the experimental and simulated variables within $J_{Tracking}$ (excluding the anterior-posterior pelvis translation difference), and the time derivatives of the generalised velocities control variables were normalised by 10% of each variables experimental range (determined from the trial being tracked. The anterior-posterior pelvis translation difference was normalised by 0.01 m to ensure it was tracked accurately. The remainder of the variables within $J_{Control}$ were normalised by their respective upper bounds.

The initial guess alongside the lower and upper bounds of the state and control variables were set using the experimental data of the trial being tracked where possible. The splined experimental kinematics were used to initialise q, v and $u_{\dot{v}}$, and their bounds were set to be 25% more than and less than the maximum and minimum of the values, respectively, obtained from the splined kinematics. The initial guess for the u_{UL} was set using the results from the inverse dynamics analysis. The u_{RES} and u_{GRF} were initialised as zero, with bounds of $\pm$ 10 Nm (40 Nm MTP DOFs) and $\pm$ 2500 N, respectively. The same initial guess and bounds as Falisse *et al.* (2019a) was used for F_T, a, $u_{\dot{F}_T}$ and $u_{\dot{a}}$.

4.3.5 Predictive simulations

In previous predictive simulation studies of sporting tasks, for instance jumping (Porsa *et al.*, 2016) and sprinting (Celik and Piazza, 2013), the objective has been to predict novel movements without considering technique changes. However, the primary objective of the predictive simulations carried out in this investigation was to explore how modifications in

sprinting technique can lead to improvements in performance during the early acceleration phase. We explored modifications to sprinting technique from a net joint moments paradigm as they are the drivers for movement, as described previously, and we specifically focused on the net ankle, knee, and hip flexor-extensor moments. Specifically, the predictive simulations were performed by enabling either individual or combinations of the listed net joint moments to freely vary whilst the remaining net joint moments within the predictive simulations aimed to coincide with those determined from the data-tracking simulation. The net joint moments which we were not attempting to modify were tracked to permit subsequent inferences to changes in performance to be attributed to the net joint moments which we gave the freedom to change. Seven predictive simulations were performed in total. Three of the predictive simulations enabled the net ankle, knee, and hip flexor-extensor moments to independently vary freely (A-free, K-free and H-free), another three predictive simulations enabled combinations of two of the net joint moments to independently vary freely (A-K-free, A-H-free and K-H-free) and the final simulation enabled all three of the net joint moments to independently vary freely (A-K-H-free). The time horizon duration was also treated as a variable to be determined from each of the predictive simulations. The following constraints were imposed for each predictive simulation:

$$[\boldsymbol{q}_1^1 \; \boldsymbol{v}_1^1]^T = \begin{bmatrix} \boldsymbol{q}_{1_{Track}}^1 \; \boldsymbol{v}_{1_{Track}}^1 \end{bmatrix}^T \tag{6.1}$$

$$q_{pelvis_{x_1}}^{END} = q_{pelvis_{x_{1_{Track}}}}^{END} \tag{6.2}$$

$$-\boldsymbol{10°} \leq \boldsymbol{q}_{JointAngles_1^{END}} - \boldsymbol{q}_{JointAngles_{1_{Track}}^{End}} \leq \boldsymbol{10°} \tag{6.3}$$

the first constraint (6.1) was imposed to ensure the state variables of the musculoskeletal model's multibody dynamics at the beginning of the simulation matched with those determined from the data-tracking simulation; the second constraint (6.2) ensured that the anterior-posterior displacement of the musculoskeletal model's pelvis segment at the end of the simulation matched with the value obtained from the data-tracking simulation; and the third constraint (6.3) was imposed to ensure that the relative joint angles of the musculoskeletal model at the end of the simulation fell within ± 10° of those obtained from the data-tracking simulation.

For each of the predictive simulations, the cost function $J_{PredSim}$ consisted of four terms: a duration of time horizon minimisation term J_{Time}, a tracking term $J_{Tracking}$ that minimised the

differences between certain data-tracking simulation and predictive simulation net joint moments, an effort term J_{Effort} that minimised the activations, and a control variables term $J_{Control}$ that minimised the reserve actuators control variables and those control variables introduced to permit the implicit dynamics formulation ($\boldsymbol{u}_{\dot{v}}$ $\boldsymbol{u}_{\dot{F}_T}$ $\boldsymbol{u}_{\dot{a}}$):

$$J_{PredSim} = J_{Time} + J_{Tracking} + J_{Effort} + J_{Control} \tag{5.1}$$

$$J_{Time} = W_1 t_f^{Pred} \tag{5.2}$$

$$J_{Tracking} = W_2 \sum_{a=1}^{31} w_a^\tau \int_0^{t_f^{Pred}} \left(\frac{\tau_a^{Track} - \tau_a^{Pred}}{range(\tau_a^{Track})} \right)^2 dt \tag{5.3}$$

$$J_{Effort} = W_3 \sum_{i=1}^{92} \int_0^{t_f^{Pred}} \left(\frac{F_i^{max} a_i^{SIM^2}}{\sum_{i=1}^{92} F_i^{max}} \right) dt \tag{5.4}$$

$$J_{Control} = W_4 \sum_{m=1}^{17} \int_0^{t_f^{Pred}} \left(\frac{u_{res_m}^{SIM}}{bound(u_{res_m}^{SIM})} \right)^2 dt + W_5 \sum_{j=1}^{37} \int_0^{t_f^{Pred}} \left(\frac{u_{\dot{v}_j}^{SIM}}{range(\ddot{q}_j^{EXP})} \right)^2 dt$$

$$+ W_6 \sum_{i=1}^{92} \int_0^{t_f^{Pred}} \left(\frac{u_{\dot{F}_{T_i}}^{SIM}}{bound\left(u_{\dot{F}_{T_i}}^{SIM}\right)} \right)^2 dt + W_6 \sum_{i=1}^{92} \int_0^{t_f^{Pred}} \left(\frac{u_{\dot{a}_i}^{SIM}}{bound(u_{\dot{a}_i}^{SIM})} \right)^2 dt \tag{5.5}$$

where t_f^{Pred} represents the to be determined duration of the time horizon, τ_a^{Track} and τ_a^{Pred} denote the a'th tracking and predictive simulation net joint moment, W_i are the weights of the being minimised or tracked ($\boldsymbol{W} = [50\ 0.1\ 0.01\ 1\ 0.0001\ 0.1]$), and $\boldsymbol{w}^\tau$ is a ones-vector with the indices of the net joint moments not tracked changed to zero for each of the seven predictive simulations. The data-tracking simulation and predictive simulation variable differences within $J_{Tracking}$ were normalised by 2% of their respective range as determined from the data-tracking simulation. This was done to ensure that the net joint moments which we did not want to freely change were still tracked reasonably accurately. The threshold selected coincided with a permissible error of 5 Nm assuming a 250 Nm peak. The variables within $J_{Control}$ were normalised as per the data-tracking simulation.

The initial guess for the state and control variables for each simulation were set to the values determined from the data-tracking simulation. The lower and upper bounds of the state and control variables were identical to those used in the data-tracking simulation. The lower bound

of t_f^{Pred} was set to 5% less than the original value of t_f used in the data-tracking simulation (0.414 s), whilst the upper bound was kept at the original value of t_f.

4.3.6 Optimal control problem solution approach

The data-tracking and predictive simulations were formulated in MATLAB (2017b; MathWorks Inc., Natick, MA, USA) using CasADi (Andersson *et al.*, 2019), and solved using IPOPT (Wächter and Biegler, 2006) with an adaptive barrier parameter strategy and NLP convergence tolerance of 10^{-3}. The variables for each NLP were scaled to lie on the interval [-1,1] and the constraints were scaled to improve the convergence rate and numerical conditioning as per recommendations of Betts (2010).

4.3.7 Outcome measures

The data-tracking simulation was evaluated by calculating the root mean squared difference (RMSD) between the tracked experimental data and simulated data, and the reported RMSDs are of categories of variables (e.g., global pelvis translations and net lower-limb flexor-extensor joint moments). The performance of the data-tracking and predictive simulations was quantified using average horizontal external power (Bezodis *et al.*, 2010) and was calculated as the rate of change in kinetic energy between the start and end of each simulation. The horizontal CoM velocity at the end of each simulation and the time horizon duration were also extracted as performance outcomes. The horizontal impulses (net, propulsive and braking) were calculated across each stance phase using trapezoidal quadrature and previously identified kinematics-based technique variables at touchdown and takeoff instances were also extracted. To further foster comparison between the data-tracking and predictive simulations from a net joint moments perspective, the peak flexor and extensor net joint moments during stance were extracted.

4.4 Results

4.4.1 Data-tracking simulation

The kinematics and kinetics from the data-tracking simulation were found to closely match the corresponding experimental data (Supplementary material Figures 4.7–1 to 4.7–4). The average RMSDs were less than 1° and 0.3 cm for the global pelvis angles and translations, respectively, and less than 1° for the relative joint angles. For the right and left stance phase ground reaction force components, they were tracked with an RMSD of 0.050 and 0.054 BW

(anterior-posterior), 0.034 and 0.033 BW (vertical) and 0.003 and 0.009 BW (medial-lateral). The average RMSDs of the tracked net joint moments and the net lower-limb joint moments were 16.3 and 17.5 Nm, respectively. These results demonstrate that the modelling and simulation framework used was a sufficient representation of reality and therefore suitable for performing the proposed predictive simulations.

4.4.2 Predictive simulations

Performance Outcomes

Each of the predictive simulations performed resulted in improvements to overall performance as indicated by the average horizontal external power (Figure 4.4–1). The greatest improvement in performance was found for A-K-H-free (22.0%; 1401.2 vs. 1148.7 W), and this simulation also led to the greatest improvements in terminal horizontal CoM velocity (3.2%; 6.05 vs. 5.86 m/s) and time horizon duration (-4.4%; 0.417 vs. 0. 436 s).
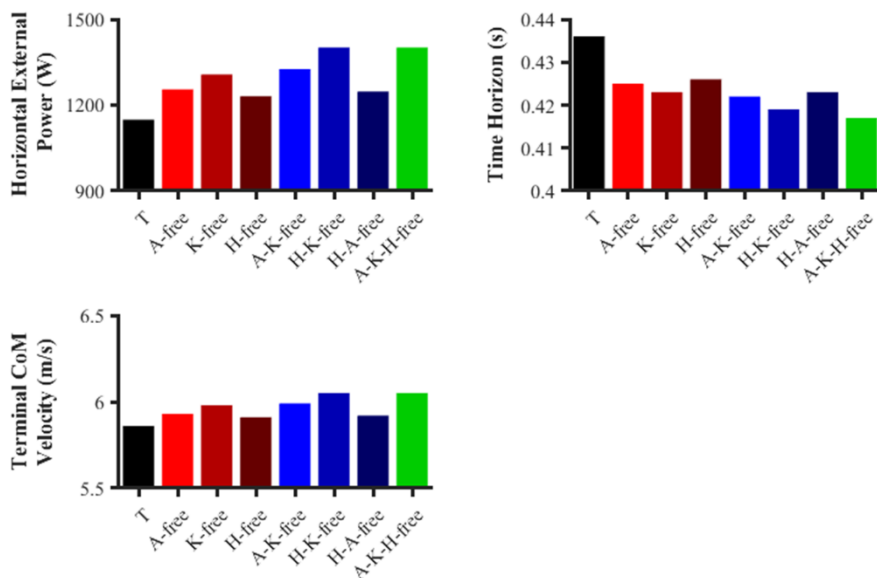
Figure 4.4–1 Metrics to quantify the sprint performance in the data-tracking (T) and predictive simulations (A-free, K-free, H-free, A-K-free, H-K-free, H-A-free, A-K-H-free). Bar colours are matching the colour code used in the previous figures (black, red, scarlet, cranberry, blue, indigo, navy, green).

Horizontal Impulses

All the predictive simulations were found to generate greater net horizontal impulse during the right foot stance phase compared to the data-tracking simulation (68.4 (average) vs. 58.8 Ns). For the left foot stance phase, the net horizontal impulse generated was lower in several of the predictive simulations (A-free, H-free, A-K-free, H-A-free) compared to the data-tracking

simulation (Figure 4.4–2), but not for the predictive simulation that led to the largest performance improvements (A-K-H-free). Despite the lower net horizontal impulse of those simulations, the net horizontal impulse surplus they generated during the right foot stance was still sufficient to produce an overall improvement in performance (average horizontal external power and terminal horizontal CoM velocity) (Figure 4.4–1).
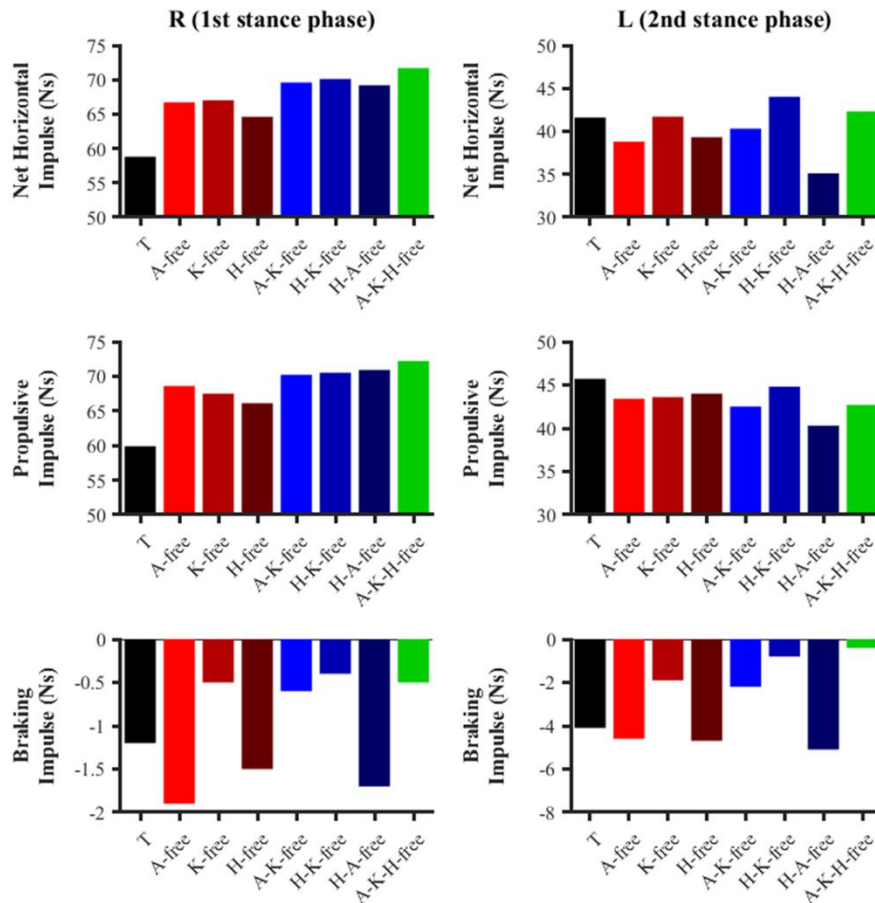
Figure 4.4–2 Right (R) and left (L) stance phase anterior-posterior impulses for the data-tracking (T) and predictive simulations (A-free, K-free, H-free, A-K-free, H-K-free, H-A-free, A-K-H-free). Bar colours are matching the colour code used in the previous figures (black, red, scarlet, cranberry, blue, indigo, navy, green).

The predictive simulations were found to generate greater propulsive impulse during the right foot stance phase compared to the data-tracking simulation (69.4 (average) vs. 59.9 Ns). In comparison to the data-tracking simulation, all the predictive simulations were found to produce less propulsive impulse during the left foot stance phase (45.7 vs. 43.0 (average) Ns) (Figure 4.4–2). There was not a clear trend in the simulation results for the braking impulse, although the predictive simulations which led to the greatest improvements in performance (A-K-H-free and H-K-free) produced lower braking impulses (average left: -0.5, average right: -0.6 Ns).

Figure 4.4–3 Right and left anterior-posterior, vertical and medial-lateral GRF from right foot touchdown to left foot takeoff for the data-tracking (T) and predictive simulations (A-free, K-free, H-free, A-K-free, H-K-free, H-A-free, A-K-H-free). The horizontal bars at the top of the figure indicate the periods of stance.

Kinematics and Timings

Very minor differences in the duration of the right foot stance phases were observed between the data-tracking and predictive simulations (0.189 vs. 0.185 (average) s), however potentially more meaningful reductions were found for the left foot stance phases (0.169 vs. 0.159 (average) s). A trend was observed for the horizontal foot touchdown velocity of the left stance phase to be lower as performance was found to increase (Figure 4.4–4). The lowest horizontal foot touchdown velocity of the left stance was found to be 0.99 m/s for A-K-H-free. There was no noticeable trend for the horizontal CoM-foot touchdown distance of the left stance phase, with values ranging between -3.1 and 0.9 cm.
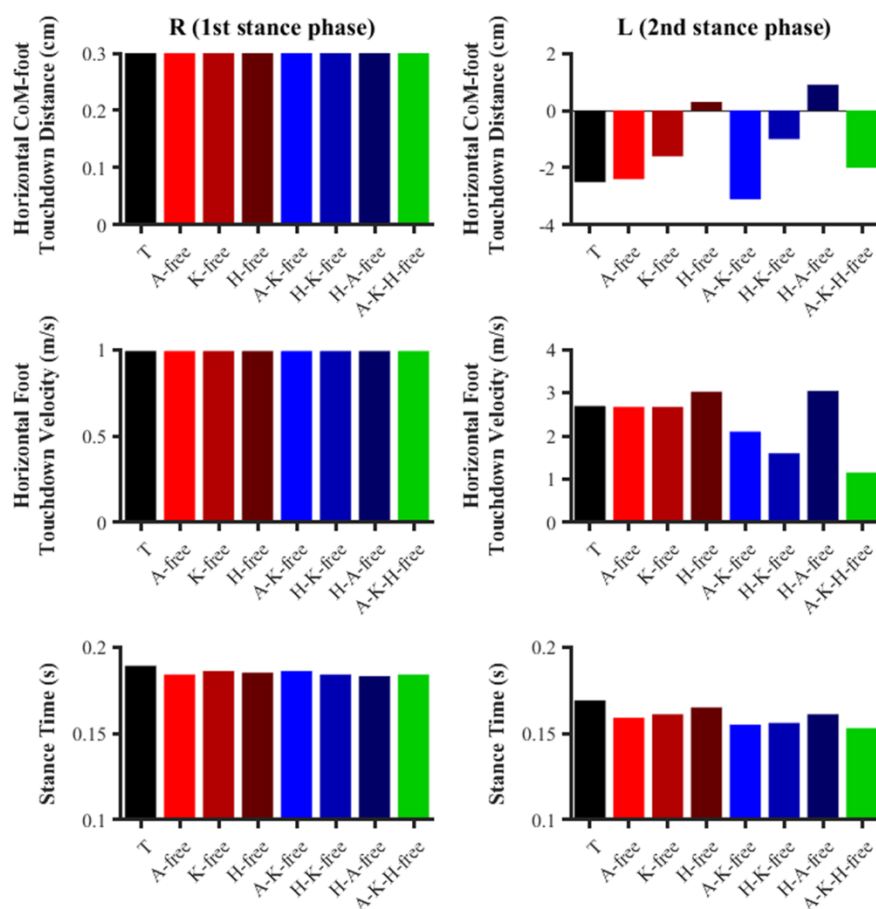
Figure 4.4–4 Right (R) and left (L) touchdown kinematics and stance phase durations for the data-tracking (T) and predictive simulations (A-free, K-free, H-free, A-K-free, H-K-free, H-A-free, A-K-H-free). Bar colours are matching the colour code used in the previous figures (black, red, scarlet, cranberry, blue, indigo, navy, green). *Note:* horizontal CoM-foot touchdown distance and horizontal foot touchdown velocity are identical for right foot touchdown as the state variables of the musculoskeletal model's multibody dynamics at the beginning of each simulation were constrained to match those determined from the data-tracking simulation. A negative horizontal CoM-foot touchdown distance indicates that the foot was behind the CoM.

There was no clear trend in hip extension (-1° to -10°) and knee flexion (-22° to -31°) takeoff angles for the right foot stance phases of the predictive simulations compared to the data-tracking simulation (Figure 4.4–5). All the predictive simulations achieved a hip extension takeoff angle of approximately -7° for the left foot stance phase, and this also matched with the data-tracking simulation. All the predictive simulations reached a knee flexion takeoff angle of approximately -30° for the left foot stance phase, whilst for the data-tracking simulation the knee was more extended (-21°).
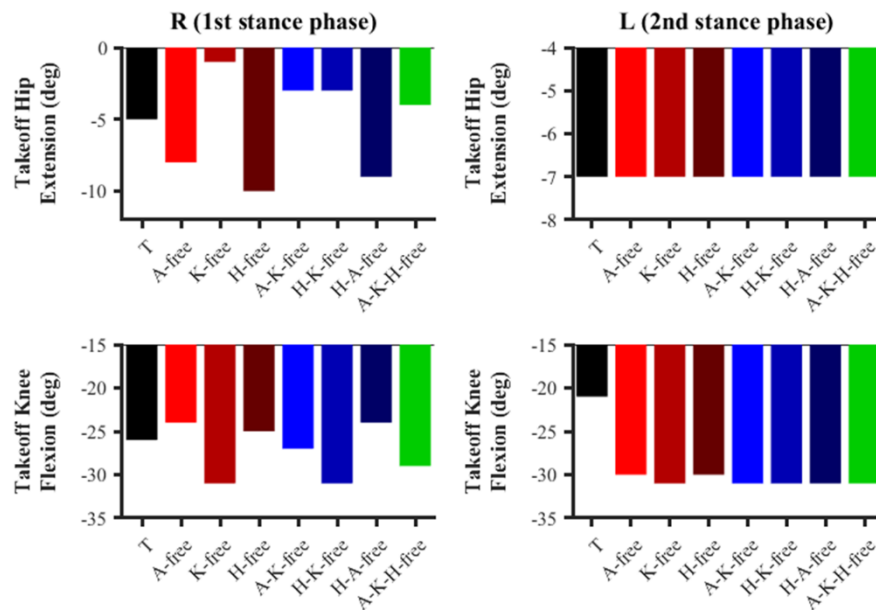
Figure 4.4–5 Right (R) and left (L) hip extension and knee flexion angles at takeoff for the data-tracking (T) and predictive simulations (A-free, K-free, H-free, A-K-free, H-K-free, H-A-free, A-K-H-free). Bar colours are matching the colour code used in the previous figures (black, red, scarlet, cranberry, blue, indigo, navy, green). *Note:* full knee extension = 0° and knee flexion is negative; thigh aligned vertically with pelvis corresponds to hip flexion-extension = 0°, and hip flexion is positive and hip extension is negative. These are consistent with the model's definitions.
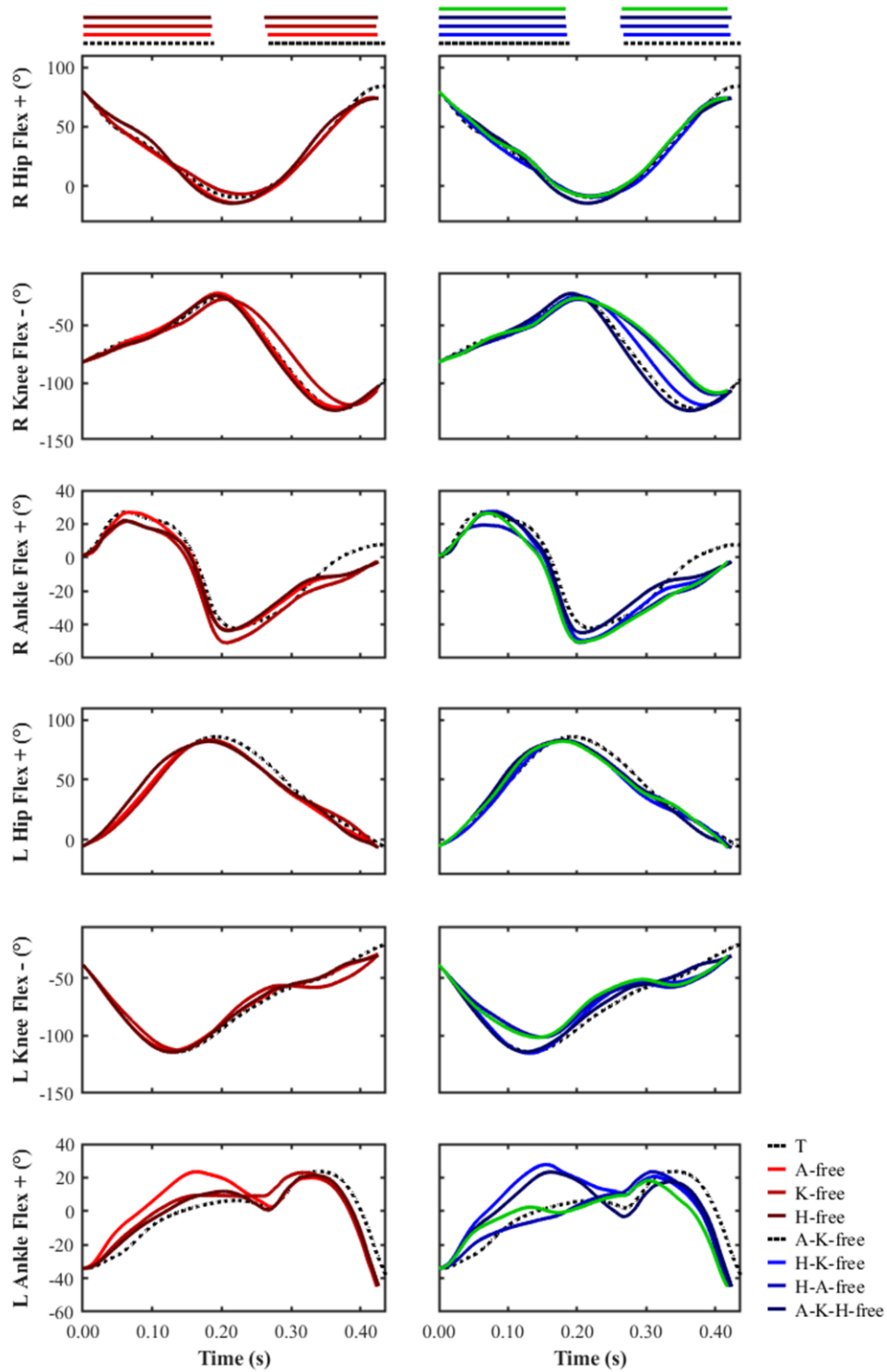
Figure 4.4–6 Right and left ankle, knee, and hip flexion-extension angles from right foot touchdown to left foot takeoff for the data-tracking (T) and predictive simulations (A-free, K-free, H-free, A-K-free, H-K-free, H-A-free, A-K-H-free). The horizontal bars at the top of the figure indicate the periods of stance.
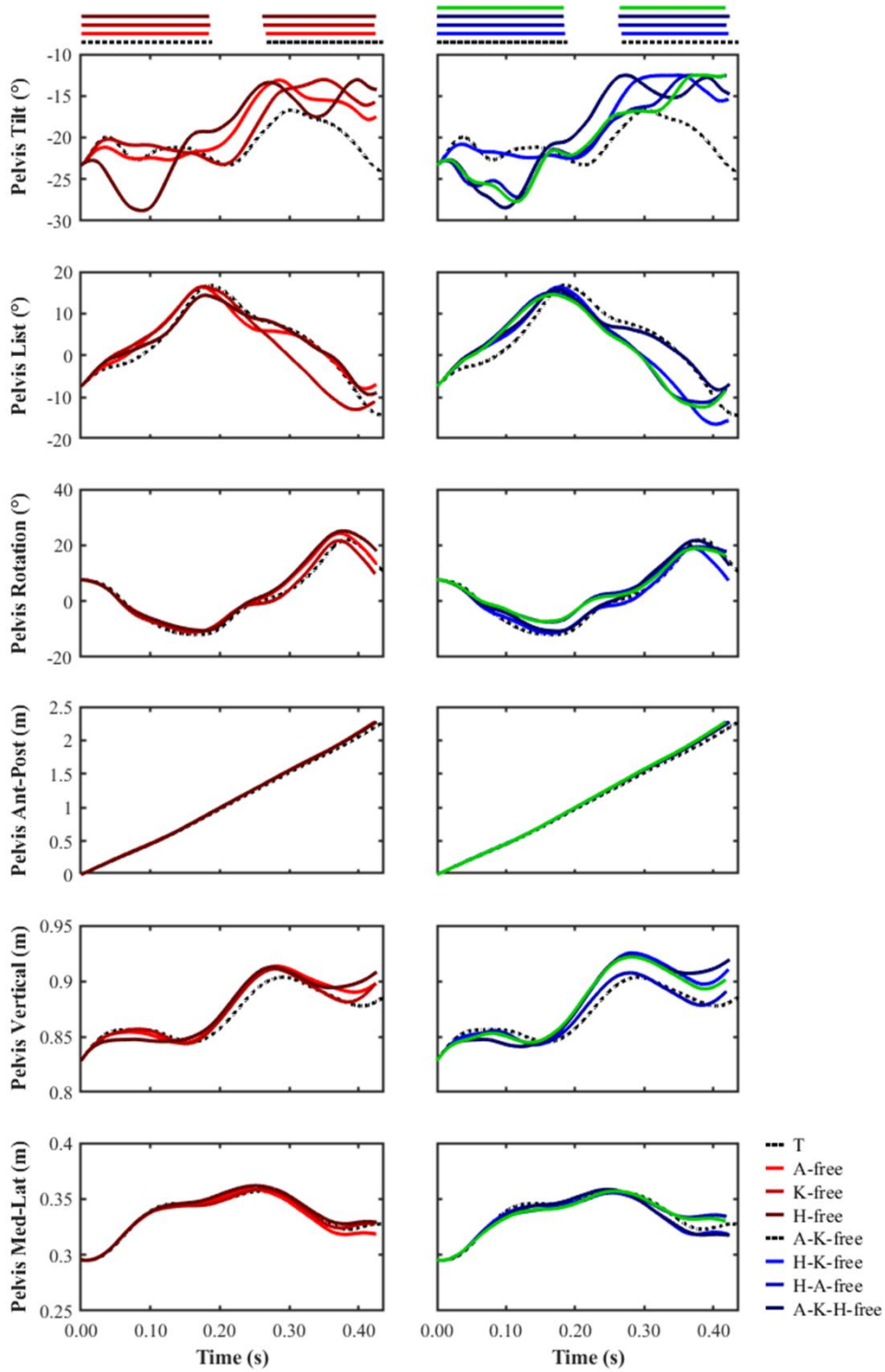
Figure 4.4–7 Global pelvis angles and translations from right foot touchdown to left foot takeoff for the data-tracking (T) and predictive simulations (A-free, K-free, H-free, A-K-free, H-K-free, H-A-free, A-K-H-free). The horizontal bars at the top of the figure indicate the periods of stance.

Peak Net Flexor and Extensor Moments

The most discernible differences in the peak net flexor and extensor moments were observed for the knee and hip (Figure 4.4–8). The 'knee-free' simulations were found to generate a greater peak net knee flexor (average 100.3%; 141.2 vs. 70.5 Nm) and extensor moment (average 37.1%; 188.5 vs. 137.5 Nm) across both right and left stance phases compared to the data-tracking simulation. The H-K-free and A-K-H-free predictive simulations were found to generate a greater peak net hip flexor (average 23.6%; 194.5 vs. 157.3 Nm) and extensor moment (average 20.2%; 266.9 vs. 222.9 Nm) across both stance phases in comparison to the data-tracking simulation.
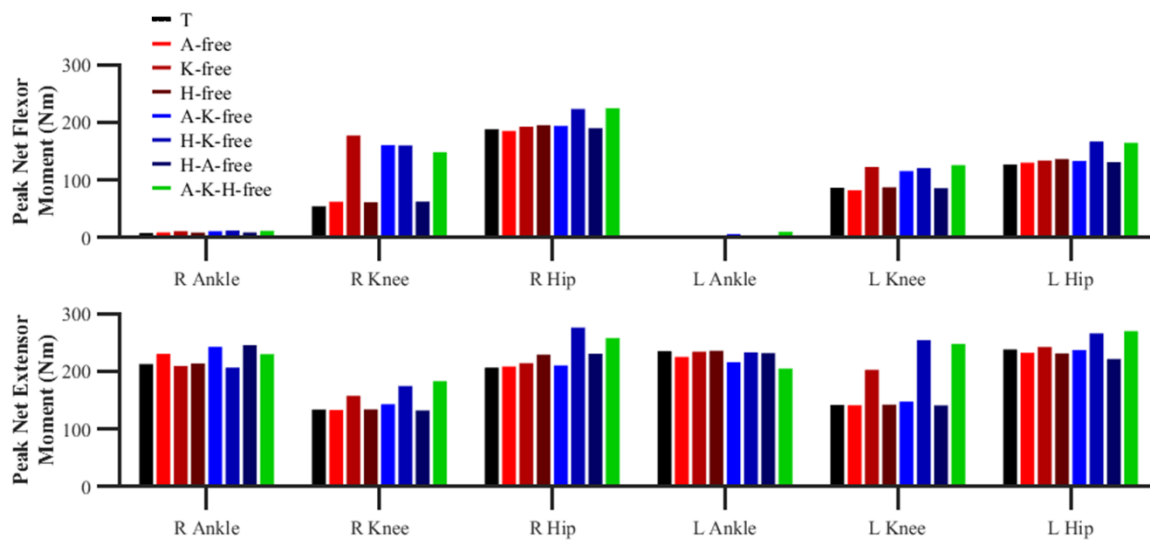
Figure 4.4–8 Right (R) and left (L) peak ankle, knee, and hip net flexor and extensor moments during the right and left stance phases for the data-tracking (T) and predictive simulations (A-free, K-free, H-free, A-K-free, H-K-free, H-A-free, A-K-H-free). Bar colours are matching the colour code used in the previous figures (black, red, scarlet, cranberry, blue, indigo, navy, green).
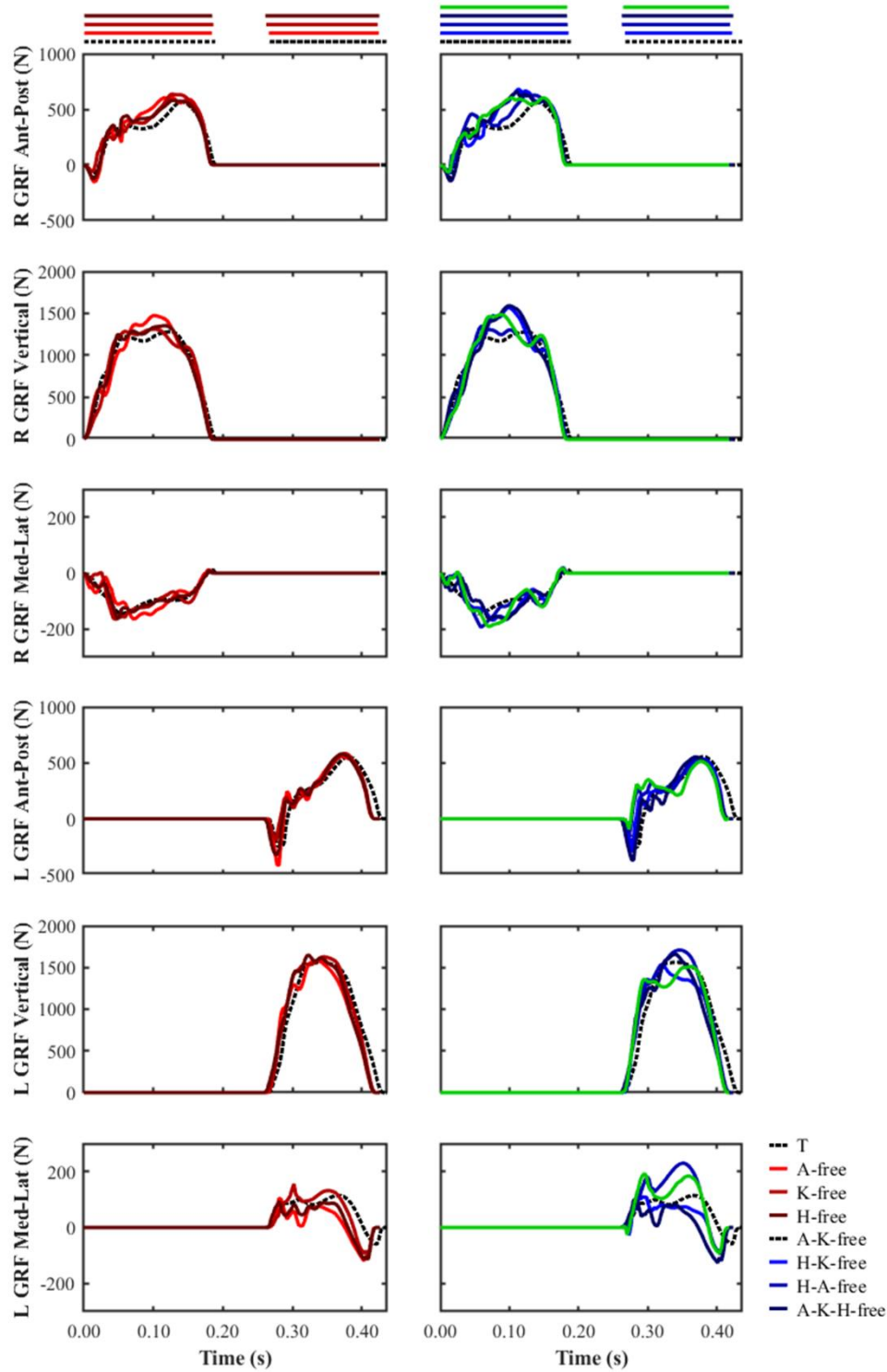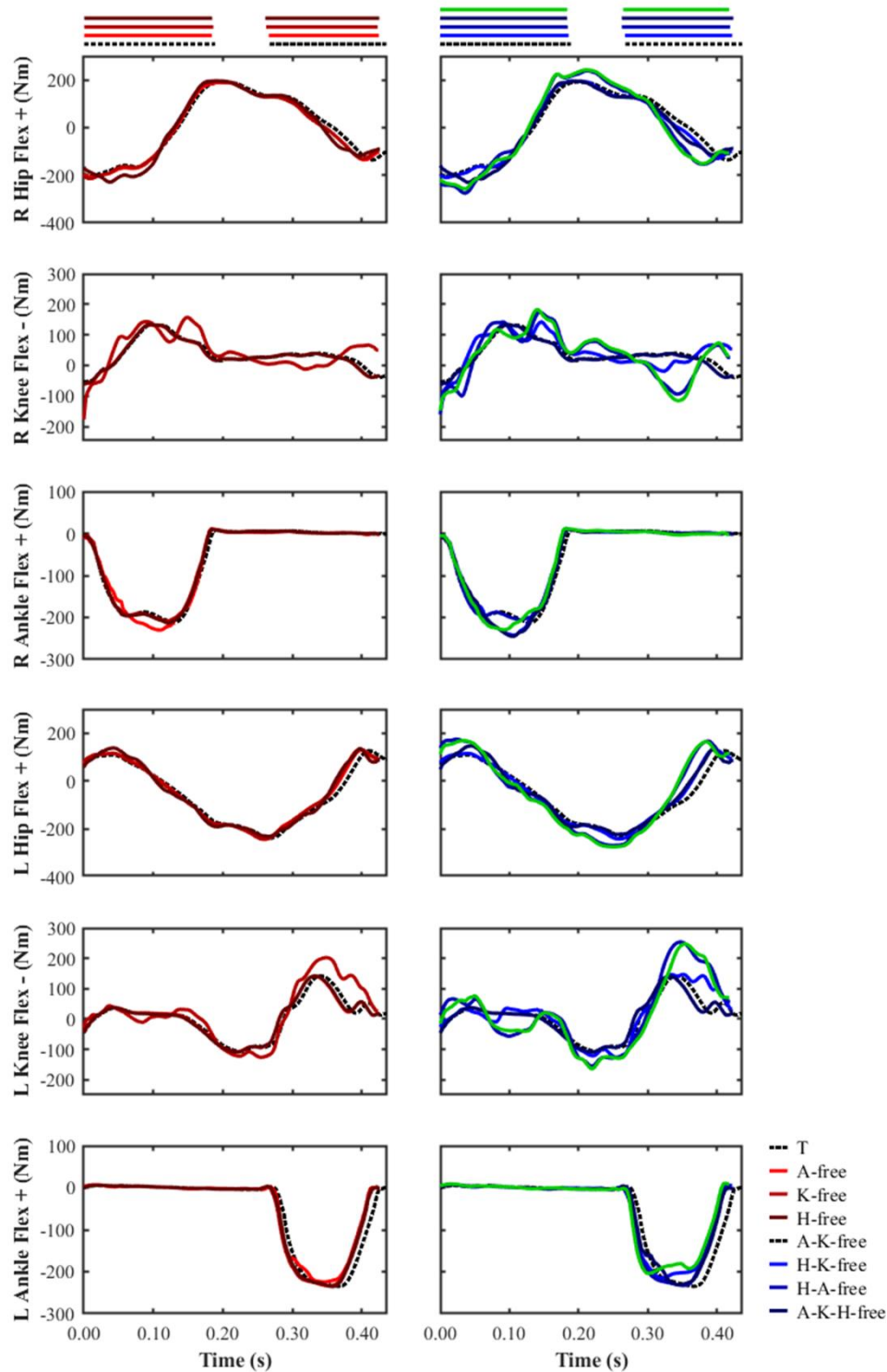
Figure 4.4–9 Right and left ankle, knee, and hip net flexor-extensor moments from right foot touchdown to left foot takeoff for the data-tracking (T) and predictive simulations (A-free, K-free, H-free, A-K-free, H-K-free, H-A-free, A-K-H-free). The horizontal bars at the top of the figure indicate the periods of stance.

4.5 Discussion

The primary purpose of this investigation was to identify how modifications in technique influence performance during the preliminary steps of accelerative sprinting. This was achieved by using a predictive simulation and modelling approach where the major lower-limb (ankle, knee, and hip) flexor-extensor net joint moments were modified individually and in combination. We found that the predictive simulations which enabled the net knee moments to vary (K-free) resulted in the greatest improvements in performance. More specifically, the K-free and K-H-free predictive simulations resulted in a 13.8% and 21.9% increase of average horizontal external power, respectively. The predictive simulation which permitted all the targeted net joint moments to change, A-K-H-free, was found to improve average horizontal external power production the greatest (22.0%) compared to all the other predictive simulations. The secondary aim of this study was to provide further insights into the front-side mechanics coaching framework, for which there is currently a limited amount of literature. The subset of 'hip-free' predictive simulations were found to coincide with the front-side mechanics coaching framework from a joint kinetics perspective, as we observed earlier and greater generation of net hip flexor moment during stance. However, the results from our predictive simulations did not provide evidence in support of the kinematics-based aspects of the front-side mechanics coaching framework. Videos of the kinematics from the data-tracking and predictive simulations, in addition to the data files, can be accessed online at https://doi.org/10.6084/m9.figshare.14988051.

The predicted changes in the timings and magnitude of the targeted lower-limb net joint moments are responsible for the improvements in performance, and the subset of 'knee-free' predictive simulations resulted in the greatest performance enhancement. For those predictive simulations, a greater and earlier net knee flexor moment during the late swing phase prior to the initiation of the left foot stance phase was found in comparison to the data-tracking simulation (Figure 4.4–9). The potential benefit of this aspect of technique is to reduce the magnitude of the braking impulse by driving the lower-limb backwards at touchdown and therefore reducing the horizontal touchdown velocity of the foot (Hunter *et al.*, 2005; Mann and Sprague, 1980). Indeed, for the 'knee-free' predictive simulations, the magnitude of the braking impulse decreased (Figure 4.4–2), together with a reduction in the horizontal touchdown velocity of the foot (Figure 4.4–3). The net hip extensor moment during the late swing phase has been suggested to perform a similar role as the net knee flexor moment (Hunter *et al.*, 2005; Mann and Sprague, 1980), and we observed this phenomenon in the H-free and

H-K-free predictive simulations (Figure 4.4–9). Greater reductions in the horizontal foot touchdown velocity (left foot stance phase) and the braking impulses were observed in the H-K-free predictive simulation, thus demonstrating the combined benefits of the actions of those net joint moments. The technique improvements from those net joint moments are potentially due to an enhanced coordination of the hamstring muscles, as they are responsible for both knee flexion and hip extension. Furthermore, Morin *et al.* (2015a) identified the significance of the hamstring muscles in the late swing phase in relation to ground reaction force production based on electromyography measurements. The computational modelling and simulation approach utilised in this study permitted exploring the behaviour of the hamstring muscles more thoroughly, however it was deemed beyond the scope of this study. In further work we will perform a detailed analysis of the results we have obtained in this study at a muscle level to explore potential changes in the coordination of the hamstring muscles.

The above findings demonstrate that a key feature of improving acceleration performance is by minimising the braking impulses during the early portion of the stance phase via the generation of greater net knee flexor and net hip extensor moments. However, previous experimental studies (Colyer *et al.*, 2018a; Morin *et al.*, 2015b; Nagahara *et al.*, 2018) have found that improved early accelerative sprinting is based on an individual's ability to generate greater propulsive impulses as opposed to reduced braking impulses, which tends to differentiate sprinters more in the latter stages of accelerative sprinting. A potential explanation for this discrepancy is due to the different study designs embraced. The studies by Colyer *et al.* (2018a), Morin *et al.* (2015b) and Nagahara *et al.* (2018) used a cross-sectional study approach, whilst the predictive simulations carried out in this study can almost be viewed as enabling a highly controlled intervention study, where individualised enhancement in performance was achieved via reducing the braking impulses. However, it is possible that with a different athlete for which the musculoskeletal model was scaled to, the strategy for improving performance may have been different (i.e., increase propulsive impulses) due to differing organismic constraints (e.g., inertial or MTUs parameters) (Glazier and Davids, 2009; McErlain-Naylor *et al.*, 2021). Nevertheless, we believe that this is a particular strength of the approach adopted, as individualised technique recommendations to improve performance can be administered instead of group level recommendations which may or may not be beneficial for a particular athlete.

The 'knee-free' predictive simulations were found to increase the magnitude of the peak net knee extensor moment during the late stance phase in comparison to the data-tracking simulation. This finding is in line with a previous study (Bezodis *et al.*, 2014), which focused on the lower-limb net joint kinetics of three international calibre athletes during the first stance phase of accelerative sprinting. Specifically, Bezodis *et al.* (2014) identified that the most distinguishing feature of technique in relation to performance was the net knee extensor moment, as the highest performing athlete was found to generate a greater and earlier net knee extensor moment. The results from our predictive simulations therefore provide further evidence to support the existing notion of the link between the behaviour of the net knee extensor moment and early accelerative sprinting performance. Interestingly, Schache *et al.* (2019) found that there was a strong association between the impulses of the net hip and ankle extensor moments and forward acceleration during accelerative sprinting. Interpreting our findings together with the work of Schache *et al.* (2019) and Bezodis *et al.* (2014) suggest that the net knee joint moments have a major performance benefitting role in early accelerative sprinting. However, the net ankle and hip joint moments are also fundamental to continue enabling an athlete to accelerate their CoM whilst sprinting.

In the A-K-H-free predictive simulation all the targeted net joint moments were able to vary, and we therefore anticipated that the optimal technique uncovered would likely coincide with the greatest improvements in performance. In fact, the A-K-H-free predictive simulation identified the optimal combination of the net joint moments that resulted in the greatest overall average horizontal external power improvement (22.0%). However, the performance improvement was not much greater than the H-K-free predictive simulation (Figure 4.4–1). A potential explanation for why we did not observe a greater improvement in performance for the A-K-H-free predictive simulation is due to the intrinsic physiological constraints of the MTUs (e.g., multiple roles per joint and biarticular), as they are required to both reproduce the tracked net joint moments whilst also generate the non-tracked net joint moments, and thus the scope for further improvements is limited due to a reduced space of potential solutions. It is also possible that the results we have obtained are due to the gradient-based optimal control approach we have used, which may have led to a local optimum solution as opposed to a global optimum solution. To assess this issue a previous study (Porsa *et al.*, 2016), using similar methods to those used in this study, explored the use of different initial guesses. Nevertheless, in this study, the same initial guess was used to initialise each of the predictive simulations. For simple OCPs with low complexity models it is feasible to initialise them with different

initial guesses to prevent the possibility of achieving a local optimal solution. However, given the complexity of our OCPs and the model we have used we did not explore this, as in our experience a poor initial guess can lead to simulations not converging or making very trivial progress between iterations. Thus, we opted to initialise each of the predictive simulations from a feasible solution, which was in this case the data-tracking solution.

A-free

H-K-free

K-free

H-A-free

H-free

A-K-H-free

A-K-free
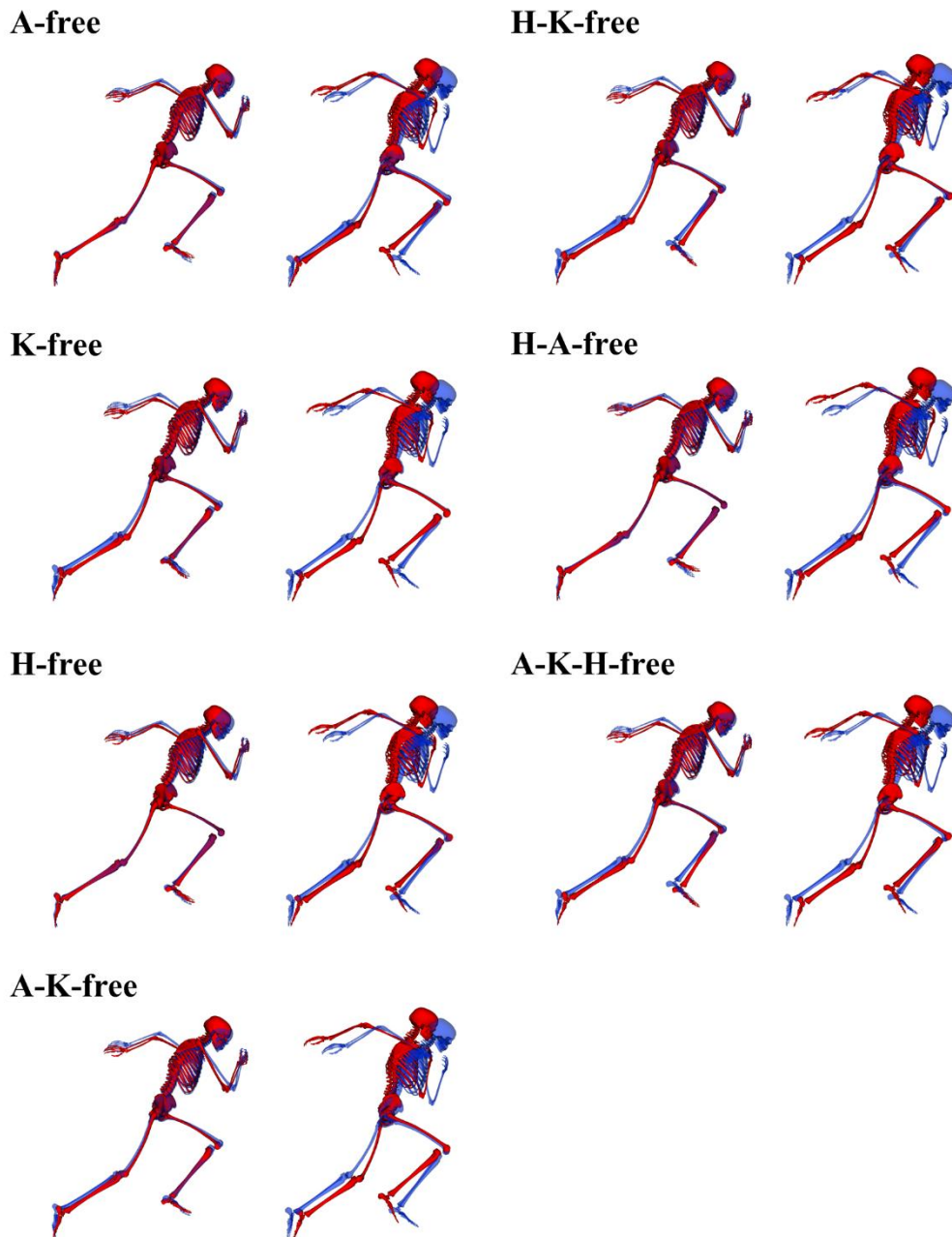
Figure 4.5–1 Right and left takeoff configurations for the data-tracking (blue model) and predictive simulations (red model).

A further important aspect of technique we identified was the increase in magnitude and timing of the net hip flexor moment, particularly for the second stance phase, in the 'hip-free' predictive simulations. This technique aspect has been suggested to be imperative for reversing the rotation of the hip (extension to flexion), and Mann and Murphy (2015) have stipulated that the highest calibre athletes generate a net hip flexor moment for the latter ~75% of the stance phase. More specifically, it is thought to prevent unnecessary extension at the hip and permits front-side mechanics dominance. In the 'hip-free' predictive simulations we see the transition to earlier and greater net hip flexor moments when compared to the data-tracking simulation, with ~60% of the stance phase been net hip flexor moment dominant. This provides some evidence towards the front-side mechanics coaching framework.

Interestingly, the discrete kinematics variables suggested to be important for demonstrating front-side mechanics, for example knee flexion and hip extension angles at takeoff (Figure 4.4–5), did not reveal any clues to further support or reject the front-side mechanics coaching framework. Furthermore, the pose of the model at takeoff was not found to demonstrate front-side mechanics (Figure 4.5–1). For the predictive simulations, the trunk was found to become more vertical at takeoff and this was accompanied by a concomitant reduction in thigh extension, however the reduced thigh extension was not sufficient to clearly demonstrate front-side mechanics at takeoff. It is possible that the kinematics-based criteria of front-side mechanics did not emerge from the predictive simulations due to the margins of improvement in performance. For instance, the eight male finalists, competing at the 2018 60 m World Athletics Championships, achieved second and third stance phase durations between 0.153-0.193 and 0.120-153 s, respectively, (Walker *et al.*, 2019). Meanwhile the lowest second and third stance phase durations for the predictive simulations were 0.183 and 0.153 s, respectively, and a previous study has reported a strong association between stance phase duration and accelerative sprinting performance have been reported (Morin *et al.*, 2012). Whilst these stance phase durations give credibility to the predictive simulation results, the lack of front-side mechanics may explain why they are higher than the lower bounds achieved by the finalists. This also coincides with the beliefs held by Mann and Murphy (2015), in which only the highest calibre athletes are able to perform with front-side mechanics. The lack of clear front-side mechanics dominance emerging from our predictive simulations may also be due to insufficient strength within the musculoskeletal model or the properties and geometry of the MTUs not been representative of sprinters. For instance, the moment arms of the major knee extensor muscles have been shown to be greater in sprinters compared to non-sprinters (Miyake *et al.*,

2017). Future work should therefore aim to disentangle the ability to perform front-side mechanics by potentially using a predictive computational modelling and simulation approach, as per this study, with a subject-specific model informed by medical imaging (e.g., magnetic resonance imaging) to explore the confounding factors described above.

Previous studies have performed predictive simulations of sprinting to address a variety of research purposes (Bezodis *et al.*, 2015; Celik and Piazza, 2013; van den Bogert and Ackermann, 2009). However, to the authors' knowledge this is the first study to perform predictive simulations of sprinting whilst using state-of-the-art computational modelling and simulation approaches (e.g., three-dimensional musculoskeletal model) for the purposes of exploring the interactions between technique and performance. In previous studies, model complexity and simulation duration were sacrificed likely due to the large computational cost incurred to solve an OCP together with the inefficient means of discretising the OCP. In this study we performed predictive simulations of sprinting by transcribing the OCP using direct collection, formulated the musculoskeletal dynamics implicitly and used algorithmic differentiation, and together they have been shown to increase computational efficiency and the ability of obtaining an optimal solution (De Groote *et al.*, 2016; Porsa *et al.*, 2016). Furthermore, previous studies which have performed predictive simulations of walking, running, or sprinting (Falisse *et al.*, 2019b; van den Bogert and Ackermann, 2009) have imposed a symmetry constraint at the end of their simulations to improve computational tractability, however this is not appropriate in circumstances in which asymmetry between steps is likely, such as accelerative sprinting which was the form of locomotion studied in this investigation.

The simulation approach used in this study was similar to the approaches utilised by Meyer *et al.* (2016) and van den Bogert *et al.* (2012) for performing predictive simulations of walking and running, respectively. In those cited studies, the cost functions also included a tracking element, which in our case was a subset of the entire set of net joint moments. We opted to embrace such an approach to ensure we were subsequently able to infer changes in performance through systematic modifications to the net ankle, knee, and hip flexor-extensor moments, and to ensure the predicted outputs were still representative of accelerative sprinting. However, we recognise this is a limitation of our study as assigning different weightings to the tracking (subset of the entire net joint moments) and performance (minimisation of the time horizon duration) terms would have led to different results. Interestingly, the weighting assigned to the

minimisation of the time horizon duration meant that it never reached its lower bound, and we believe that this ensured a balancing of the two terms in the cost function such that neither was too heavily minimised.

An interesting finding from the predictive simulations was that they tended to show a trend of increasing the net and propulsive impulses in the first stance phase compared to the data-tracking simulation, whilst the net and propulsive impulses of the second stance were less than those obtained in the data-tracking simulation. Considering that all the predictive simulations improved performance compared to the data-tracking simulation, a greater surplus of net impulse from the first stance phase had to be produced by the predictive simulations such that overall performance was still enhanced. We believe that this result can be attributed to the inequality constraint enforcing that the relative joint angles at the end of the predictive simulations were within $\pm 10°$ of those obtained at the end of the data-tracking simulation, as this may have restricted the possibility of achieving optimal solutions featuring greater net and propulsive impulses for the second stance phase. We imposed the inequality constraint to ensure that the musculoskeletal model was posed such that it had the possibility of performing a subsequent step. Without imposing this type of constraint, the final solution obtained by the algorithm more closely resembled jumping/hopping/diving as opposed to accelerative sprinting, as we found in our preliminary work (Haralabidis *et al.*, 2020). In further work it would be interesting to simulate more than two stance phases as done in this investigation to explore whether the imposed inequality constraint was the cause of this result.

4.6 Conclusion

The results from the predictive simulations highlighted that modifications in technique due to the timing and magnitude of the net knee flexor-extensor moments resulted in the greatest improvements to overall performance. The 'hip-free' predictive simulations revealed a net hip flexor moment pattern in support of the front-side mechanics coaching framework, specifically an earlier net hip flexor moment during the stance phase. However, the variables previously linked to front-side mechanics were not sufficiently conclusive to support the plausibility of the front-side mechanics coaching framework. It is worthwhile noting that the improvements in accelerative sprinting performance we found can be viewed as short-term technique modifications, as opposed to long-term adaptations via strength and conditioning programs for example, as the properties of the musculoskeletal model were kept constant between predictive simulations. Lastly, for coaches and sport scientists working to improve the early accelerative

sprinting performance of their athletes, the major technique-based recommendations rely on the actions of the net knee and hip flexor-extensor moments, particularly during the late swing phase and the stance phase, and therefore cueing the actions of those joints based on the accompanying kinematics patterns is recommended.

4.7 Supplementary material

Time histories of the flexion-extension ankle, knee, and hip joint angles and net joint moments, pelvis kinematics, and ground reaction forces for the data-tracking simulation together with the tracked experimental data are presented in Figures 4.7–1 to 4.7–4.
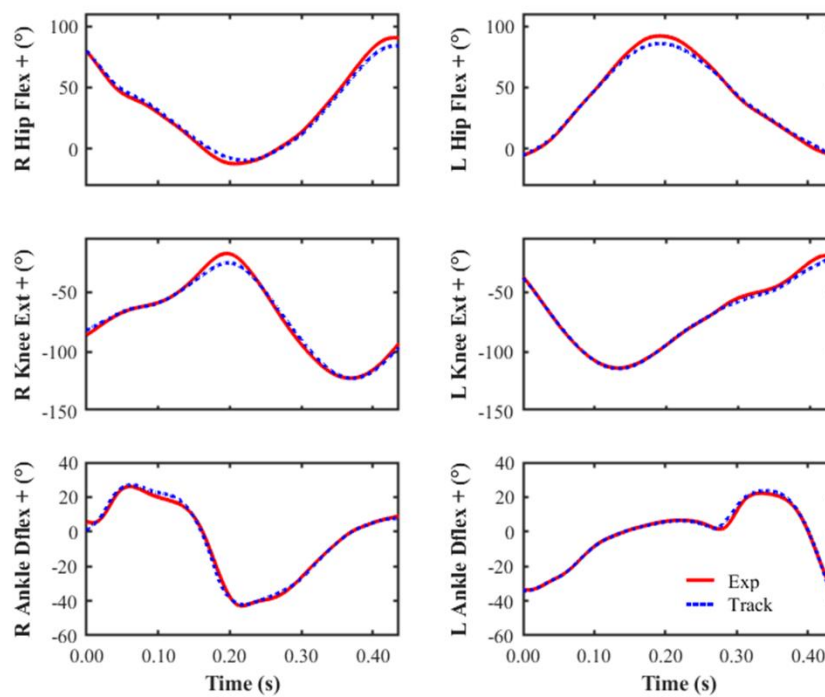
Figure 4.7–1 Right and left ankle, knee, and hip flexion-extension angles from right foot touchdown to left foot takeoff. Experimental joint angles are denoted by solid red lines (EXP). Simulated joint angles are denoted by dashed blue lines (TRACK).
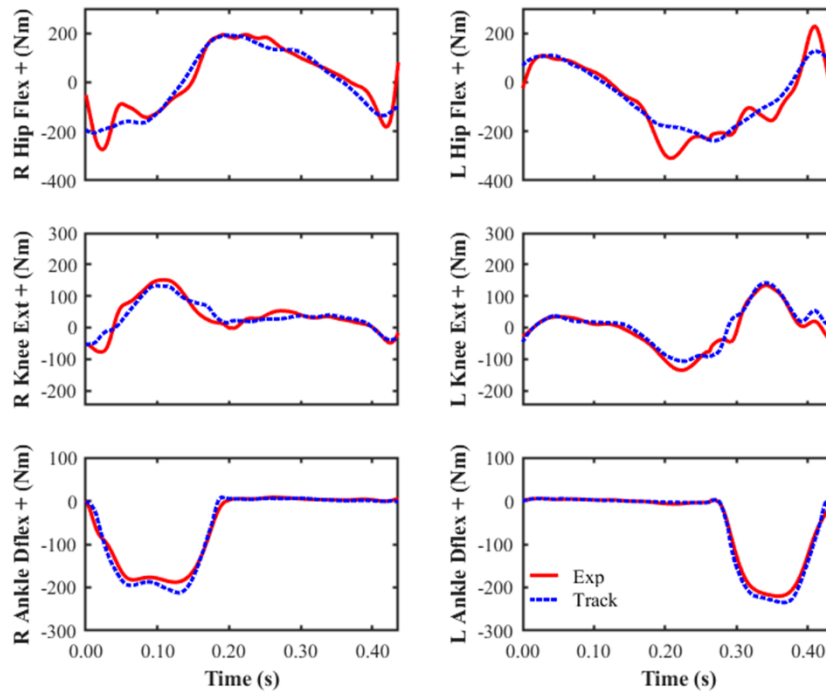
Figure 4.7–2 Right and left net ankle, knee, and hip flexor-extensor moments from right foot touchdown to left foot takeoff. Experimental net joint moments are denoted by solid red lines (EXP). Simulated net joint moments are denoted by dashed blue lines (TRACK).
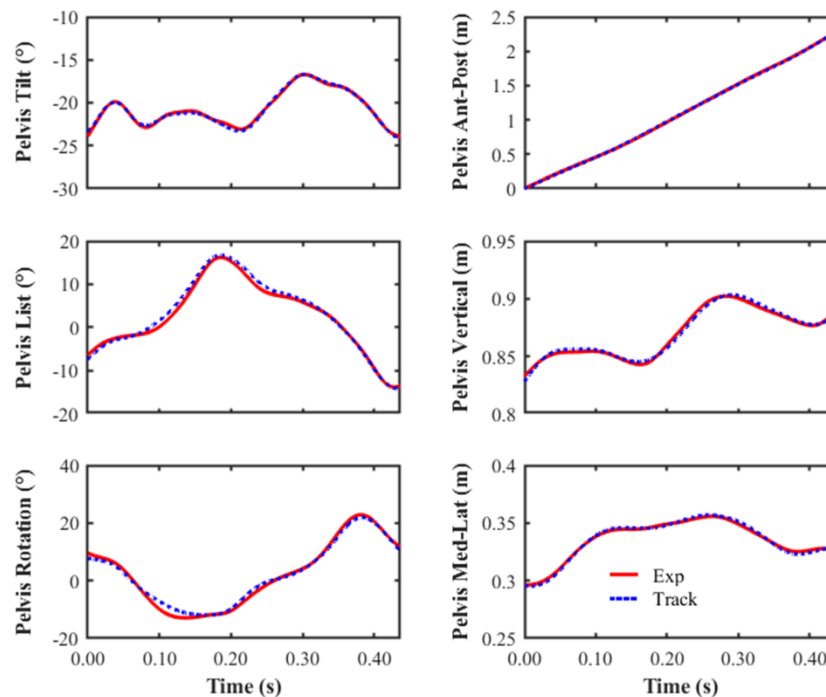
Figure 4.7–3 Global pelvis angles and translations from right foot touchdown to left foot takeoff. Experimental global pelvis angles and translations are denoted by solid red lines (EXP). Simulated global pelvis angles and translations are denoted by dashed blue lines (TRACK).
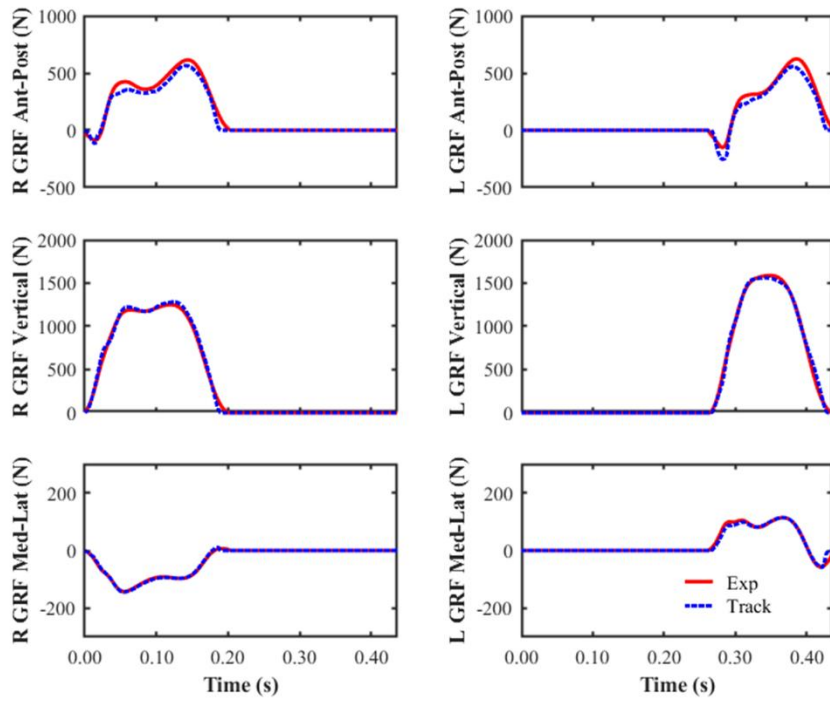
Figure 4.7–4 Right and left anterior-posterior, vertical and medial-lateral GRF from right foot touchdown to left foot takeoff. Experimental GRF components are denoted by solid red lines (EXP). Simulated GRF components are denoted by dashed blue lines (TRACK).

Chapter 5
General Discussion

5.1 Summary

The overarching purpose of this thesis was to develop a computational modelling and simulation framework to enable technique modifications in relation to accelerative sprinting performance to be explored. An important novelty of the framework developed in this thesis is that it provides individualised recommendations for improving performance, instead of group level or generic recommendations as provided by the existing body of cross-sectional experimental studies. Furthermore, the technique changes identified by the framework were compared with those of the existing literature and coaching frameworks to further inform, and potentially challenge, current coaching practices. To achieve the purpose of this thesis a computational modelling and simulation framework, which combined a complex three-dimensional musculoskeletal with a direct collocation optimal control approach, was developed.

The first study featured the development of the computational modelling and simulation framework and evaluating its ability to reproduce ground-truth sprinting data by performing a series of data-tracking simulations. A novel aspect of this investigation was that it also enabled dynamically consistent simulated outputs to be obtained for a highly dynamic activity whilst still ensuring the simulated outputs were a close match with reality. It is therefore recommended that a similar approach be adopted to avoid dynamic inconsistencies. The study featured the acquisition of conventional biomechanical experimental data (three-dimensional marker trajectories, GRF and EMGs) from an international-level male sprinter as they performed a series of maximal effort sprints. This data was subsequently used to linearly scale a three-dimensional musculoskeletal model and further procedures (inverse kinematics and dynamics analyses) were performed to generate the ground-truth data to be tracked and evaluated. The data-tracking simulations also enabled the foot-ground contact model parameters to be determined. Calibration data-tracking simulations, in the form of either tracking experimental data from a single trial individually or from several separate trials simultaneously, were performed to initially identify the foot-ground contact model parameters. The foot-ground contact model parameters obtained from the simultaneous data-tracking simulation, which featured data from the early acceleration, mid-acceleration and maximum

velocity phase trials being tracked simultaneously, were used to perform a subsequent data-tracking validation simulation. A validation data-tracking simulation was performed to assess how well the calibrated foot-ground contact model parameters were able to reproduce data from the trial they were not calibrated from. The outputs from the data-tracking simulations, calibration and validation, were found to be a close match with the ground-truth data, which provided confidence in the framework's ability to be used to perform predictive simulations.

The body of sprinting literature contains technique-based recommendations for improving performance, alas limited studies have documented how modifications to technique affect performance, especially from an individualised perspective. Furthermore, arguably the most widely adopted sprinting coaching framework, front-side mechanics, has received limited evidence to either support or reject its claims. In the second study, for the first time in the literature, dynamically consistent modifications to sprinting technique, which led to performance improvements, were identified and compared to the technique-based recommendations from the existing literature and the front-side mechanics coaching framework during the early acceleration phase. Sprinting during the acceleration phase was selected due to its importance within track and field sprinting but also for team-based sport athletes, for whom accelerative sprinting features prominently. In doing so, the applicability of the findings to the real world could be maximised.

The second study featured the same musculoskeletal model used in the first study to perform a data-tracking simulation and a series of predictive simulations. A data-tracking simulation was initially performed to provide a reference of performance and technique for comparative purposes with the outputs from the predictive simulations. The predictive simulations explored modifications to technique from a net joint moments perspective. More specifically, individual and combinations of the major lower-limb flexor-extensor net joint moments (ankle, knee, and hip) were allowed to vary within the physiological limits of the musculoskeletal model, whilst the remaining net joint moments were tracked during each of the predictive simulations.

The subset of predictive simulations which gave the freedom to the net knee flexor-extensor moments to vary were found to lead to the greatest improvements in performance, as indicated by average horizontal external power production compared to the data-tracking simulation. In those simulations, a greater net knee flexor moment was found to be produced during the late swing phase and at touchdown compared to the data-tracking simulation, which were also

accompanied by reductions in the braking impulse and the horizontal touchdown velocity of the foot. Furthermore, freely varying the hip flexor-extensor moments led to these variables been further improved upon. These findings are extremely novel as they emphasise that improvements in performance on an individualised basis are due to a strategy that collectively reduced the braking impulse. A greater peak net knee extensor moment during the stance phase was also identified during the 'knee-free' predictive simulations, which coincided with the associations noted by Bezodis *et al.* (2014) during accelerative sprinting in elite male athletes. In the 'hip-free' predictive simulations it was identified that a greater and earlier net hip flexor moment was produced when compared to the data-tracking simulation, with 60% of the stance phase been net hip flexor moment dominant. This provides some evidence in favour towards the front-side mechanics coaching framework, which states that the highest calibre sprinters generate a net hip flexor moment for almost 75% of the stance phase. However, discrete kinematics variables suggested to be important for demonstrating front-side mechanics were not found to occur with the optimal techniques uncovered by the predictive simulations, thus providing unconvincing evidence to further support the front-side mechanics coaching framework.

5.2 Limitations and future work

The work produced in this thesis carries with it some limitations that need to be considered. In this section those limitations are acknowledged, and an overview of how further work can be performed to potentially overcome them is provided.

Model personalisation

The investigations carried out in this thesis featured a linearly scaled three-dimensional musculoskeletal model that was originally developed from a combination of participants that were from a nonathletic background. Thus, it is very likely that the inertial and MTUs parameters, for example, are not representative of an elite-level sprinter. For example, a previous study has shown that sprinters have 22% greater lower-limb muscle volume than non-sprinters, with markedly larger hip- and knee-crossing muscles (Handsfield *et al.*, 2017), and this is important to acknowledge as muscle volume plays a critical role in the overall moment generating capacity of muscle (Fukunaga *et al.*, 2001). In addition, previous studies have also demonstrated morphological differences in terms of moment arms between sprinters and non-sprinters, with sprinters possessing shorter and longer ankle plantarflexor (Baxter *et al.*, 2012) and knee extensor (Miyake *et al.*, 2017) moment arms, respectively. Furthermore, a forefoot

segment was included within the model to permit MTP motion as it has been shown to undergo a substantial range of motion during sprinting (Smith *et al.*, 2014), which is novel as the foot is often modelled as a single segment. Nevertheless, more work is needed to permit the net MTP plantarflexor moment capacity to match with measured values without necessarily relying on an idealised reserve actuator. To account for these discrepancies within our model future work should consider exploring a personalised musculoskeletal model from medical images, such as magnetic resonance imaging. Barriers to this do, however, exist in the form of segmenting the medical images and creating a model that is compatible with standard musculoskeletal modelling software together with hours of processing and specialised training and they have prevented their usage. However, in recent times semi-automatic and automatic tools for segmenting the images (Burton II *et al.*, 2020) and generating the models (Modenese and Renault, 2021) have been developed to aid in the creation of personalised models. There has been a surge in the past decade to develop the tools needed to create personalised models for enhancing the rehabilitation/surgery given to patients, and therefore there is also the scope for the development of personalised models to aid with the training recommendations administered to athletes on an individualised basis.

Multiple steps

One of the major advantages of developing a predictive modelling and simulation framework is that it could be used to simulate multiple steps of walking, running or sprinting. Despite this, previous studies have enforced symmetry from touchdown to the subsequent touchdown (Ackermann and van den Bogert, 2010; Falisse *et al.*, 2019b). However, to gain insights into the techniques used by athletes to accelerate across successive steps this was not a viable approach for this programme of work. In the second investigation of this thesis, successive stance phases of the early acceleration phase were simulated with a complex three-dimensional model, and whilst this demonstrates the feasibility of simulating multiple steps, simulating 10 m of the acceleration phase, for example, would have enabled further insights into sprinting technique and performance to be obtained. However, the size of the OCPs based on our formulations would have potentially become too large, in which case the NLP solver may have found difficulties in reaching an optimal solution. A potential means of overcoming this, that is yet to be explored from a biomechanics perspective, still involves the use of direct collocation optimal control, but instead of using low order polynomials to approximate the state variables between mesh intervals, a higher order polynomial is used for the entire interval. By utilising this approach, the number of discretised state variables needed to be optimised for would

reduce, and in doing so create a more computationally tractable problem to solve. However, it is worthwhile noting that due to the transient dynamics at touchdown and takeoff that this approach may encounter difficulties.

In the predictive simulations performed, a terminal inequality constraint was also specified to ensure that the state variables pertaining to the multibody dynamics would enable the model to be suitably posed for performing a subsequent step, as without this constraint the model appeared to dive at the end, which would not be ideal for an investigation during the acceleration phase. Celik and Piazza (2013) demonstrated the possibility of performing predictive simulations of sprinting using a simple two-dimensional model and found encouraging results. The same authors also attempted to utilise a more complex model, including ankle and knee joints, however their optimal solutions were not found to be too dissimilar to their initial guess. To address these shortcomings, it may also be worthwhile exploring approaches from the computer graphics and robotics literature, such as contact invariant optimisation (Mordatch *et al.*, 2012; Mordatch *et al.*, 2013) and through-contact (Posa *et al.*, 2014), as these approaches have been applied to simulate successive steps of movement for humanoids and robots with remarkably encouraging results. A further alternative to explore this difficulty is reinforcement learning. This approach has recently found application within the biomechanics and computer science community whereby a competition was hosted (Kidziński *et al.*, 2018a) to determine the control variables for a two-dimensional musculoskeletal model that travelled as far as possible in 10 s. The results from this competition also look promising (Kidziński *et al.*, 2018b) and are worthy of future exploration.

Objective function

The objective function used to perform the predictive simulations in the second study featured a performance term, minimisation of time horizon duration, and a tracking term, minimisation of error between subset of predictive and data-tracking simulation net joint moments. Different weightings were assigned to each of the terms, and this was a compromise between attempting to improve performance whilst still retaining the net joint moments for those joints which were tracked. We acknowledge that different weightings on the two terms would have led to different results. The tracking term was included in an attempt to permit subsequent inferences to changes in performance to be explained by the net joint-moments which were free to vary. This approach was embraced as it coincides with modifying a single variable to assess its influence (cause-effect relationship), which is one of the often-cited advantages of predictive computer

simulation and modelling approaches. However, the approach embraced presents some difficult issues that warrant acknowledging, as the tracked net joint moments combined with a reduction in time lead to differing joint angular displacements. In a simple scenario such as determining the magnitude of the moment to move a pendulum upwards in the least amount of time, applying the same pattern and magnitude of moment in half the time leads to half the angular displacement. Furthermore, because of dynamic coupling, each net joint moment (alongside the gravitational forces etc.) is capable of accelerating all the joints (Zajac and Gordon, 1989). Care must therefore be exercised when interpreting the findings of this study by acknowledging the above limitations. A potential way in which to further explore the findings from this study would be to apply an induced acceleration analysis. The challenge of performing predictive simulations to inform technique and performance therefore still remains. Perhaps performing the predictive simulations by means of progressively reducing the lower bound of the time horizon duration between simulations and not tracking any data would have been a better approach to explore technique modifications and performance. However, the difficulty with this approach is that many of the variables change and it therefore becomes difficult to ascertain what is causing performance to change. Furthermore, the athlete used in the investigations was an international-level sprinter and consequently drastic improvements in technique were not anticipated, which therefore suggests that such an approach (e.g., no tracking terms) was not warranted.

Dynamics formulations

In the two studies carried out in this thesis, the musculoskeletal model's dynamics were formulated implicitly as opposed to explicitly. Formulating the dynamics implicitly together with a direct collocation method has been previously shown to improve the computational efficiency of obtaining an optimal solution (De Groote *et al.*, 2016). To do so requires the introduction of additional control variables, and in the case of the multibody dynamics introducing time derivatives of the generalised velocities. The performance benefit of doing so is believed to be due to bypassing the necessity of calculating the time derivatives of the generalised velocities from the multibody dynamics equations, which can lead to difficulties due to needing to invert the model's mass matrix (Serrancolí and Pàmies-Vilà, 2019; van den Bogert *et al.*, 2011). Serrancolí and Pàmies-Vilà (2019) stated that the benefit in performance from the implicit formulation required including the additional control variables in the cost function. In the studies carried out in this thesis the variables introduced due to the implicit formulations were minimised within the respective cost functions, although it is questionable

whether for highly demanding tasks that this is appropriate, in which case an explicit formulation may have been more appropriate. Future studies exploring the differences between the two formulations are warranted, particularly during maximal effort sporting movements.

Translating the findings

The findings from the second investigation carried out in this thesis have contributed to the sprinting biomechanics and coaching literature, although the findings were not translated to a real world setting to improve performance, despite the framework's ability to accurately reproduce experimental sprinting data. However, this also appears to be a recurrent theme for studies which have performed predictive simulations of sporting movements to optimise performance, and this can be seen within cricket fast-bowling (Felton *et al.*, 2020), triple jumping (Allen *et al.*, 2013), gymnastics (Hiley *et al.*, 2015), golf (Brown *et al.*, 2020) and track cycling (Jansen and McPhee, 2020). Hatze (1983) provides the only evidence of the findings from predictive simulations been transferred to enhance sporting performance in the real world, although the evidence of this is circumstantial and limited. Hatze (1983) states that the technique-based recommendations (delaying hip joint extension at takeoff) for improving the performance of an athlete's long jump based on the findings of his 1981 study (Hatze, 1981) were implemented, and within three weeks the athlete improved their PB performance from 6.96 to 7.12 m. A similar trend is also noticeable within the clinical biomechanics field, with the only evidence of translating the findings from predictive simulations to the real world in a knee osteoarthritis setting (Fregly *et al.*, 2007). Fregly *et al.* (2007) performed a predictive simulation of walking that featured minimisation of the net knee adduction moment, which is linked with medial knee osteoarthritis generation, and they subsequently trained the patient to walk in the manner predicted by the simulation and reported that the osteoarthritis risk reduced by a factor of 10. Future work should therefore involve translating the findings from predictive simulations to the real world, in doing so this will also improve the acceptance of applying the findings and build a reputation for their merit.

5.3 Conclusion

This thesis has focused on developing and applying state-of-the-art modelling and simulation approaches to explore how technique modifications affect sprinting performance. In the first investigation, the developed modelling and simulation framework was found to be a suitable match with reality (e.g., experimental sprinting data). Novel aspects of the first investigation included dynamically consistent simulated outputs and the calibration of foot-ground contact

model parameters from tracking multiple trials simultaneously. The second investigation featured using the evaluated modelling and simulation framework to perform a series of predictive simulations to explore how technique modifications affect accelerative sprinting performance and how they coincide with the front-side mechanics coaching framework. A novelty of the second investigation was that it featured identifying an individualised strategy for improving accelerative sprinting performance, which was predominantly based upon the actions of the net knee flexor-extensor moments. A further novelty of the second investigation was the emergence of the actions of the net hip flexor-extensor moments coinciding with the front-side mechanics coaching framework, although unconvincing evidence was found for the kinematics aspects of the framework.

The work carried out in this thesis has taken an important step towards identifying how an individual athlete can improve their accelerative sprinting performance and it also has the potential to transform sports coaching practices. However, this is just the beginning, as the era of using personalised computer models to provide individualised modifications to sporting technique or long-term training adaptations based upon predictive simulations is upon us. Furthermore, two of arguably the world's most pioneering groups (Griffith Centre of Biomedical and Rehabilitation Engineering, Griffith University, Australia and Neuromuscular Biomechanics Lab, Stanford University, USA) in computational modelling and simulation for biomechanical applications have recently embarked on a mission to apply such approaches for sporting applications. The realisation of the benefits afforded by utilising computer modelling and simulation approaches within sporting contexts is there for all to see, and the next decade within this field promises to have some exciting times ahead. Hopefully within the same decade the results from the predictive simulations will have been transferred to the relevant sporting organisations to have a measurable impact.

References

1. Ackermann M, and van den Bogert AJ. 2010. Optimality principles for model-based prediction of human gait. *Journal of Biomechanics* 43:1055-1060.

2. Ae M, Ito A, and Suzuki M. 1992. The men's 100 metres. *New Studies in Athletics* 7:47-52.

3. Aeles J, Jonkers I, Debaere S, Delecluse C, and Vanwanseele B. 2018. Muscle-tendon unit length changes differ between young and adult sprinters in the first stance phase of sprint running. *Royal Society Open Science* 5:180332.

4. Alenezi F, Herrington L, Jones P, and Jones RL. 2016. How reliable are lower limb biomechanical variables during running and cutting tasks. *Journal of Electromyography and Kinesiology* 30:137-142.

5. Alexander RM. 2003. Modelling approaches in biomechanics. *Philosophical Transactions of the Royal Society of London Series B: Biological Sciences* 358:1429-1435.

6. Allen SJ, King MA, and Yeadon MR. 2013. Trade-offs between horizontal and vertical velocities during triple jumping and the effect on phase distances. *Journal of Biomechanics* 46:979-983.

7. Anderson FC, and Pandy MG. 1999. A dynamic optimization solution for vertical jumping in three dimensions. *Computer Methods in Biomechanics and Biomedical Engineering* 2:201-231.

8. Anderson FC, and Pandy MG. 2001. Dynamic optimization of human walking. *Journal of Biomechanical Engineering* 123:381-390.

9. Andersson JA, Gillis J, Horn G, Rawlings JB, and Diehl M. 2019. CasADi: a software framework for nonlinear optimization and optimal control. *Mathematical Programming Computation* 11:1-36.

10.   Austin DJ, Gabbett TJ, and Jenkins DJ. 2011. Repeated high-intensity exercise in a professional rugby league. *The Journal of Strength and Conditioning Research* 25:1898-1904.

11.   Bangsbo J, Nørregaard L, and Thorsoe F. 1991. Activity profile of competition soccer. *Canadian Journal of Sport Sciences* 16:110-116.

12.   Baxter JR, Novack TA, Van Werkhoven H, Pennell DR, and Piazza SJ. 2012. Ankle joint mechanics and foot proportions differ between human sprinters and non-sprinters. *Proceedings of the Royal Society B: Biological Sciences* 279:2018-2024.

13.   Belli AH, Kyröläinen H, and Komi PV. 2002. Moment and power of lower limb joints in running. *International Journal of Sports Medicine* 23:136-141.

14.   Betts JT. 2010. *Practical methods for optimal control using nonlinear programming*. Philadelphia, PA: SIAM.

15.   Bezodis I. 2006. Biomechanical performance variation in maximum velocity sprinting. PhD Thesis. University of Bath.

16.   Bezodis IN, Kerwin DG, and Salo AI. 2008a. Lower-limb mechanics during the support phase of maximum-velocity sprint running. *Medicine & Science in Sports & Exercise* 40:707-715.

17.   Bezodis NE, Salo AI, and Trewartha G. 2010. Choice of sprint start performance measure affects the performance-based ranking within a group of sprinters: which is the most appropriate measure? *Sports Biomechanics* 9:258-269. 10.1080/14763141.2010.538713

18.   Bezodis NE, Salo AI, and Trewartha G. 2014. Lower limb joint kinetics during the first stance phase in athletics sprinting: three elite athlete case studies. *Journal of Sports Sciences* 32:738-746.

19.   Bezodis NE, Salo AIT, and Trewartha G. 2008b. Understanding elite sprint start performance through an analysis of joint kinematics. In: Kwon Y-H, Shim J, Shim JK,

and Shin I-S, editors. Proceedings of XXVI International Symposium on Biomechanics in Sports. Seoul: Seoul National University Press. p 498-501.

20.   Bezodis NE, Trewartha G, and Salo AIT. 2015. Understanding the effect of touchdown distance and ankle joint kinematics on sprint acceleration performance through computer simulation. *Sports Biomechanics* 14:232-245.

21.   Bisseling RW, and Hof AL. 2006. Handling of impact forces in inverse dynamics. *Journal of Biomechanics* 39:2438-2444. 10.1016/j.jbiomech.2005.07.021

22.   Brown C, McNally W, and McPhee J. 2020. Optimal control of joint torques using direct collocation to maximise ball carry distance in a golf swing. *Multibody System Dynamics* 50:323-333.

23.   Burton II W, Myers C, and Rullkoetter P. 2020. Semi-supervised learning for automatic segmentation of the knee from MRI with convolutional neural networks. *Computer Methods and Programs in Biomedicine* 189:105328.

24.   Cavagna GA, Komarek L, and Mazzoleni S. 1971. The mechanics of sprinting. *The Journal of Physiology* 217:709-721.

25.   Celik H, and Piazza SJ. 2013. Simulation of aperiodic bipedal sprinting. *Journal of Biomechanical Engineering* 135:081008-081001-081008.

26.   Charalambous L, Irwin G, Bezodis IN, and Kerwin D. 2012. Lower limb joint kinetics and ankle joint stiffness in the sprint start push-off. *Journal of Sports Sciences* 30:1-9.

27.   Clark KP, Meng CR, and Stearne DJ. 2020. 'Whip from the hip': thigh angular motion, ground contact mechanics, and running speed. *Biology Open* 9:bio053546.

28.   Clark KP, and Weyand PG. 2014. Are running speeds maximized with simple-spring stance mechanics? *Journal of Applied Physiology* 117:604-615.

29.   Colyer SL, Nagahara R, and Salo AIT. 2018a. Kinetic demands of sprinting shift across the acceleration phase: novel analysis of entire waveforms. *Scandinavian Journal of Medicine and Science in Sports* 28:1784-1792.

30.   Colyer SL, Nagahara R, Takai Y, and Salo AI. 2018b. How sprinters accelerate beyond the velocity plateau of soccer players: Waveform analysis of ground reaction forces. *Scandinavian Journal of Medicine and Science in Sports* 28:2527-2535.

31.   Dalton SL, Kerr ZY, and Dompier TP. 2015. Epidemiology of hamstring strains in 25 NCAA sports in the 2009-2010 to 2013-2014 academic years. *The American Journal of Sports Medicine* 43:2671-2679.

32.   Damsgaard M, Rasmussen J, Christensen ST, Surma E, and De Zee M. 2006. Analysis of musculoskeletal systems in the AnyBody Modeling System. *Simulation Modelling Practice and Theory* 14:1100-1111.

33.   Davis DJ, and Challis JH. 2020. Automatic segment filtering procedure for processing non-stationary signals. *Journal of Biomechanics* 101:109619.

34.   De Groote F, Kinney AL, Rao AV, and Fregly BJ. 2016. Evaluation of direct collocation optimal control problem formulations for solving the muscle redundancy problem. *Annals of Biomedical Engineering* 44:2922-2936.

35.   De Groote F, Pipeleers G, Jonkers I, Demeulenaere B, Patten C, Swevers J, and De Schutter J. 2009. A physiology based inverse dynamic analysis of human gait: potential and perspectives. *Computer Methods in Biomechanics and Biomedical Engineering* 12:563-574.

36.   De Ruiter CJ, Didden WJM, Jones DA, and De Haan A. 2000. The force-velocity relationship of human adductor pollicis muscle during stretch and the effects of fatigue. *The Journal of Physiology* 526:671-681.

37.   Debaere S, Delecluse C, Aerenhouts D, Hagman F, and Jonkers I. 2013. From block clearance to sprint running: characteristics underlying an effective transition. *Journal of Sports Sciences* 31:137-149. 10.1080/02640414.2012.722225

38. Delecluse C, Van Coppenolle H, Diels R, and Goris M. 1992. A model for the scientific preparation of high level sprinters. *New Studies in Athletics* 7:57-64.

39. Delecluse C, van Coppenolle H, Willems E, van Leemputte M, Diels R, and Goris M. 1995. Influence of high-resistance and high-velocity training on sprint performance. *Medicine & Science in Sports & Exercise* 27:1203-1209.

40. Delp SL, Anderson FC, Arnold AS, Loan P, Habib A, Chand JT, Guendelman E, and Thelen DG. 2007. OpenSim: open-source software to create and analyze dynamic simulations of movement. *IEEE Transactions on Biomedical Engineering* 54:1940-1950.

41. Dembia CL, Bianco NA, Falisse A, Hicks JL, and Delp SL. 2020. Opensim moco: musculoskeletal optimal control. *PLOS Computational Biology* 16:e1008493.

42. Derrick TR, van den Bogert AJ, Cereatti A, Dumas R, Fantozzi S, and Leardini A. 2020. ISB recommendations on the reporting of intersegmental forces and moments during human motion analysis. *Journal of Biomechanics* 99:109533.

43. Di Salvo V, Baron R, González-Haro C, Gormasz C, Pigozzi F, and Bachl N. 2010. Sprinting analysis of elite soccer players during European Champions League and UEFA Cup matches. *Journal of Sports Sciences* 28:1489-1494.

44. Dorn TW, Schache AG, and Pandy MG. 2012. Muscular strategy shift in human running: dependence of running speed on hip and ankle muscle performance. *Journal of Experimental Biology* 215:1944-1956.

45. Dorschky E, Krüger D, Kurfess N, Schlarb H, Wartzack S, Eskofier BM, and van den Bogert AJ. 2019. Optimal control simulation predicts effects of midsole materials on energy cost of running. *Computer Methods in Biomechanics and Biomedical Engineering* 22:869-879.

46. Duhig S, Shield AJ, Opar D, Gabbett TJ, Ferguson C, and Williams M. 2016. Effect of high-speed running on hamstring strain injury risk. *British Journal of Sports Medicine* 50:1536-1540.

47.   Erskine RM, Jones DA, Maffulli N, Williams AG, Stewart CE, and Degens H. 2011. What causes in vivo muscle specific tension to increase following resistance training? *Experimental Physiology* 96:145-155.

48.   Ezati M, Brown P, Ghannadi B, and McPhee J. 2020. Comparison of direct collocation optimal control to trajectory optimization for parameter identification of an ellipsoidal foot-ground contact model. *Multibody System Dynamics*:1-23.

49.   Falisse A, Serrancolí G, Dembia CL, Gillis J, and De Groote F. 2019a. Algorithmic differentiation improves the computational efficiency of OpenSim-based trajectory optimization of human movement. *PLoS ONE* 14. e0217730

50.   Falisse A, Serrancolí G, Dembia CL, Gillis J, Jonkers I, and De Groote F. 2019b. Rapid predictive simulations with complex musculoskeletal models suggests that diverse healthy and pathological human gaits can emerge from similar control strategies. *Journal of The Royal Society Interface* 16:20190402.

51.   Faude O, Koch T, and Meyer T. 2012. Straight sprinting is the most frequent action in goal situations in professional football. *Journal of Sports Sciences* 30:625-631.

52.   Felton PJ, Yeadon MR, and King MA. 2020. Optimising the front foot contact phase of the cricket fast bowling action. *Journal of Sports Sciences* 38:2054-2062.

53.   Fregly BJ, Reinbolt JA, Rooney KL, Mitchell KH, and Chmielewski TL. 2007. Design of patient-specific gait modifications for knee osteoarthritis rehabilitation. *IEEE Transactions on Biomedical Engineering* 54:1687-1695.

54.   Fukunaga T, Miyatani M, Tachi M, Kouzaki M, Kawakami Y, and Kanehisa H. 2001. Muscle volume is a major determinant of joint torque in humans. *Acta Physiologica Scandinavica* 172:249-255.

55.   Gabbett TJ. 2012. Sprinting patterns of national rugby league competition. *The Journal of Strength and Conditioning Research* 26:121-130.

56. Gabbett TJ, and Gahan CW. 2016. Repeated high-intensity-effort activity in relation to tries scored and conceded during rugby league match play. *International Journal of Sports Physiology and Performance* 11:530-534.

57. Garg D, Patterson MA, Francolin C, Darby CL, Huntington GT, Hager WW, and Rao AV. 2011. Direct trajectory optimization and costate estimation of finite-horizon and infinite-horizon optimal control problems using a Radau pseudospectral method. *Computational Optimization and Applications* 49:335-358.

58. Gilchrist LA, and Winter DA. 1996. A two-part, viscoelastic foot model for use in gait simulations. *Journal of Biomechanics* 29:795-798.

59. Glazier PS, and Davids K. 2009. Constraints on the complete optimization of human motion. *Sports Medicine* 39:15-28.

60. Goldmann JP, Sanno M, Willwacher S, Heinrich K, and Brüggemann GP. 2013. The potential of toe flexor muscles to enhance performance. *Journal of Sports Sciences* 31:424-433.

61. Hamner SR, Seth A, and Delp SL. 2010. Muscle contributions to propulsion and support during running. *Journal of Biomechanics* 43:2709-2716. 10.1016/j.jbiomech.2010.06.025

62. Handsfield GG, Knaus KR, Fiorentino NM, Meyer CH, Hart JM, and Blemker SS. 2017. Adding muscle where you need it: non-uniform hypertrophy patterns in elite sprinters. *Scandinavian Journal of Medicine and Science in Sports* 27:1050-1060.

63. Haralabidis N, Serrancolí G, Colyer SL, Bezodis I, Salo A, and Cazzola D. 2020. Data-tracking and predictive simulations of sprint running. In: Robinson M, Baltzopoulos B, Lake M, and Vanrenterghem J, editors. Proceedings of the XXXVIII International Conference on Biomechanics in Sports. Liverpool, UK.

64. Haralabidis N, Serrancolí G, Colyer SL, Bezodis I, Salo A, and Cazzola D. 2021. Three-dimensional data-tracking simulations of sprinting using a direct collocation optimal control approach. *PeerJ* 9:e10975.

65. Hatze H. 1981. A comprehensive model for human motion simulation and its application to the take-off phase of the long jump. *Journal of Biomechanics* 14:135-142.

66. Hatze H. 1983. Computerized optimization of sports motions: An overview of possibilities, methods and recent developments. *Journal of Sports Sciences* 1:3-12.

67. Hatze H. 2005. Towards a comprehensive large-scale computer model of the human neuromusculoskeletal system. *Theoretical Issues in Ergonomics Science* 6:239-250.

68. Haugen T, Danielsen J, Alnes LO, McGhie D, Sandbakk Ø, and Ettema G. 2018. On the importance of "front-side mechanics" in athletics sprinting. *International Journal of Sports Physiology and Performance* 13:420-427.

69. Hay JG. 1994. *The Biomechanics of Sports Techniques.* New Jersey, USA: Prentice-Hall, Inc.

70. Helene O, and Yamashita MT. 2010. The force, power, and energy of the 100 meter sprint. *American Journal of Physics* 78:307-309.

71. Hermens HJ, Freriks B, Disselhorst-Klug C, and Rau G. 2000. Development of recommendations for SEMG sensors and sensor placement procedures. *Journal of Electromyography and Kinesiology* 10:361-374.

72. Hicks JL, Uchida TK, Seth A, Rajagopal A, and Delp SL. 2015. Is my model good enough? Best practices for verification and validation of musculosketal models and simulations of movement. *Journal of Biomechanical Engineering* 137:020905.

73. Hiley MJ, Jackson MI, and Yeadon MR. 2015. Optimal technique for maximal forward rotating vaults in men's gymnastics. *Human Movement Science* 42:117-131.

74. Hunter JP, Marshall RN, and McNair PJ. 2004a. Interaction of step length and step rate during sprint running. *Medicine & Science in Sports & Exercise* 36:261-271.

75.   Hunter JP, Marshall RN, and McNair PJ. 2004b. Segment-interaction analysis of the stance limb in sprint running. *J Biomech* 37:1439-1446. 10.1016/j.jbiomech.2003.12.018

76.   Hunter JP, Marshall RN, and McNair PJ. 2005. Relationships between ground reaction force impulse and kinematics of sprint-running acceleration. *Journal of Applied Biomechanics* 21:31-43.

77.   IAAF. 2004. 100 metres men. 28th Olympic Games, Athens 2004. *Available at https://www.iaaf.org/competitions/olympic-games/28th-olympic-games-3201/results/men/100-metres/final/result* (accessed 03/10/2017).

78.   Jacobs R, and van Ingen Schenau GJ. 1992. Intermuscular coordination in a sprint push-off. *Journal of Biomechanics* 25:953-965.

79.   Jansen C, and McPhee J. 2020. Predictive dynamic simulation of Olympic track cycling standing start using direct collocation optimal control. *Multibody System Dynamics* 49:53-70.

80.   Johnson MD, and Buckley JG. 2001. Muscle power patterns in the mid-acceleration phase of sprinting. *Journal of Sports Sciences* 19:263-272.

81.   Judson LJ, Churchill SM, Barnes A, Stone JA, Brookes IGA, and Wheat J. 2020. Measurement of bend sprinting kinematics with three-dimensional motion capture: a test-retest reliability study. *Sports Biomechanics* 19:761-777.

82.   Kawamori N, Nosaka K, and Newton RU. 2013. Relationships between ground reaction impulse and sprint acceleration performance in team sport athletes. *Journal of Strength and Conditioning Research* 27:568-573.

83.   Kersting UG. 1999. Biomechanical analysis of the sprinting events. In: Brüggemann GP, Koszewski D, and Müller H, editors. Biomechanical Research Report Athens 1997. Oxford, UK.

84.   Kidziński Ł, Mohanty SP, Ong CF, Hicks JL, Carroll SF, Levine S, Salathé M, and Delp SL. 2018a. Learning to run challenge: synthesizing physiologically accurate motion using deep reinforcement learning. In: Escalera S, and Weimer M, editors. The NIPS '17 Competition: Building Intelligent Systems The Springer Series on Challenges in Machine Learning. Basel, Switzerland: Springer.

85.   Kidziński Ł, Mohanty SP, Ong CF, Huang Z, Zhou S, Pechenko A, Stelmaszczyk A, Jarosik P, Pavlov M, Kolesnikov S, Plis S, Chen Z, Zhang Z, Chen J, Shi J, Zheng Z, Yuan C, Lin Z, Michalewski H, Milos P, Osinski B, Melnik A, Schilling M, Ritter H, Carroll SF, Hicks JL, Levine S, Salathé M, and Delp SL. 2018b. Learning to run challenge solutions: adapting reinforcement learning methods for neuromuscular environments. In: Escalera S, and Weimer M, editors. The NIPS '17 Competition: Building Intelligent Systems The Springer Series on Challenges in Machine Learning. Basel, Switzerland.

86.   Kim HY, Sakurai S, and Ahn JH. 2007. Errors in the measurement of center of pressure (CoP) computed with force plate affect on 3D lower limb joint moment during gait. *International Journal of Sport and Health Science* 5:71-82.

87.   Kristianslund E, Krosshaug T, and van den Bogert AJ. 2012. Effect of low pass filtering on joint moments from inverse dynamics: implications for injury prevention. *Journal of Biomechanics* 45:666-671.

88.   Kuitunen S, Komi PV, and Kyröläinen H. 2002. Knee and ankle joint stiffness in sprint running. *Medicine & Science in Sports & Exercise* 34:166-173.

89.   Kunz H, and Kaufmann DA. 1981. Biomechanical analysis of sprinting: decathletes versus champions. *British Journal of Sports Medicine* 15:177-181.

90.   Lai A. 2015. Muscle and tendon mechanical interactions during human locomotion. PhD Thesis. The University of Melbourne.

91.   Lai A, Schache AG, Brown NA, and Pandy MG. 2016. Human ankle plantar flexor muscle-tendon mechanics and energetics during maximum acceleration sprinting. *Journal of The Royal Society Interface* 13:20160391. 10.1098/rsif.2016.0391

92.   Lai AK, Dick TJ, Biewener AA, and Wakeling JM. 2021. Task-dependent recruitment across ankle extensor muscles and between mechanical demands is driven by the metabolic cost of muscle contraction. *Journal of The Royal Society Interface* 18:20200765.

93.   Lin YC, and Pandy MG. 2017. Three-dimensional data-tracking dynamic optimization simulations of human locomotion generated by direct collocation. *Journal of Biomechanics* 59:1-8.

94.   Lin YC, Walter JP, and Pandy MG. 2018. Predictive simulations of neuromuscular coordination and joint-contact loading in human gait. *Annals of Biomedical Engineering* 46:1216-1227.

95.   Luhtanen P, and Komi PV. 1978. Mechanical factors influencing running speed. *Biomechanics VI-B* 2:23-28.

96.   Maćkała K, and Mero A. 2013. A kinematics analysis of three best 100 m performances ever. *Journal of Human Kinetics* 36:149-160.

97.   Mai P, and Willwacher S. 2019. Effects of low-pass filter combinations on lower extremity joint moments in distance running. *Journal of Biomechanics* 95:109311.

98.   Mann R, and Herman J. 1985. Kinematic analysis of Olympic sprint performance: men's 200 meters. *Journal of Applied Biomechanics* 1:151-162.

99.   Mann R, Kotmel J, Herman J, Johnson B, and Schultz C. 1984. Kinematic trends in elite sprinters. In: Terauds J, Barthels K, Kreighbaum E, Mann R, and Crakes J, editors. Proceedings of II International Symposium on Biomechanics in Sports.

100.   Mann R, and Sprague P. 1980. A kinetic analysis of the ground leg during sprint running. *Research Quarterly for Exercise and Sport* 51:334-348.

101. Mann R, and Sprague P. 1983. Kinetics of sprinting. In: Terauds J, editor. Proceedings of I International Symposium on Biomechanics in Sports. San Diego, USA.

102. Mann RV. 1981. A kinetic analysis of sprinting. *Medicine and Science in Sports and Exercise* 13:325-328.

103. Mann RV, and Murphy A. 2015. *The mechanics of sprinting and hurdling*.

104. McCaw ST, and Devita P. 1995. Errors in alignment of center of pressure and foot coordinates affect predicted lower extremity torques. *Journal of Biomechanics* 28:985-988.

105. McErlain-Naylor SA, King MA, and Felton PJ. 2021. A review of forward-dynamics simulation models for predicting optimal technique in maximal effort sporting movements. *Applied Sciences* 11:1450.

106. Mero A. 1988. Force-time characteristics and running velocity of male sprinters during the acceleration phase of sprinting. *Research Quarterly for Exercise and Sport* 59:94-98.

107. Mero A, and Komi PV. 1985. Effects of supramaximal velocity on biomechanical variables in sprinting. *Journal of Applied Biomechanics* 1:240-252.

108. Mero A, and Komi PV. 1987. Electromyographic activity in sprinting at speeds ranging from sub-maximal to supra-maximal. *Medicine and Science in Sports and Exercise* 19:266-274.

109. Mero A, Komi PV, and Gregor RJ. 1992. Biomechanics of sprint running. A review. *Sports Medicine* 13:376-392.

110. Meyer AJ, Eskinazi I, Jackson JN, Rao AV, Patten C, and Fregly BJ. 2016. Muscle synergies facilitate computational prediction of subject-specific walking motions. *Frontiers in Bioengineering and Biotechnology* 4:77.

111. Miller RH, and Hamill J. 2015. Optimal footfall patterns for cost minimization in running. *Journal of Biomechanics* 48:2858-2864.

112. Miyake Y, Suga T, Otsuka M, Tanaka T, Misaki J, Kudo S, Nagano A, and Isaka T. 2017. The knee extensor moment arm is associated with performance in male sprinters. *European Journal of Applied Physiology* 117:533-539.

113. Modenese L, and Renault JB. 2021. Automatic generation of personalised skeletal models of the lower limb from three-dimensional bone geometries. *Journal of Biomechanics* 116:110186.

114. Mordatch I, Todorov E, and Popović Z. 2012. Discovery of complex behaviors through contact-invariant optimization. *ACM Transactions on Graphics* 31:1-8.

115. Mordatch I, Wang JM, Todorov E, and Koltun V. 2013. Animating human lower limbs using contact-invariant optimization. *ACM Transactions on Graphics* 32:1-8.

116. Morin JB, Bourdin M, Edouard P, Peyrot N, Samozino P, and Lacour JR. 2012. Mechanical determinants of 100-m sprint running performance. *European Journal of Applied Physiology* 112:3921-3930.

117. Morin JB, Edouard P, and Samozino P. 2011. Technical ability of force application as a determinant factor of sprint performance. *Medicine & Science in Sports & Exercise* 43:1680-1688.

118. Morin JB, Gimenez P, Edouard P, Arnal P, Jimenez-Reyes P, Samozino P, Brughelli M, and Mendiguchia J. 2015a. Sprint acceleration mechanics: the major role of hamstrings in horizontal force production. *Frontiers in Physiology* 6:1-14.

119. Morin JB, Slawinski J, Dorel S, de Villareal ES, Couturier A, Samozino P, Brughelli M, and Rabita G. 2015b. Acceleration capability in elite sprinters and ground impulse: Push more, brake less? *Journal of Biomechanics* 48:3149-3154.

120. Nagahara R, Matsubayashi T, Matsuo A, and Zushi K. 2014a. Kinematics of transition during human accelerated sprinting. *Biology Open* 3:689-699.

121. Nagahara R, Mizutani M, Matsuo A, Kanehisa H, and Fukunaga T. 2018. Association of sprint performance with ground reaction forces during acceleration and maximal speed phases in a single sprint. *Journal of Applied Biomechanics* 34:104-110.

122. Nagahara R, Naito H, Morin JB, and Zushi K. 2014b. Association of acceleration with spatiotemporal variables in maximal sprinting. *International Journal of Sports Medicine* 35:755-761.

123. Neptune RR. 2000. Computer modeling and simulation of human movement: applications in sport and rehabilitation. *Physical Medicine and Rehabilitation Clinics of North America* 11:417-434.

124. Novacheck TF. 1998. The biomechanics of running. *Gait & Posture* 7:77-95.

125. Oh K, and Park S. 2017. The bending stiffness of shoes is beneficial to running energetics if it does not disturb the natural MTP joint flexion. *Journal of Biomechanics* 53:127-135.

126. Pallarès-López R, Alvim FC, Febrer-Nafría M, Menegaldo LL, and Font-Llagunes JM. 2019. Assessment of residual reduction procedures for high-speed tasks. *Gait & Posture* 73:116-119.

127. Pandy MG. 2001. Computer modeling and simulation of human movement. *Annual Review of Biomedical Engineering* 3:245-273.

128. Pandy MG, and Andriacchi TP. 2010. Muscle and joint function in human locomotion. *Annual Review of Biomedical Engineering* 12:401-433.

129. Porsa S, Lin YC, and Pandy MG. 2016. Direct methods for predicting movement biomechanics based upon optimal control theory with implementation in OpenSim. *Annals of Biomedical Engineering* 44:2542-2557.

130. Posa M, Cantu C, and Tedrake R. 2014. A direct method for trajectory optimization of rigid bodies through contact. *The International Journal of Robotics Research* 33:69-81.

131. Quinn MD. 2003. The effects of wind and altitude in the 200-m sprint. *Journal of Applied Biomechanics* 19:49-59.

132. Rasmussen J, Holmberg LJ, Sørensen K, Kwan M, Andersen MS, and de Zee M. 2012. Performance optimization by musculoskeletal simulation. *Movement & Sport Sciences-Science & Motricité* 75:73-83.

133. Robertson DGE, and Dowling J. 2003. Design and responses of Butterworth and critically damped digital filters. *Journal of Electromyography and Kinesiology* 13:569-573.

134. Saibene F, and Minetti AE. 2003. Biomechanical and physiological aspects of legged locomotion in humans. *European Journal of Applied Physiology* 88:297-316.

135. Salo AI, Keränen T, and Viitasalo JT. 2005. Force production in the first four steps of sprint running. In: Wang Q, editor. Proceedings of XXIII International Symposium on Biomechanics in Sports. Beijing, China. p 313-317.

136. Salo AIT, Bezodis IN, Batterham AM, and Kerwin DG. 2011. Elite sprinting: are athletes individually step-frequency or step-length reliant? *Medicine & Science in Sports & Exercise* 43:1055-1062.

137. Samozino P, Rabita G, Dorel S, Slawinski J, Peyrot N, Saez de Villarreal E, and Morin JB. 2016. A simple method for measuring power, force, velocity properties, and mechanical effectiveness in sprint running. *Scandinavian Journal of Medicine and Science in Sports* 26:648-658.

138. Santuz A, Ekizos A, Kunimasa Y, Kijima K, Ishikawa M, and Arampatzis A. 2020. Lower complexity of motor primitives ensures robust control of high-speed human locomotion. *bioRxiv*. 10.1101/2020.04.24.055277

139. Sasaki K, Neptune RR, and Kautz SA. 2009. The relationships between muscle, external, internal and joint mechanical work during normal walking. *Journal of Experimental Biology* 212:738-744.

140. Schache AG, Blanch PD, Dorn TW, Brown NA, Rosemond D, and Pandy MG. 2011. Effect of running speed on lower limb joint kinetics. *Medicine and Science in Sports and Exercise* 43:1260-1271.

141. Schache AG, Brown NA, and Pandy MG. 2015. Modulation of work and power by the human lower-limb joints with increasing steady-state locomotion speed. *Journal of Experimental Biology* 218:2472-2481.

142. Schache AG, Dorn TW, Williams GP, Brown NA, and Pandy MG. 2014. Lower-limb muscular strategies for increasing running speed. *Journal of Orthopaedic & Sports Physical Therapy* 44:813-824.

143. Schache AG, Lai AKM, Brown NAT, Crossley KM, and Pandy MG. 2019. Lower-limb joint mechanics during maximum acceleration sprinting. *Journal of Experimental Biology* 222:jeb209460. doi: 10.1242/jeb.209460

144. Schultz G, and Mombaur K. 2010. Modeling and optimal control of human-like running. *IEEE/ASME Transactions on Mechatronics* 15:783-792.

145. Serrancolí G, Falisse A, Dembia CL, Vantilt J, Tanghe K, Lefeber D, Jonkers I, and De Groote F. 2019. Subject-exoskeleton contact model calibration leads to accurate interaction force predictions. *IEEE Transactions on Neural Systems and Rehabilitation Engineering* 27:1597-1605.

146. Serrancolí G, and Pàmies-Vilà R. 2019. Analysis of the influence of coordinate and dynamic formulations on solving biomechanical optimal control problems. *Mechanism and Machine Theory* 142:103578.

147. Sherman MA, Seth A, and Delp SL. 2011. Simbody: multibody dynamics for biomedical research. *Procedia IUTAM* 2:241-261.

148. Sides DL. 2014. Kinematics and kinetics of maximal velocity sprinting and specificity of training in elite athletes. PhD Thesis. University of Salford.

149. Slawinski J, Termoz N, Rabita G, Guilhem G, Dorel S, Morin JB, and Samozino P. 2017. How 100-m event analyses improve our understanding of world-class men's and women's sprint performance. *Scandinavian Journal of Medicine and Science in Sports* 27:45-54.

150. Smith G, Lake M, and Lees A. 2014. Metatarsophalangeal joint function during sprinting: a comparison of barefoot and sprint spike shod foot conditions. *Journal of Applied Biomechanics* 30:206-212.

151. Spencer M, Lawrence S, Rechichi C, Bishop D, Dawson B, and Goodman C. 2004. Time-motion analysis of elite field hockey, with special reference to repeated-sprint activity. *Journal of Sports Sciences* 22:843-850.

152. Toon D, Kamperman N, Ajoku U, Hopkinson N, and Caine M. 2006. Benchmarking stiffness of current spring spikes and concept selective laser sintered nylon outsoles. In: Moritz EF, and Haake S, eds. *The Engineering of Sport 6*. Berlin: Springer-Verlag, 415-420.

153. Umberger BR, and Miller RH. 2017. Optimal control modeling of human movement. In: Müller B, Wolf SI, Bruggemann GP, Deng Z, McIntosh A, Miller F, and Selbie WS, eds. *Handbook of Human Motion*. 1st ed. New York City, USA: Springer International Publishing.

154. van den Bogert AJ, and Ackermann M. 2009. Effect of a prosthetic limb on sprint running performance. XXII Congress of the International Society of Biomechanics. Natal, Brazil.

155. van den Bogert AJ, Blana D, and Heinrich D. 2011. Implicit methods for efficient musculoskeletal simulation and optimal control. *Procedia IUTAM* 2.

156. van den Bogert AJ, Hupperets M, Schlarb H, and Krabbe B. 2012. Predictive musculoskeletal simulation using optimal control: effects of added limb mass on energy cost and kinematics of walking and running. *Proceedings of the Institution of*

Mechanical Engineers, Part P: Journal of Sports Engineering and Technology 226:123-133.

157. van den Bogert AJ, and Nigg BM. 2007. Simulation. In: Nigg BM, and Herzog W, editors. Biomechanics of the Musculo-skeletal System. New York, USA: John Wiley & Sons.

158. van Ingen Schenau GJ, de Koning JJ, and de Groot G. 1994. Optimisation of sprinting performance in running, cycling and speed skating. *Sports Medicine* 17:259-275.

159. Vaughan CL. 1984. Computer simulation of human motion in sports biomechanics. . *Exercise and Sport Science Reviews* 12:373-398.

160. Volkov NI, and Lapin VI. 1979. Analysis of the velocity curve in sprint running. *Medicine & Science in Sports* 11:332-337.

161. von Lieres Und Wilkau HC. 2017. Understanding biomechanical differences in technique between phases of a sprint. PhD Thesis. Cardiff Metropolitan University.

162. von Lieres Und Wilkau HC, Bezodis NE, Morin JB, Irwin G, Simpson S, and Bezodis IN. 2020. The importance of duration and magnitude of force application to sprint performance during the initial acceleration, transition and maximal velocity phases. *Journal of Sports Sciences* 38:2359-2366.

163. Wächter A, and Biegler LT. 2006. On the implementation of an interior-point filter line-search algorithm for large-scale nonlinear programming. *Mathematical Programming* 106:25-57.

164. Walker J, Tucker C, Paradisis GP, Bezodis I, Bissas A, and Merlino S. 2019. Biomechanical report for the IAAF World Indoor Championships 2018: 60 Metres Men. Birmingham, UK.

165. Weyand PG, Sternlight DB, Bellizzi MJ, and Wright S. 2000. Faster top running speeds are achieved with greater ground forces not more rapid leg movements. *Journal of Applied Physiology* 89:1991-1999.

166. Wiemann K, and Tidow G. 1995. Relative activity of hip and knee extensors in sprinting - implications for training. *New Studies in Athletics* 10:29-49.

167. Winter DA. 2009. *Biomechanics and Motor Control of Human Movement*. Toronto, Canada: John Wiley & Sons.

168. Wood GA. 1987. Biomechanical limitations to sprint running. In: van Gheluwe B, and Atha J, editors. Current Research in Sports Biomechanics. Basel, Switzerland: Karger Publishers.

169. Yamaguchi GT. 2005. *Dynamic modeling of musculoskeletal motion: a vectorized approach for biomechanical analysis in three dimensions.* New York, USA: Springer Science & Business Media.

170. Yeadon MR, Atha J, and Hales FD. 1990. The simulation of aerial movement - IV. A computer simulation model. *Journal of Biomechanics* 23:85-89.

171. Yeadon MR, and Challis JH. 1994. The future of performance-related sports biomechanics research. *Journal of Sports Sciences* 12:3-32. 10.1080/02640419408732156

172. Yeadon MR, and King MA. 2007. Computer simulation modelling in sport. In: Payton CJ, and Bartlett RM, eds. *Biomechanical Evaluation of Movement in Sport and Exercise*. London, UK: Routledge.

173. Yeadon MR, King MA, and Wilson C. 2006. Modelling the maximum voluntary joint torque/angular velocity relationship in human movement. *Journal of Biomechanics* 39:476-482.

174. Yong JR, Silder A, and Delp SL. 2014. Differences in muscle activity between natural forefoot and rearfoot strikers during running. *Journal of Biomechanics* 47:3593-3597.

175. Yu J, Sun Y, Yang C, Wang D, Yin K, Herzog W, and Liu Y. 2016. Biomechanical insights into differences between the mid-acceleration and maximum velocity phases of sprinting. *Journal of Strength and Conditioning Research* 30:1906-1916.

176. Zajac FE. 1989. Muscle and tendon: propeties, models, scaling, and application to biomechanics and motor control. *Critical Reviews in Biomedical Engineering* 17:359-411.

177. Zajac FE, and Gordon ME. 1989. Determining muscle's force and action in multi-articular movement. *Exercise and Sport Science Reviews* 17:187-230.

178. Zatsiorsky VA. 2002. *Kinetics of Human Motion*. Champaign, IL: Human Kinetics.